NBS TECHNICAL NOTE 902

U.S. DEPARTMENT OF COMMERCE / National Bureau of Standards

Evaluation, Revision and Application of the NBS Stylus/Computer System for the Measurement of Surface Roughness

NATIONAL BUREAU OF STANDARDS

The National Bureau of Standards [1] was established by an act of Congress March 3, 1901. The Bureau's overall goal is to strengthen and advance the Nation's science and technology and facilitate their effective application for public benefit. To this end, the Bureau conducts research and provides: (1) a basis for the Nation's physical measurement system, (2) scientific and technological services for industry and government, (3) a technical basis for equity in trade, and (4) technical services to promote public safety. The Bureau consists of the Institute for Basic Standards, the Institute for Materials Research, the Institute for Applied Technology, the Institute for Computer Sciences and Technology, and the Office for Information Programs.

THE INSTITUTE FOR BASIC STANDARDS provides the central basis within the United States of a complete and consistent system of physical measurement; coordinates that system with measurement systems of other nations; and furnishes essential services leading to accurate and uniform physical measurements throughout the Nation's scientific community, industry, and commerce. The Institute consists of the Office of Measurement Services, the Office of Radiation Measurement and the following Center and divisions:

Applied Mathematics — Electricity — Mechanics — Heat — Optical Physics — Center for Radiation Research: Nuclear Sciences; Applied Radiation — Laboratory Astrophysics [2] — Cryogenics [2] — Electromagnetics [2] — Time and Frequency [2].

THE INSTITUTE FOR MATERIALS RESEARCH conducts materials research leading to improved methods of measurement, standards, and data on the properties of well-characterized materials needed by industry, commerce, educational institutions, and Government; provides advisory and research services to other Government agencies; and develops, produces, and distributes standard reference materials. The Institute consists of the Office of Standard Reference Materials, the Office of Air and Water Measurement, and the following divisions:

Analytical Chemistry — Polymers — Metallurgy — Inorganic Materials — Reactor Radiation — Physical Chemistry.

THE INSTITUTE FOR APPLIED TECHNOLOGY provides technical services to promote the use of available technology and to facilitate technological innovation in industry and Government; cooperates with public and private organizations leading to the development of technological standards (including mandatory safety standards), codes and methods of test; and provides technical advice and services to Government agencies upon request. The Institute consists of the following divisions and Centers:

Standards Application and Analysis — Electronic Technology — Center for Consumer Product Technology: Product Systems Analysis; Product Engineering — Center for Building Technology: Structures, Materials, and Life Safety; Building Environment; Technical Evaluation and Application — Center for Fire Research: Fire Science; Fire Safety Engineering.

THE INSTITUTE FOR COMPUTER SCIENCES AND TECHNOLOGY conducts research and provides technical services designed to aid Government agencies in improving cost effectiveness in the conduct of their programs through the selection, acquisition, and effective utilization of automatic data processing equipment; and serves as the principal focus within the executive branch for the development of Federal standards for automatic data processing equipment, techniques, and computer languages. The Institute consists of the following divisions:

Computer Services — Systems and Software — Computer Systems Engineering — Information Technology.

THE OFFICE FOR INFORMATION PROGRAMS promotes optimum dissemination and accessibility of scientific information generated within NBS and other agencies of the Federal Government; promotes the development of the National Standard Reference Data System and a system of information analysis centers dealing with the broader aspects of the National Measurement System; provides appropriate services to ensure that the NBS staff has optimum accessibility to the scientific information of the world. The Office consists of the following organizational units:

Office of Standard Reference Data — Office of Information Activities — Office of Technical Publications — Library — Office of International Relations — Office of International Standards.

---

[1] Headquarters and Laboratories at Gaithersburg, Maryland, unless otherwise noted; mailing address Washington, D.C. 20234.

[2] Located at Boulder, Colorado 80302.

Evaluation, Revision and Application of the NBS Stylus/Computer System for the Measurement of Surface Roughness

E. Clayton Teague

Mechanics Division
Institute for Basic Standards
National Bureau of Standards
Washington, D.C. 20234

U.S. DEPARTMENT OF COMMERCE, Elliot L. Richardson, *Secretary*

James A. Baker, III, *Under Secretary*

Dr. Betsy Ancker-Johnson, *Assistant Secretary for Science and Technology*

U.S. NATIONAL BUREAU OF STANDARDS, Ernest Ambler, *Acting Director*

Issued April 1976

National Bureau of Standards Technical Note 902
Nat. Bur. Stand. (U.S.), Tech. Note 902, 151 pages (Apr. 1976)
CODEN: NBTNAE

U.S. GOVERNMENT PRINTING OFFICE
WASHINGTON: 1976

For sale by the Superintendent of Documents, U.S. Government Printing Office, Washington, D.C. 20402
(Order by SD Catalog No. C13.46:902). Price $2.70 (Add 25 percent additional for other than U.S. mailing).

TABLE OF CONTENTS

LIST OF FIGURES

LIST OF TABLES

EVALUATION, REVISION AND APPLICATION OF THE NBS STYLUS/COMPUTER SYSTEM FOR THE MEASUREMENT OF SURFACE ROUGHNESS

E. Clayton Teague

This report describes in detail the hardware and software used at NBS to implement on a stylus instrument/minicomputer system the process of calibrating the system with an interferometrically measured step and the calculation of important characterizations of surface profiles. The characterizations of a profile which may be calculated include the arithmetic average value, the mean square value, the amplitude density function, the autocorrelation function and the average wavelength. The report also includes a statistical evaluation, using empirical and analytical techniques, of the calibration procedure's long term stability.

Key words: Amplitude density function; arithmetic average; autocorrelation function; average wavelength; kurtosis; minicomputer software; random error; skewness; surface microtopography; surface roughness; surface texture; systematic error.

INTRODUCTION

In February 1974, NBS announced a new procedure for calibrating precision roughness specimens which utilized a computerized system for measuring surface roughness. The purpose of developing a computerized system was to increase the accuracy and reliability of the arithmetic average, AA, measurements made by NBS for industrial consumers and to expand NBS's capability for characterizing surface roughness with parameters and functions other than AA. The computerized system has improved the accuracy of AA measurement, relative to American National Standard B46.1-1962 and the International Length Standard, from 7% to 5% in the 0.25 μm AA range and from 5% to 2% in the 2.5 μm AA range. Reliability of the AA value assigned to a particular specimen has been enhanced because the system may be conveniently calibrated at each use with an interferometrically measured step and because the computer's operational speed enables one to perform roughness measurements at a large number of positions on the specimen's surface. With the computerized system, NBS now has the capability to calculate the amplitude density function, the autocorrelation function, the average wavelength, the average slope and the RMS value for the profile of any arbitrary roughness specimen.

Precision roughness measurements at NBS and throughout the world in their earliest form followed the same conceptual procedure used in NBS's computerized system. An interferometrically measured step was used to calibrate the stylus instrument by relating the height produced in the graphical output to the measured step height. The resulting calibration constant for the graphical output was then coupled with manual planimetry of surface profiles to calculate AA values of reasonably high accuracy. The technique, before the availability of computers, was however very time consuming and limited in accuracy by visual estimations of step heights, by the precision of the planimeter and by operator skill.

Due to these difficulties, the procedure evolved to one in which a roughness specimen under test was compared to a master artifact with the use of AA values produced by an analog integrating meter. The master artifact employed by NBS for calibrations was measured at NBS using the step-calibrated planimetry and corrobrated in a blind round robin with other laboratories where similar measurements were made. Even though this one step transfer decreased the time required for calibrating a given specimen, its overall systematic error was greater than the earlier procedure. Increased systematic error arises from a 3% of full scale error for the integrating meter and from the error produced by subjective interpolation between scale divisions. In addition, the method is limited because individual calibrations are referred to the historical values of roughness assigned to the master artifact which is subject to loss, damage and deterioration with ordinary use. With the availability of dedicated minicomputers, the earlier and more basic calibration procedure may be implemented to bypass the comparison method's errors and to reduce the "planimetry" calculations to fractions of a second.

This report describes in detail the hardware and software used at NBS to implement on a minicomputer the calculation of step-calibrated AA values and the other parameters mentioned earlier. The report also describes an evaluation of the new procedure and its correlation with the one previously used. Initial development of the stylus/computer system was performed by Dennis A. Swyt and is described in his report on the system, NBSIR 73-106. To make the present report self-contained, relevant parts of his report, hereafter referred to as DASR, have been included, primarily as appendices.

Following development, the stylus/computer system was subjected to a thorough evaluation for 14 months. The satisfactory results which were obtained after completing the evaluation and its indicated revisions of the system served as a basis for announcing the new procedure. The evaluation consisted of:

1) checking the dynamic and static operation of the system software,

2) statistically evaluating the calibration procedure's long (months) and short (hours) term stability,

3) studying both empirically and analytically various components of the procedure's systematic error,

4) measuring the system hardware's operating characteristics,

and

5) examining the correlation between roughness values obtained from the master-artifact-comparison procedure and the values obtained with the step-calibrated stylus/computer system.

The final system described in this report is the product of many iterations of an evaluate-revise process. As an explanation to those readers who received the announcement of an availability date for this report of April 1974, two delays in the writing of the summary report were due to major revisions of the system software and to subsequent evaluations which were then necessary. Other than the addition of software for the new parameters, the principal change from the system described in DASR is that made in the step height calculations. Here it was found that the metric (in a geometrical context) transformation from computer coordinates to spatial co-ordinates was incomplete. When this conversion is carried out completely, one also finds that the slope factors given in DASR are not needed at the accuracies of the present system. The other revisions of system hardware and software will not be discussed any further since they are dominantly software details. Appropriate changes to the extracted parts of DASR have been made.

1.0 SYSTEM OPERATION

The NBS computerized system for measuring surface roughness consists of a Talysurf 4 stylus instrument* used to generate a profile of the test specimen's surface, an Interdata 3 minicomputer* with data acquisition circuitry for processing the profile in digital form, a digital to analog converter with the associated electronics needed to drive a strip chart recorder used for displaying the results of computer analysis and a Teletype model 33* for system control and output. Appendix A gives a complete description of the electronics necessary for interfacing the system components.

Operations which may be performed with the system are represented by the flowchart in figure 1. To bring the system hardware (appendix A) to this operational state the set of instructions described in appendix B must be loaded into the minicomputer. Convenient use of the minicomputer is then made possible by the properties of the instructional subset named, Monitor. The system is put in a "ready" state by addressing the minicomputer to Monitor's command interpreter located at the hexadecimal address, 3C80. In this state the system accepts commands from the teletype (TTY) and may be directed to perform any of the operations indicated in the flowchart by entering the appropriate letter at the teletype. If additional inputs, from either the stylus instrument or the operator, are required the minicomputer is programmed to type a command or question at the teletype.

To avoid unnecessary usage of minicomputer memory, only the paths through the calibration, roughness and step height measurement procedures are at a near conversational level (appendix Q). Correct execution of the other operations is more dependent on the operator's understanding of the system. Two of the most important examples of this operator dependence are in measuring average wavelength and in calculating the amplitude density function (ADF) and the autocorrelation function (ACF). In both of these cases, the sequence of operations executed, with respect to figure 1, must follow a general top to bottom and left to right pattern. The top to bottom sequence is required since the five operations in the lower half of figure 1 assume that a calibration constant has been measured and that at least one roughness profile has been obtained. A left to right order is necessary since the average wavelength and slope calculation destroys the profile data required for both the amplitude density and

---

*Certain commerical equipment, instruments, or materials are idendified in this paper in order to adequately specify the experimental procedure. In no case does such identification imply recommendation or endorsement by the National Bureau of Standards, nor does it imply that the material or equipment identified is necessarily the best available for the purpose.

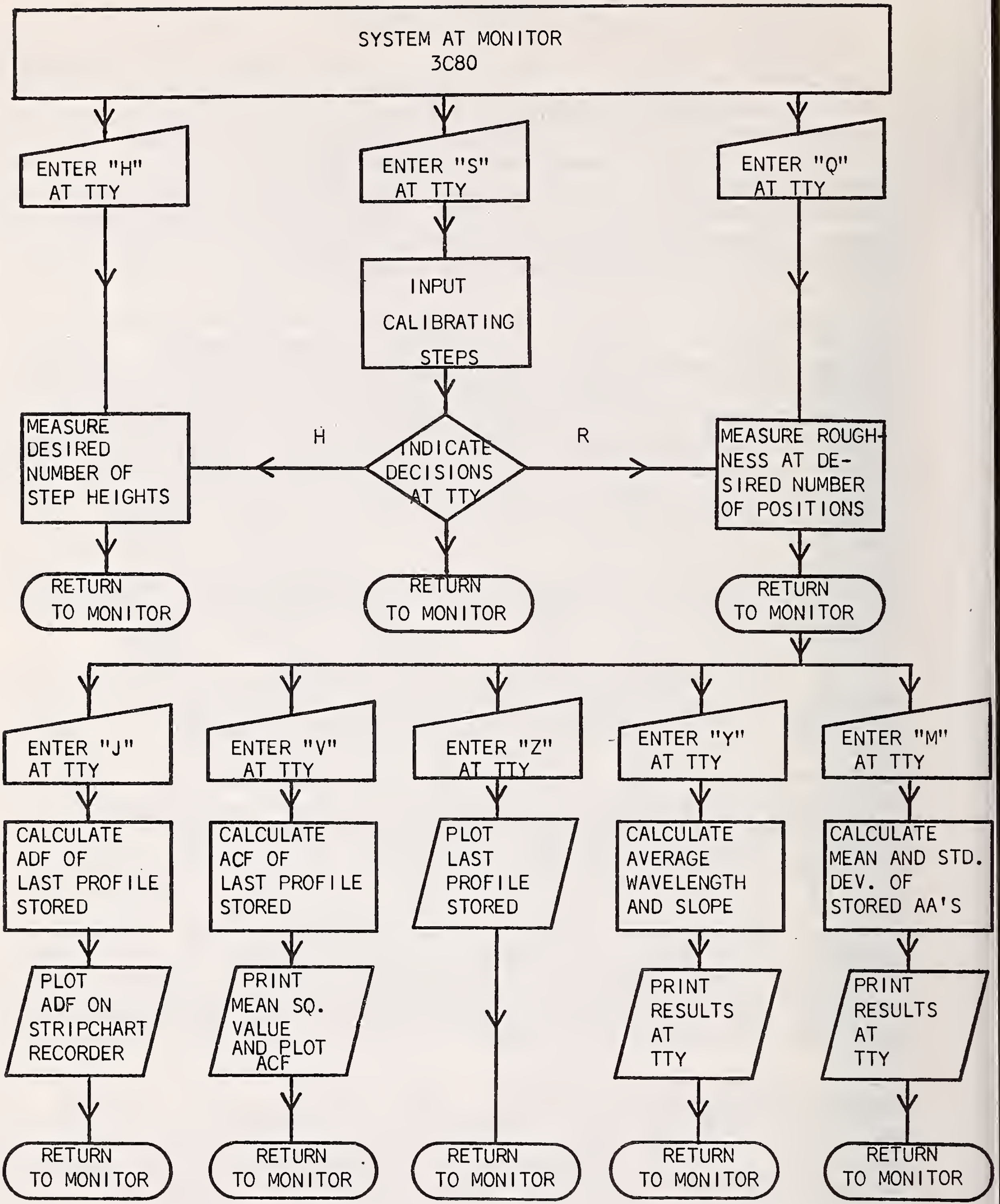

Figure 1. Flowchart of Overall operation of the Computerized System for Surface Roughness Measurement.

autocorrelation function calculations. The operator dependence of this procedure is balanced by its flexibility. Within the sequence just outlined the operator has, following the input of a calibrating step, as many as five correct operations which may be executed. The most common operational sequences are:

I $*\to S\to *\to H\to *$,

II $*\to S\to *\to Q\to *\to M\to *$,

III $*\to S\to *\to Q\to *\to J\to *\to V\to *\to Y\to *$,

and

IV $*\to S\to *\to J\to *\to Q\to *\to J\to *$,

where a letter symbolizes the keyboard entry and its associated operations and, *, symbolizes a return to Moitor's command interpreter. In the first three sequences, the paths from S→H and S→Q may utilize the conversational routes as an alternative to bypass returns to monitor. The fourth sequence is used to obtain a step-calibrated display of the amplitude density function. A rough timetable for these four operational sequences is given in appendix C.

1.1 DATA ACQUISITION*

The means by which topographical profiles are converted to surface roughness data is represented by the functional schematic in figure 2. When the stylus is traversed across a surface, the profile is indicated on strip chart recorder A; the signal driving the recorder, amplified and filtered, appears at the analog-to-digital converter (A/D).

At a particular point in the stroke, the stylus arm activates a relay, which in turn generates two pulses. The first pulse, one second long, appears at the common input of the recorder and interface amplifier. (The source of the event pulse is in the information channel only for the duration of the pulse). Coincident with the leading edge of the event pulse is a fifty-microsecond interrupt pulse to the A/D converter. On receipt of the interrupt at the A/D, a programmed one-second delay is executed, and the analog signal at the filter output is converted to binary data points and stored sequentially in computer memory. (Thus the event mark, recorded on the strip chart, does not appear in the digital data.)

---

*Sections 1.1, 1.2, 1.3, and 1.4, are slightly revised parts of DASR.

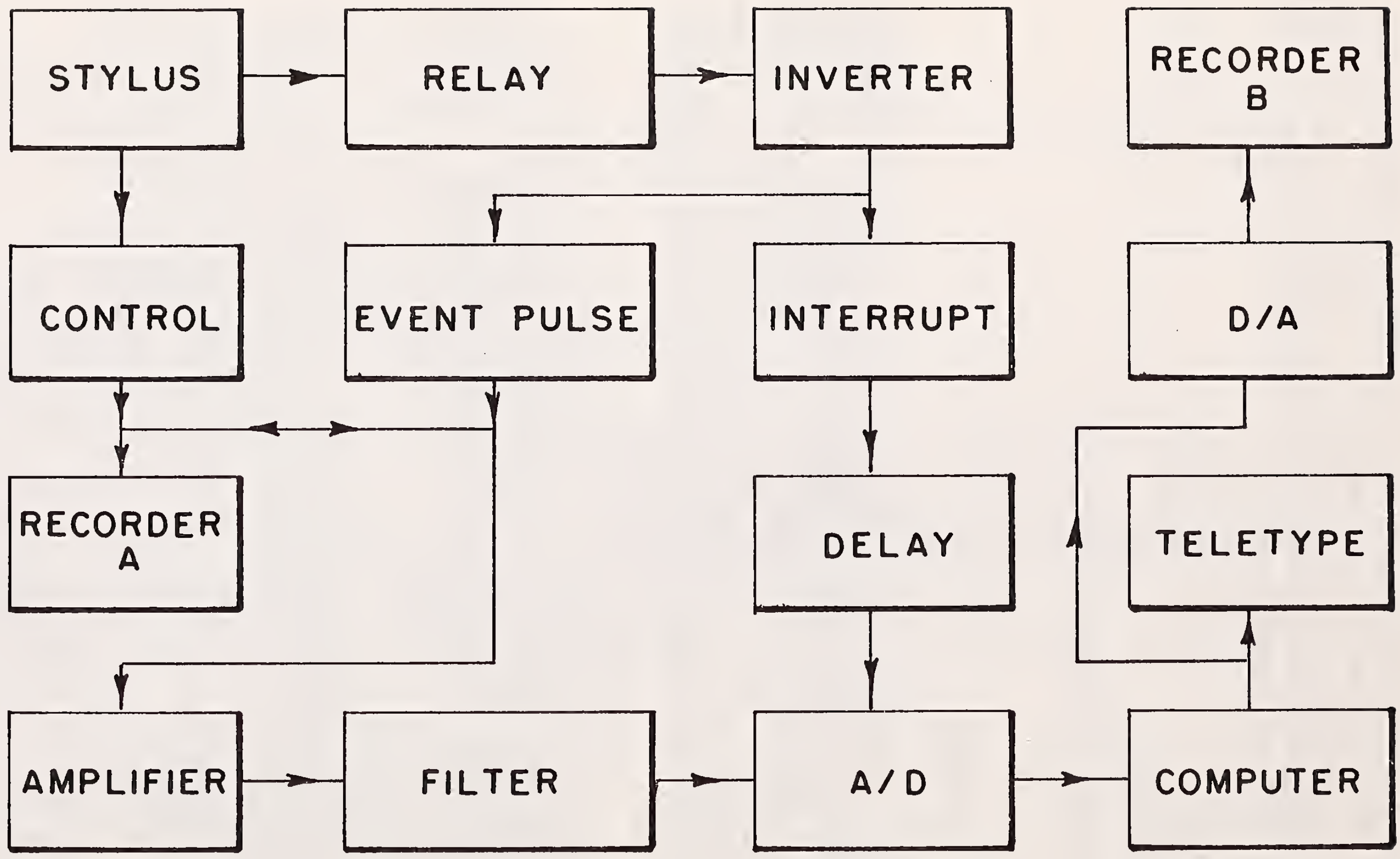

FUNCTION DIAGRAM OF STYLUS INSTRUMENT/MINICOMPUTER SYSTEM

Figure 2

1.2 DATA ANALYSIS OF STEP HEIGHTS

In order to efficiently handle the discontinuity in the trace which comprises the step height and to eliminate restrictions on the alignment of the step artifact, a mathematical model of the step data in the computer memory has been devised. Figure 3a represents a general step profile in which the traces on opposite sides of the discontinuity are wavy and parallel neither to each other nor to the sides of the strip chart.

Linear least-sequares curves are fitted to the segments designated by L1 and L2 in figure 3b (appendix D); the segments are located at the operator's discretion relative to the event mark (appendix E), are of equal lengths and constitute one-half of the total trace. From the slopes and intercepts of the two computed lines, S1 and S2 in figure 3C, are calculated the distances Hi, i = 1, 2....,8 (appendix F); these heights are simply taken as the ordinate differences at equally spaced intervals along the horizontal distance between the ends of the line segments selected by the operator. H1, H3, H5, and H8 are printed at the teletype to inform the operator of the two line segment's relative slopes. The distance HM in figure 3d is the arithmetic mean (or H4) of the distances between the two calculated lines over the region separating the line segments.

1.3 DATA ANALYSIS OF SURFACE ROUGHNESSES

The AA roughness for a surface profile is computed from the data in memory in a manner analogous to the operation of an integrating meter. Since the profile signal has wavelength cut-off restrictions imposed by analog filtering (appendix A), no digital filtering or signal conditioning is involved. The value corresponding to the center line of the profile is the arithmetic average of all points in the record. The AA value is the arithmetic average of the magnitudes of the deviations of each from the mean.

1.4 CALIBRATION OF STEP HEIGHTS AND AA VALUES

When the binary value, HM, of the calibration step profile has been computed and the decimal value, H0, of the interferometrically measured calibration step entered at the Teletype, a conversion constant, KCAL, is computed:

KCAL = HO (decimal)/HM (binary).

a)
b)
c)
d)

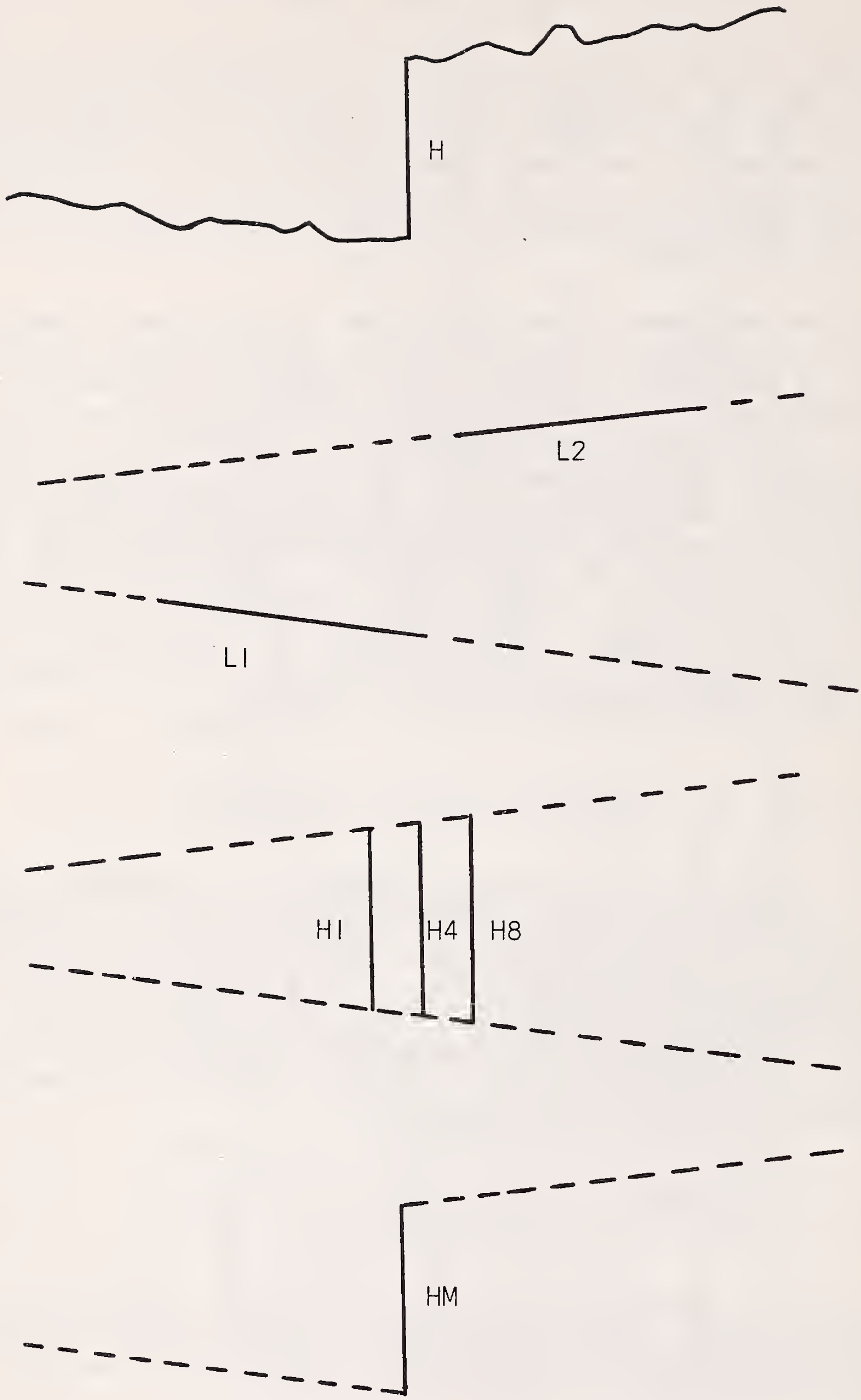

Figure 3: STEP HEIGHT CALCULATION

a) Step Profile Input
b) Least Squares Line Segments
c) Calculated Distances at X_m Between the two Lines
d) Mean Distance of Step Height

The calibrated values of unknown steps and surface roughnesses are then of the form:

$$HM \text{ (decimal)} = HM \text{ (binary)} \times KCAL$$

and

$$AA \text{ (decimal)} = AA \text{ (binary)} \times KCAL$$

1.5 EXAMPLE OF SYSTEM OPERATION

An example of the procedure for step-calibrating the system followed by the measurement of an unknown step height and a surface roughness may be illustrative. A sample teletype output is given in figure 4. Further details appear in appendix Q. This example assumes the operator follows a conversational route through the procedure.

After an appropriate magnification has been selected, the corresponding calibration step is aligned on the Talysurf and program execution begun by entering an S at the teletype. At the proper point in the program the operator is informed at the teletype to begin the stylus stroke in order to enter the calibration step profile. The signal from the stylus instrument is amplified by a factor of 10, filtered (appendix A), converted to 512 twelve-bit data points over a 25 second record length and stored in the computer memory. The operator is then instructed to enter HO, the interferometrically measured value of the calibration step height, at the teletype; this four-digit decimal number is converted to binary and stored. The operator now enters the information at the teletype which locates the step discontinuity in the stored data; the information is derived from the chart trace and the step locator chart (appendix E).

The step heights are then computed, converted to decimal values and printed. The calibration constant is also calculated with the hexadecimal value being printed. To obtain a more complete sampling of the data output from the step measurement process, the procedure described in these paragraphs is repeated five times to produce an average calibration constant AVG. KCAL for subsequent use.

The operator now aligns the specimen to be measured on the stylus instrument. On being queried at the teletype, the operator indicates the type of artifact by entering command characters at the teletype keyboard. If it is a step, an H is entered and the procedures for entering a step profile and its related information repeated. If a roughness is to be measured, the proper filter cutoff and stoke speeds are selected, an R entered at the teletype and the stroke begun. In roughness measurement, the signal from the stylus instrument is amplified by a factor of 10, filtered, converted to 4096 twelve-bit data points over a 2.5 second record length and stored in

```
>S        STEP/SURFACE ROUGHNESS CALIBRATION


ENTER DATA/ IN ENTER HO 5105 ENTER UNITS -7 ENTER A1 11C2 ENTER A2 124A
H1       H3       H5       H7       HM       UNITS          KCAL= 000031B2
00005123 00005113 00005102 00005091 00005104 -7 MM
ENTER DATA/ IN ENTER HO 5105 ENTER UNITS -7 ENTER A1 11C2 ENTER A2 124A
H1       H3       H5       H7       HM       UNITS          KCAL= 0000318A
00005102 00005103 00005105 00005107 00005105 -7 MM
ENTER DATA/ IN ENTER HO 5105 ENTER UNITS -7 ENTER A1 11C2 ENTER A2 124A
H1       H3       H5       H7       HM       UNITS          KCAL= 0000310C
00005096 00005101 00005106 00005110 00005104 -7 MM
ENTER DATA/ IN ENTER HO 5105 ENTER UNITS -7 ENTER A1 11C2 ENTER A2 124A
H1       H3       H5       H7       HM       UNITS          KCAL= 00003158
00005121 00005111 00005102 00005093 00005105 -7 MM
ENTER DATA/ IN ENTER HO 5105 ENTER UNITS -7 ENTER A1 11C2 ENTER A2 124A
H1       H3       H5       H7       HM       UNITS          KCAL= 00003190
00005100 00005103 00005106 00005108 00005105 -7 MM
AVG KCAL =00003170
MORE? YH OR R? H
ENTER DATA/ IN ENTER HO  ENTER UNITS -7 ENTER A1 11C2 ENTER A2 124A
H1       H3       H5       H7       HM       UNITS
00005091 00005096 00005101 00005105 00005099 -7 MM
MORE? YH OR R? H
ENTER DATA/ IN ENTER HO  ENTER UNITS -7 ENTER A1 11C2 ENTER A2 124A
H1       H3       H5       H7       HM       UNITS
00000000 00000000 00000000 00000000 00000000 -7 MM
MORE? YH OR R? H
ENTER DATA/ IN ENTER HO  ENTER UNITS -7 ENTER A1 11C2 ENTER A2 124A
H1       H3       H5       H7       HM       UNITS
00005077 00005076 00005075 00005074 00005075 -7 MM
MORE? YH OR R? R
AA       UNITS
00000935 -8 MM   00000920 -8 MM   00000914 -8 MM         MORE? Y
00000873 -8 MM   00001009 -8 MM   00000854 -8 MM         MORE? Y
00000856 -8 MM   00000878 -8 MM   00000953 -8 MM         MORE? Y
00000864 -8 MM   00000846 -8 MM   00000835 -8 MM         MORE? Y
00000885 -8 MM   00000827 -8 MM   00000817 -8 MM         MORE? Y
00000912 -8 MM   00000887 -8 MM   00000806 -8 MM         MORE? Y

00006408 -8 MM   00006279 -8 MM   00006294 -8 MM         MORE? Y
00006391 -8 MM   00006491 -8 MM   00006495 -8 MM         MORE? N


FINI
>
```

Figure 4: SAMPLE TELETYPE OUTPUT

the computer memory. The computer calculates either a step height or roughness AA, prints the result, and asks if more measurements are to be made from the same calibration. Roughness values are obtained in groups of three and may be stored for future statistical analysis by entering a space at the teletype; the roughness value is not stored if a K is entered. If more measurements are to be made from the same calibration, a Y is entered at the teletype and the measurement of the unknown as described in this section repeated. If no more measurements or those at a different magnification are to be made, an N is entered to return the system to Monitor.

2.0 ANALYTICAL AND EMPIRICAL STUDIES OF THE NEW CALIBRATION PROCEDURE'S ACCURACY

Following the achievement of a reliably operating software system for measuring step heights and roughness (appendix B), the measurement system's roughness data output was subjected to a preliminary evaluation. Data for the statistical evaluation was extracted from the results of four calibration studies which NBS had performed for industry. The calibration studies had employed the stylus/computer system simply as a more accurate readout than the Talysurf 4's AA meter, with the reported AA values being referenced to the NBS master. The pattern of observations made on a precision roughness specimen at this time was that of making 6 measurements at each of 5 positions on a roughness area. Results of this preliminary evaluation along with the increased accuracy of the computer calculation showed that position-to-position variations in specimen roughness and variations in day-to-day transfers from the NBS master were the dominant sources of random error.

Based upon the preliminary evaluation, the complete interferometrically calibrated stylus/minicomputer system was used to obtain roughness measurements over a three month period. In these measurements the pattern of observations was changed at first to that of 3 traverses at each of 6 positions, then later to 3 traverses at each of 10 positions over each roughness area (appendix H). Only a small area of each roughness patch was used for the study in order to minimize the effect of positional variations in the surface roughness on the resultant data. The data was analyzed by Joseph Cameron of the Office of Measurement Services at NBS. Results of this analysis (appendix H) show that:*

1) the computed standard deviation, σ_W, of the average of three measurements at one surface location on a particular day was 0.028 μin for the 20-μin AA patch and 0.31 μin for the 125-μin AA patch,

2) the computed standard deviation, σ_B, of the day-to-day component of the average of measurements at 10 (or 6) surface positions was 0.132 μin for the 20-μin AA patch and 0.337 μin for the 125-μin AA patch,

3) assuming a uniform roughness specimen i.e., one with no position-to-position variations in roughness, the estimated 3 standard deviations limit for assessing the uncertainty of roughness measurements employing an average from measurements at 10 positions was 0.40 μin for the 20-μin AA patch and 1.1 μin for the 125-μin AA patch, or 2.0% and 0.9% of the respective mean roughness values.

*English units are used in referring to the precision roughness specimens in deference to their conventional use.

4) no significant correlation between the magnitude of KCAL, the calibration constant, and the daily averages was apparent.

This last conclusion is important since correlation between KCAL and roughness values would imply that the step calibration procedure was not properly correcting for gain drifts in the system electronics.

Overall uncertainty in a measurement process may be described in terms of two categories; systematic uncertainty and random uncertainty. Systematic uncertainties describe those properties of the measurement process which are fixed prior to and during the procedure of obtaining data. Random uncertainties describe the variations in a measurement process's results during repetitions of the procedure to obtain data.

The aspects of the measurement process which are classed as being parts of a repetition is always arbitrary to some extent. For instance, should one repeat a roughness measurement with the use of two or more stylus tips of nominally the same radius to determine the uncertainty in the roughness value produced by this aspect of the process? Should one repeat a computation of KCAL with the use of two or more interferometrically measured steps approximately equal in height? A consistent definition of a repetition for the roughness measurement process results when one fixes all artifacts of the measurement apparatus i.e. one roughness specimen, one calibrating step, one stylus tip, one roughness filter and one environment (noise level). A "repetition" is then defined as a completely new and independent measurement with this fixed set of apparatus and artifacts including a recomputation of KCAL, repositioning the test specimen, etc., such as would be involved if the values were obtained one or more days apart.

Based on this definition, all the uncertainty components revealed by the three month evaluation would be random uncertainties. Possible systematic uncertainties describing the difference between an AA value obtained with the use of the NBS stylus/computer system and that obtained with a similar system are as follows:

1) Uncertainty in the interferometrically measured height of the calibrating step. An estimated 3 standard deviation of these measurements is 25 nm (section 2.1).

2) Uncertainty in stylus tip radius. The resultant error in an AA measurement is dependent on the profile's waveform but an estimate based on the highly sloped 20-μin (0.508-μm) precision roughness specimen's waveform is $\pm$ 5-nm AA with the stylus tip in current use at NBS, (appendix I). An estimate of the relationship between tip radius uncertainty and AA uncertainty was made through the use of a correction chart given in appendix C of American National Standard B46.1-1962.

3) Lack of conformity of the NBS system's roughness filter characteristics to those specified in American National Standard B46.1. The filter-amplifier bandpass characteristics given in appendix A and the uniformity and magnitude of the stylus traversal speed given in appendix O demonstrate that the NBS system performance conforms to the American National Standard B46.1 specifications. Since tolerances on the filter characteristics of the standard allow greater variations in the cutoff points etc., than the electrical component specifications of the NBS system no uncertainty estimates on this effect will be made.

4) A bias error produced by the system's mechanical and electrical noise. The AA value of the combined system noise is 5 to 6 nm (appendix J). The positive bias of the noise on AA measurements would be additive according to the expression $\sqrt{(\text{roughness AA})^2 + (\text{noise AA})^2}$ since no correlation between the noise and the signal from the specimen roughness should be present. For roughness values above 100 nm the effect of noise on the calculated AA value is small e.g.

$$\frac{\sqrt{(100)^2 + (5)^2} - 100}{100} = 0.12\% \ .$$

5) A component to account for the deviation of the profile obtained with the specified tip radius from the true profile, i.e., the profile which would be obtained with a tip radius approaching zero. Whitehouse [1]* has explored this problem and concludes that if the tip radius is small compared to the correlation length (section 3.3) of the profile, AA values will be reduced only one to two percent from the true profile AA. This particular value is based on the use of a tip radius of 2-3 μm and correlation lengths of 25 μm or greater. The systematic uncertainty from this effect is therefore not given further consideration. All calibration and test reports issued by NBS do however report measured AA values relative to a specified tip radius.

Analytical and further empirical studies of the components of the measurement process random uncertainty are presented in the following sections. These studies show that the net random uncertainty may be attributed to three sources: (1) the variations, due to the surface finish of the calibrating step, in KCAL, (2) the variations, due to sampling and digitizing processes, software computations and

*Figures in brackets indicate the literature reference.

nonlinearities in the stylus instrument transducer and in the interface hardware, in KCAL and (3) in measured AA values, for a fixed KCAL.

Section 2.2 shows that the 3 standard deviations of step heights calculated from profiles of a specimen with an RMS surface finish of q is 1.08 q. An estimate of a 3 standard deviations values for the second source of uncertainty based on the results of section 2.2 and 2.3 is 1.0% of the measured AA value. A 3 standard deviations value of 1.4% of the measured AA value for the third component is obtained from the three month evaluation (see appendix H). Since profiles of typical roughness specimens have peak-to-valley heights of three to eight times the profile AA value, step heights approximately six times the expected AA value are used for calibrating the system. Thus the net random uncertainty in the measurement process is given by the relation:

$$\text{Net Random Uncertainty} = \left[\left(\frac{27\ \text{nm}}{6}\right)^2 + (0.01\ \text{AA nm})^2 + (0.014\ \text{AA nm})^2\right]^{1/2},$$

where an RMS surface finish of 25 nm has been assumed. This relation holds since the components are uncorrelated.

The systematic uncertainties that are included in an NBS statement of calibration accuracy are the components 1, 2 and 4 as described earlier. The net systematic uncertainty is therefore given by the relation:

$$\text{Net Systematic Uncertainty} = \left[\left(\frac{25\ \text{nm}}{6}\right)^2 + (5\ \text{nm})^2\right]^{1/2}.$$

Effects of the fourth component of systematic uncertainty are corrected for in stated AA values.

The calibration uncertainty of the NBS system for measuring surface roughness is taken as the sum of the system's random uncertainty and its systematic uncertainty. The calibration uncertainty (CU) as a function of the specimen AA roughness is therefore:

$$\text{CU(AA nm)} = 6.5\ \text{nm} + [20.25\ \text{nm}^2 + 2.96 \times 10^{-4}\ (\text{AA nm})^2]^{1/2}.$$

A plot of this equation is given in figure 5.

Calibration and test reports issued by NBS briefly describe these systematic and random uncertainties and give a net value based on the calibrating step height used for the measurements; the usual height is approximately six times the AA value. Finally, an overall measurement uncertainty is stated which is the sum of the calibration uncertainty and a three-standard-deviation limit of the data obtained in 3 stylus traverses at each of 10 positions of the test specimen's surface.

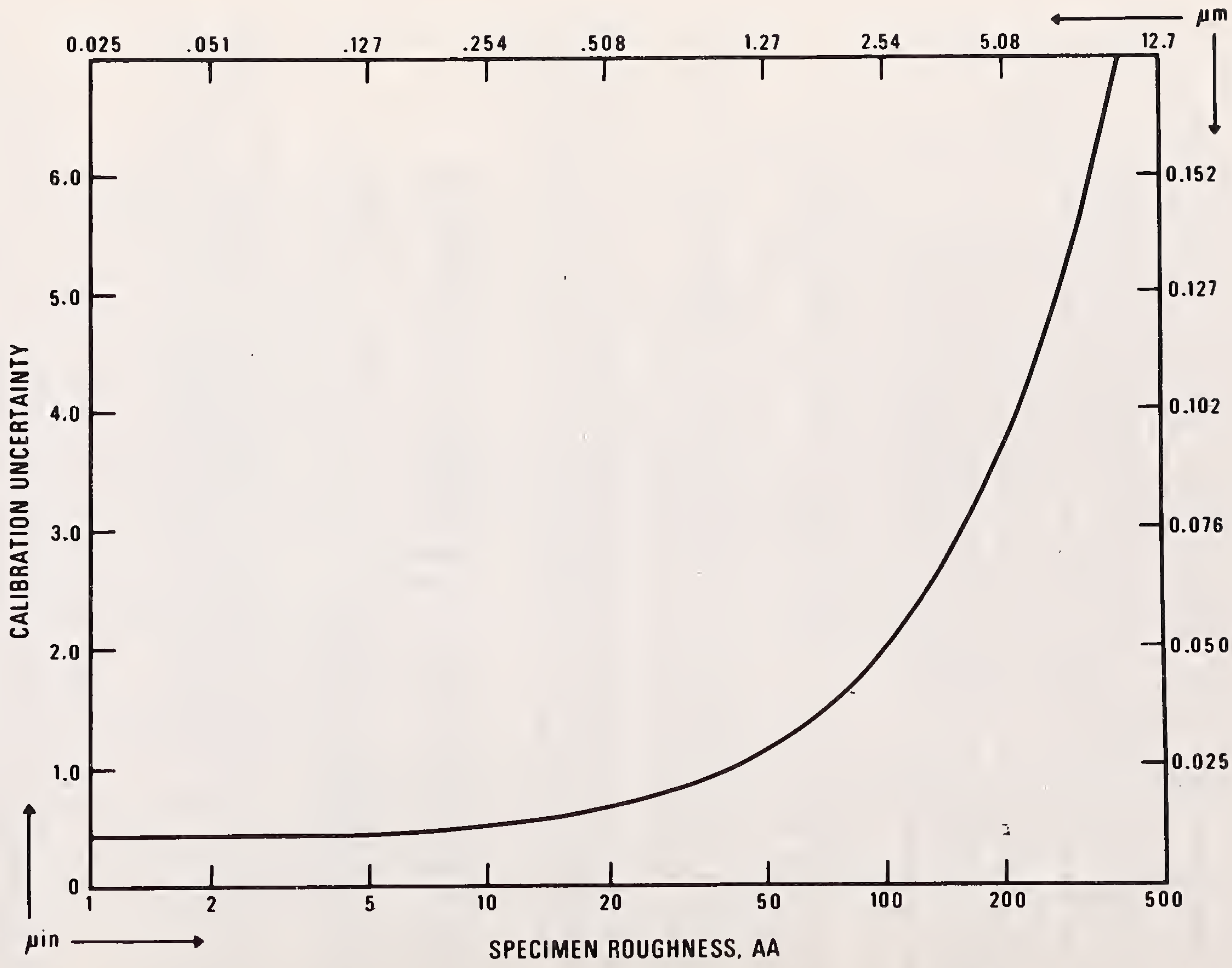

Figure 5: PLOT OF ROUGHNESS CALIBRATION ACCURACY AS A FUNCTION OF SPECIMEN ROUGHNESS.

The results of the study of the correlation between roughness values obtained from the master-artifact comparison procedure and the values obtained with the step calibrated stylus/computer system are also presented in the following sections. The study confirms that a smooth transition between the two measurement processes was made.

2.1 THE EFFECT OF GEOMETRY ON STEP HEIGHT MEASUREMENT

Step artifacts used to calibrate the stylus/minicomputer system typically have many unavoidable geometrical errors; surfaces on both sides of the step have a microscopic texture, the surfaces are not flat and the two sides of the step are not parallel. One cross-section of such a step obtained from a stylus trace at a 5000 to 1 vertical to horizontal distortion is shown in figure 6. These geometrical errors affect both the precision of measuring step heights interferometrically and the precision of transferring the measured value to the stylus instrument.

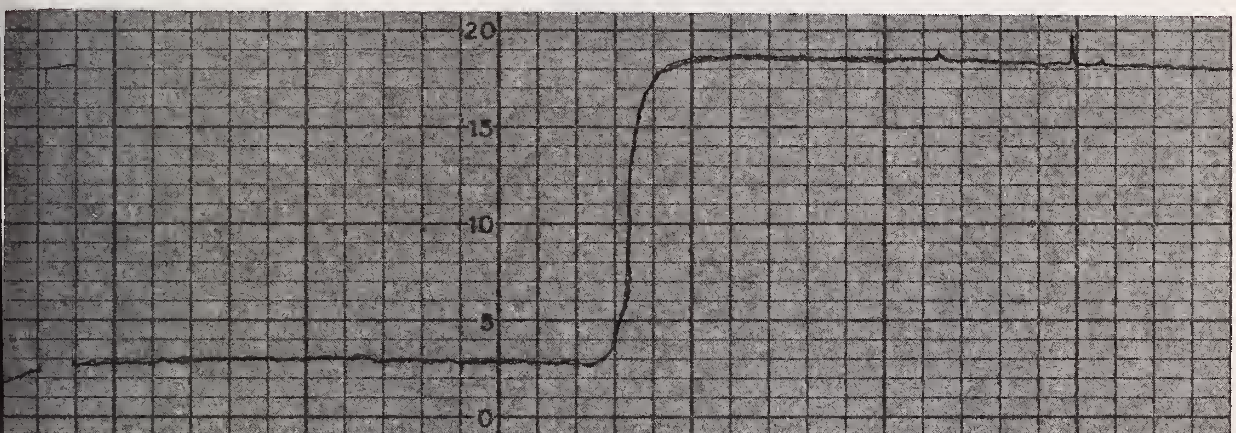

Figure 6: Profile of a 0.501 μm step. The vertical to horizontal magnification ratio is 5000 to 1.

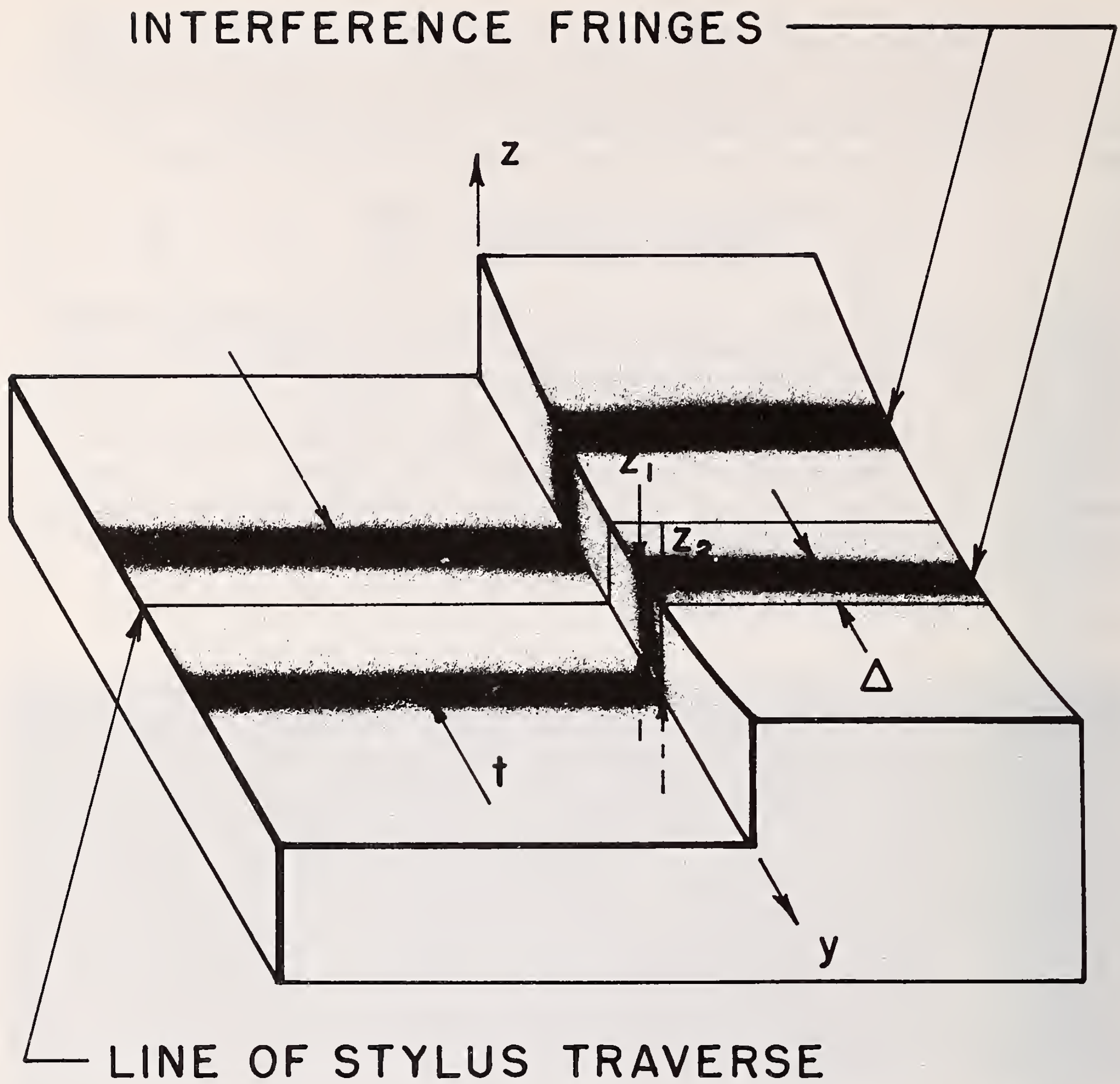

Figure 7. The Effect of Geometry Errors on the Measurement of Step Heights.

As an introduction to some effects of geometrical errors on the interferometric measurement of step heights, consider the illustration in figure 7. In the usual two beam or multiple beam interferometry the measured height will be some function of the fringe spacing, t; the lateral displacement of the fringe, Δ; and properties of the illuminating radiation. Assuming one has well collimated light of wavelength λ and an ideal step artifact (flat and parallel sides) the height, h, is given by the well known equation:

$$h = \left(n + \frac{\Delta}{t}\right) \lambda/2. \qquad \text{Equation 1.}$$

The order of the displaced fringe, n, is determined by "following the fringe" or by deduction from measurements with several different wavelengths of illumination.

Figure 7 was composed to show that the heights measured on a step artifact with interferometry and with a stylus instrument may differ significantly. This is particularly true if interferometry at magnifications of about 10X is employed. Here the lateral displacement of the two fringes used in measuring Δ may be as much as 5 mm; assuming no magnification and 5 fringes in a 2.5 cm field of view. Thus, with reference to figure 7, some mean of z_1 and z_2 would be measured with interferometry, while the value measured with a stylus instrument with the indicated stylus traverse would be less than this mean.

Figure 8 is an interferogram obtained from a specimen with some typical geometry errors; the planes on the two sides of the step are not parallel in either the direction perpendicular or parallel to the step's edge. From the bottom of the interferogram, fringe displacements at the step edge are respectively, 1.74, 1.77 and 1.81 of the mean fringe spacing. Magnification of this interferogram (∿ 20X) is such that the field of view contains approximately the distance traversed, in the fringe direction, by the stylus during step height measurement, (3.8 mm). Notice that the lateral displacement of the fringes at the step is ∿ 2 mm.

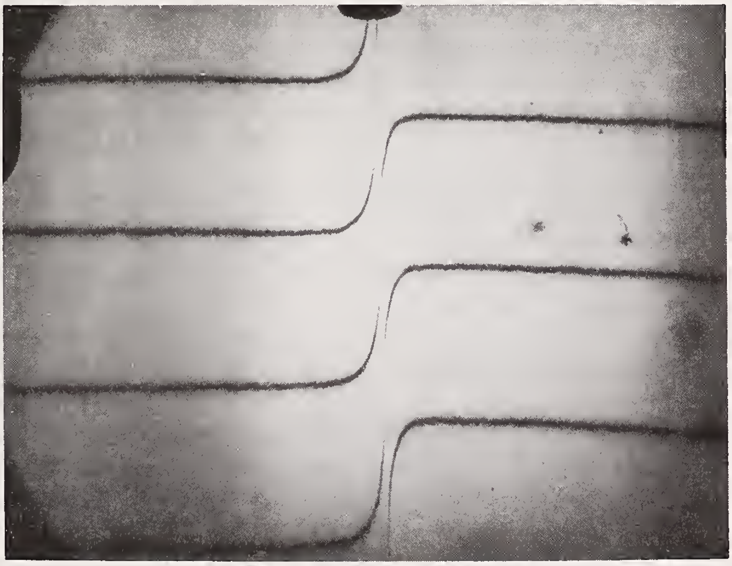

Figure 8: Representative Interferogram of a Step Specimen. Wavelength of the Light Used was 589 nm.

For an ideal artifact the fractional error in a step height measurement using equation 1 is given by:

$$\frac{dh}{h} < \frac{\varepsilon}{\Delta} \left(1 + \frac{\Delta}{t} + \frac{\varepsilon}{t}\right) \left(\frac{1}{1 + \frac{nt}{\Delta}}\right), \qquad (2)$$

where ε is the error in measuring either Δ or t. This expression includes the second order error $\varepsilon^2/\Delta t$ and assumes that the error produced by uncertainty in λ is negligible. For real step artifacts additional error terms must be added to account for the artifact's imperfect geometry and for the lateral averaging of interferometry. One possible way of incorporating these errors into equation 1 is to let h be a function of the dispersion, $s = \Delta/t$, such that:

$$h = n\,\lambda/2 + g(s)\,\lambda/2,$$

where for small geometrical errors, $g(s) = s + \delta(s)$. With these assumptions the errors may be expressed by the equation:

$$dh = ds\,\lambda/2 + \frac{d\delta}{ds}\,ds\,\lambda/2.$$

The first term in this equation is the error for an ideal artifact discussed before. The second term is the error arising from geometry and lateral averaging.

An illustration of this mixing of geometrical errors and averaging by lateral fringe displacement such that the height measured is a function of dispersion is given in figure 9. For the particular geometry shown the height measured with interferometry could therefore change by as much as $0.12\,\lambda/2$. The approximate mean deviation from planarity for the example is $0.15\,\lambda/2$. If the amplitude of this deviation is halved to approximately $0.08\,\lambda/2$ then the difference measured for the dispersions shown is also $\sim 0.08\,\lambda/2$. The close correspondence between the difference measured and the mean deviation from planarity is a coincidence generated by the two dispersions used for the example. Other dispersions do not show this correspondence. Experimentation with other geometrical errors shows that the variation of height measured is strongly dependent on the particular geometry and its general slope relative to that of the reference surface. Geometrical errors in the lower part of the step and in the reference surface would also contribute to the total uncertainty of a height measurement in a manner similar to the one surface considered in the example.

Carrying the discussion further to obtain an explicit relationship between $\delta(s)$ and a particular geometry is not fruitful. The principal point of the discussion was to demonstrate that to properly measure a step height with interferometry and to characterize the measurement's uncertainty the geometry of the surfaces on both sides of the step in

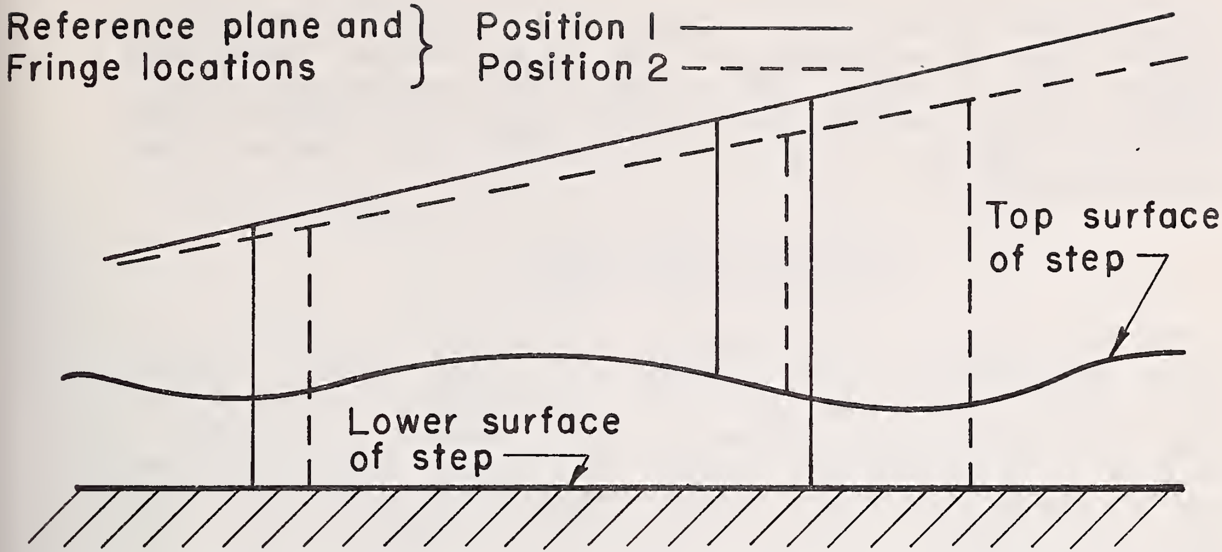

Figure 9a. Side View of Step and Reference Plane with Fringe Locations Shown for Two Reference Plane Positions Assuming λ = 3.5 cm.

Position 1. Step height measured = Δ_1 / t_1 = 0.836 $\lambda/2$

Position 2. Step height measured = Δ_2 / t_2 = 0.720 $\lambda/2$

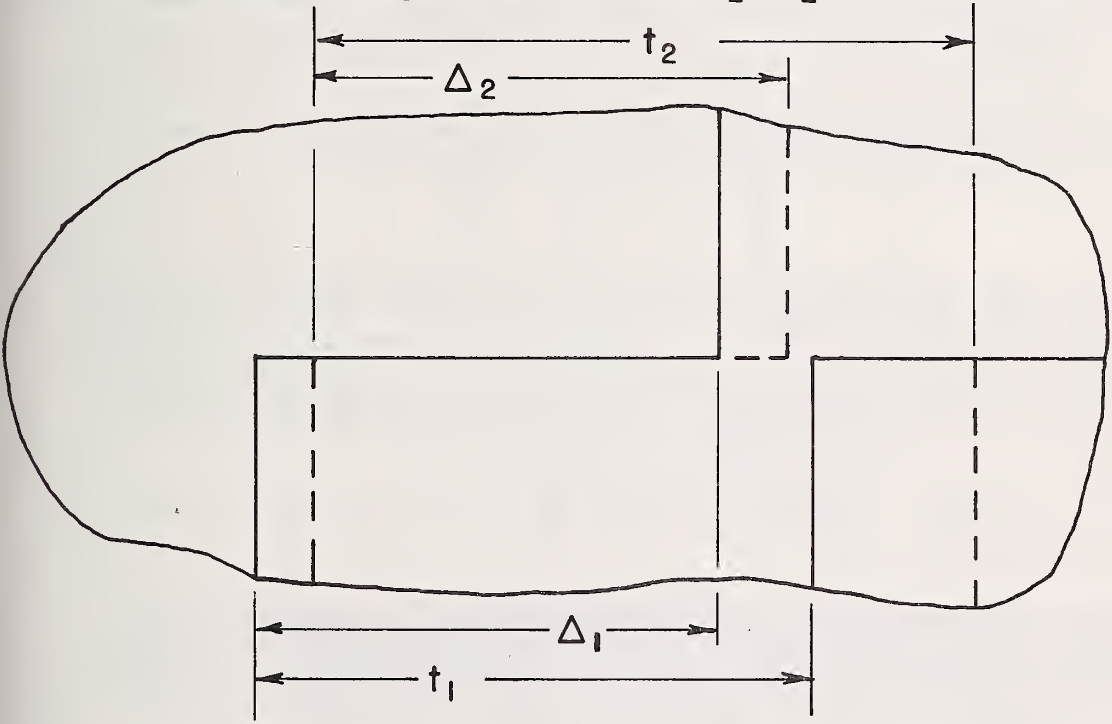

Figure 9b. Top View of Fringe Pattern Across the Step Shown in Figure 9a.

the neighborhood of the measured region must be determined. Step artifacts used to calibrate the NBS stylus/computer system are therefore routinely checked for flatness and parallelism. The 3 standard deviation uncertainty of 25 nm assigned to this aspect of the calibration procedure reflects in part the errors produced by imperfect geometry.

2.2 THE EFFECT OF SURFACE TEXTURE ON STEP HEIGHT MEASUREMENT

The microscopic surface texture on both sides of the step also affects the measurement and transfer of a step height. Surface texture affects the measurement of a step height by increasing the fringe width and therefore increasing ε, the error in measuring Δ and/or t. The microscopic texture is usually unresolved at the customary magnifications used for step height measurement in the 10-μm range. The primary effect of the surface texture is to limit the overall accuracy of transferring a step height into the stylus/computer system.

As described in section 1.2, the step height is transferred to the stylus/computer system by performing a linear least-squares fit to the data taken from each side of the step, then calculating the step height from the position of the two resulting lines. Least-squares methods for estimating the coefficients of a relation such as, $y = ax + b$, are strictly valid only when[2]:

a) the random variations in the y's, for many traverses across a step, have a zero mean and a common variance;

and

b) the random variations in the y's are mutually independent in the statistical sense.

In addition for strict validity of the confidence interval estimations given in the following discussion, an additional assumption must be satisfied:

c) the random variations affecting the y's have a normal distribution.

Studies of the amplitude density function and the autocorrelation function for profiles of highly polished surfaces similar to the ones on the calibrating step specimens have been performed[3]. The results of these studies show that assumptions a and c are realized and that assumption b is approximated. Thus, while these studies do not completely justify the application of least-squares methods for fitting the step profiles and estimating confidence intervals, they do provide a basis for using a model of the surfaces which has the necessary properties required by a, b, and c.

Therefore, assume a model of the calibrating step which has no geometrical errors other than surface texture whose profile meets requirements a, b, and c. If the texture has an RMS value (≈AA value) of q, what is the 3 standard deviation of the step heights calculated when the height routines are applied to profiles obtained from such a step? Let the line $y = ax + b$ be least square fit to N data pairs (X_i, Y_i). Then the estimated variance, σ^2, of a point (x', y'), on the predicted line is given by the equation [4, 5]:

$$\sigma^2 = S_y^2 \left[\frac{1}{N} + \frac{(x' - \bar{X})^2}{\sum_{i=1}^{N} (X_i - \bar{X})^2} \right]$$

where

$$X = \frac{1}{N} \sum_{i=1}^{N} X_i$$

and S_y is the sample standard deviation of the set of Y_i about the predicted line $y = ax + b$. It is calculated from the equation:

$$S_y^2 = \frac{\sum_{i=1}^{N} (Y_i - y_i)^2}{N-2} .$$

Thus with the assumed profile properties, $S_y^2 = q^2$ and

$$\sigma^2 = q^2 \left[\frac{1}{N} + \frac{(x' - \bar{X})^2}{\sum_{i=1}^{N} (X_i - \bar{X})^2} \right]$$

The data format for the step height routines uses N=128 and X_i = (constant) i, where i is an integer, so that for a particular abcissa specified by i',

$$\sigma^2 = q^2 \left[\frac{1}{N} + \frac{(i' - 64)^2}{\sum_{i=1}^{N} (i - 64)^2} \right] .$$

The position of the point used for step height calculations may vary over a range such that; $64 < |i'-64| < 192$, depending on where the operator chooses A1 and A2. A typical value for $|i'-64|$ is 100.

Substituting this value and evaluating the summation gives the result:

$$\sigma^2 = q^2 \,(0.0650)$$

or:

$$\sigma = 0.255\, q.$$

If one assumes that the fits to the two sides of the steps are uncorrelated, a 3 standard deviation uncertainty, 3σ, for the calculated step height is therefore:

$$3\sigma = 3\sqrt{\sigma_L^2 + \sigma_R^2} = 1.08q.$$

Two other random error components are produced by the system electrical and mechanical noise and by the quantization error resulting from digitizing the step profile. Measurements of the first of these gave an estimated value of $q_N = 6$ nm (see appendix J). The quantization error gives rise to an equivalent RMS error of [6];

$$q_Q = 0.29 \, \frac{\text{Full Scale Range}}{\text{Number of quantized intervals}} = 0.29 \, \frac{50\text{mm/Magnification}}{4096}$$

For a magnification of 1000, the quantization thus produces an RMS error of 3.2 nm. These three random error components are uncorrelated so that a net RMS error q_o is:

$$q_o = (q^2 + q_N^2 + q_Q^2)^{\frac{1}{2}} .$$

Assuming $q = 12$ nm and a magnification of 1000, $q_o = 14$ nm. For higher magnifications the quantization error becomes insignificant and q_o drops to 13 nm, with $q = 12$ nm. An experimental study of the random error of calculated step heights for a 12.7-µm step with a surface finish of 12-nm AA and a 0.51 µm step with a surface finish of 6-nm AA is described in appendix K. The results are in good agreement with the analytical calculations given here.

Surface finish of calibrating step artifacts is typically 6-12-nm AA. Profiles of the calibrating step often contain the cross section of discrete scratches or dust particles which greatly increases the uncertainty of transferring the step height. Step profiles are carefully examined before being used for calibration, but small discrete imperfections probably escape detection. A conservative value of the calibration step's surface finish of 25-nm AA is therefore used for estimating the system's systematic error.

2.3 EFFECTS OF STYLUS-TRANSDUCER AND INTERFACE HARDWARE NON-LINEARITIES ON ARITHMETIC AVERAGE AND STEP HEIGHT MEASUREMENTS

To consider the effects on roughness, let the overall nonlinearity of the signal path from the transducer to the computer memory be described by the equation;

$$V(y) = by + cy^2, \tag{3}$$

where V is the number stored in memory for a tip displacement y. Then the AA calculated from V, exclusive of digital data acquisition effects, may be related to the AA of the profile y(x) by means of the amplitude density function, ADF (section 3.2). Given the ADF of a profile y(x), the profile's AA may be calculated from the equation:

$$AA_{y(x)} = \int_{-\infty}^{+\infty} |y| \, ADF(y) \, dy. \tag{4}$$

Similarly the AA of V(x) is given by:

$$AA_{V(x)} = \int_{-\infty}^{+\infty} |V| \, ADF(V) \, dv. \tag{5}$$

Expanding equation 5 in terms of y requires a relation between ADF(V) and ADF(y). With the assumed quadratic relationship between V and y one may show that [7]:

$$ADF(V) = \frac{ADF(y)}{b + 2cy} \; . \tag{6}$$

Substituting equations (6) and (3) into equation (5) then yields:

$$AA_{V(x)} = \int_{-\infty}^{+\infty} |by + cy^2| ADF(y) \, dy.$$

Since:

$$|b||y| - |c|y^2 < |by + cy^2| \leq |b||y| + |c|y^2,$$

the fractional error, e_{LQ}, between the AA value measured with a linear system, AA_L, and that measured with a quadratic system, AA_Q, is:

$$e_{LQ} = \frac{AA_L - AA_Q}{AA_L} = \frac{b_L - b_Q}{b_L} \pm \frac{|c|}{b_L \; AA_y} \int_{-\infty}^{+\infty} y^2 \, ADF(y) \, dy.$$

The integral in the last term of this equation is the mean square value, MS, of the profile. For most profiles the MS/AA ratio is less than 4AA; for a profile with a Gaussian ADF the ratio is 1.57 AA. Thus a maximum expected normalized error is:

$$e_{LQ} = \frac{b_L - b_Q}{b_L} \pm 4 \frac{|c|}{b_L} AA_y .$$

Using the measured values for b_L, b_Q, and c for the transducer which are given in appendix L, the maximum value for each term for AA values less than 10 μm is:

$$e_{LQ} = 0.0027 \pm 0.0018.$$

For the interface hardware both terms are less than 0.001.

In relating these nonlinearities to the increase in random error resulting from sample repositioning in the long term stability study, the best association of the error is with a $\pm$ 3 standard deviation limit equal to the maximum value of e_{LQ}. This association, in-stead of considering the component as a known bias error, follows since the coefficient's uncertainties are comparable with the difference, b_L-b_Q, and with the coefficient c. If the nonlinearity uncertainties from the transducer and interface hardware are simply added, the expected error in AA measurements due to the system nonlinearities analyzed thus far is about 0.6% while the difference in random error due to repositioning was 0.7 to 1.0%. The remainder of the random error may be attributed to nonlinearities in the analog-to-digital conversion process. These nonlinearities probably were not characterized by the simple quadratic relationship assumed in the analysis given here because of their random nature.

The effects of system nonlinearities on step height measurements may be analyzed by again assuming the relationship given in equation 3. Then, if the profile mean values for each side of the step are respectively y_1 and y_2, the fractional error, S_{LQ}, between the value calculated with a linear system and with a quadratic system is:

$$S_{LQ} = \frac{b_L - L_Q}{b_L} - \frac{c}{b_L} (y_2 + y_1).$$

Using the measured values for b_L, b_Q and c given in appendix L:

$$S_{LQ} = 0.0027 - 4.6 \times 10^{-5}\ \mu m^{-1} (y_2 + y_1).$$

Since y_2 and y_1 may be of either sign, S_{LQ} may range from 0.38% to 0.15% of the linear values when a typical step height of one half full scale is used on the Talysurf's 1000 magnification. For the same reason given in the roughness considerations, the maximum value of S_{LQ} should again be taken to estimate a $\pm$ 3 standard deviation limit for the uncertainty in step height generated by transducer nonlinearity. Adding the nonlinearity of the interface hardware then gives a $\pm$ 0.5% uncertainty in the step height measurements due to these nonlinearities.

The arguments then confirm that for these two measurements the system nonlinearity as defined in appendix L and the uncertainties generated from the nonlinearity are approximately equal.

2.4 UNCERTAINTIES IN ARITHMETIC AVERAGE MEASUREMENT DUE TO DATA ACQUISITION PROCESSES

Three aspects of the data acquisition process which produce uncertainties in the roughness measurements are:

1. record lingth is finite,
2. data are sampled,

and

3. data are digitized to a finite precision.

The arithmetic average value will change in magnitude from record to record when it is calculated from a finite record length of profiles with a random shape or when it is calculated from a periodic profile which is randomly phased with respect to the finite record. Arguments are given in appendix M to show that the 3 standard deviation limit expected from AA measurements of precision roughness specimens with the standard 3.8 mm record length will be:

0.05 to 0.3% of the mean AA value for the 0.5-μm (20-μin) patch,

and

0.3% of the mean AA value for the 3.17-μm (125-μin) patch.

How accurately does the sampled sequence $\{y_i\}$ represent the continuous profile y(t)? The sampling theorem [8] states that for physically realizable profiles with a power spectral density equal to zero for frequencies greater than B, the use of sampling intervals $\Delta t<1/2B$ enables one to reconstruct the continuous function y(x) uniquely. The bandpass of the NBS system (appendix A) extends to 300 Hz as the -3db point for a 12dB/octave attenuation filter for all higher frequencies. The sampling interval for roughness measurements is 610 μs (length equivalent is 0.93 μm) or 1640 Hz. At $B = 1/2\Delta t$ = 820 Hz the system electronics has a transmission factor of approximately 0.09. Thus, the possibility exists that up to 9% of the power of frequency components > 820 Hz will be aliased into the AA value measured. The only frequency components > 820 Hz which will likely be present are electrical noise frequencies since the sampling rate already gives 3 to 4 points across the stylus tip radius of 3.4 μm. Any effect from the power folded back into the measured frequency range would be accounted for in the usual system noise check. As discussed in section 2.0 to total, true plus any possible aliasing, is negligible for AA values greater than 100 nm.

The accuracy with which the sequence $\{y_i\}$ represents $y(t)$ is also dependent on how closely the sampling process approaches a Dirac-delta function sampling process. The error produced by obtaining a discrete value for the signal by averaging for a finite time is known as aperture error. It is minimized by making the aperture or averaging time small with respect to the sampling interval. In the present NBS system aperture time is 50 μs while the sampling interval is 610 μs.

The digitization of each sampled datum point to a finite precision produces an equivalent RMS noise of 0.29 scale unit. (Section 2.2) With the 12 bit analog to digital conversion used in the NBS system this aspect of the data acquisition process only produces 3.2 nm RMS or AA on the Talysurf's 1000 magnification and decreases proportionally with increasing magnification.

2.5 SYSTEM SHORT TERM STABILITY

The time between step-calibration of the NBS system and the completion of 3 traverses at each of 10 positions is less than 30 minutes. Thus, short term relative to the NBS system implys times of this magnitude.

During early checks of the system, repetitive step height measurements showed that irregular changes of 5 to 10% in the overall gain of the system took place during the first one to two hours after turning the system on at the beginning of a workday. After this period of "warmup" the system remained stable. Confirmation of this stability is given in the step height measurements reported in appendix K. Each step height measurement requires approximately 1 minute, so the measurements given in the appendix cover the 30 minutes required to investigate the system's short term stability. No overall or random change in system gain is observable in the data. However, any effect from the short term variations in system gain would be included in the experimental confirmations of the uncertainty produced by the calibrating step's surface finish. Since reasonable agreement was obtained between the analytical and experimental effects of surface finish, the effect must have been negligible.

All calibrations are now performed only after a two hour system warmup or after the system has remained "on" overnight.

2.6 SUMMARY OF THE SYSTEM UNCERTAINTY BUDGET FOR ROUGHNESS CALIBRATIONS

The motivation for the error analysis given in sections 2.0 through 2.5 was threefold:

1. to firmly establish experimentally the overall system uncertainty for calibrations at the most commonly used roughness values;

2. to extend the range of known uncertainties so that it covers in a continuous form the operating bounds of the system (the extension was based on the empirical and analytical studies described in these sections).

3. to analyze the system's uncertainty so that major components could be reduced in future system improvements.

A comparison of the analytical and experimental values for the various uncertainty components of the calibration procedure for 0.5 μm and 3.17 μm precision roughness specimens is given in tables 1 and 2. The computational accuracies were computed as ± one bit out of 12 bits or 1/4096 for step height measurements and ∓ the quantization error for roughness measurements. The differences between the RMS-sum of the components of $3\sigma_B$ and the value measured in the three-month study is 0.005 and 0.002 for the 0.5 μm and the 3.17 μm AA measurements, respectively. Due to the existence of this difference the uncertainty assigned to nonlinearities, computations and other parts not taken into account is ± 1%. As stated in section 2.0 the net random uncertainty is assigned a value based on this 1% and the other experimental values from the three-month study. The sources of the remaining 0.7% random uncertainty are unknown. A study of the system's transient response was made in search of an explanation for this remainder, (see appendix H). No significant source of uncertainty was revealed by the investigation.

2.7 COMPARISON OF THE AA VALUES MEASURED RELATIVE TO THE NBS-1 MASTER ARTIFACT WITH THOSE MEASURED WITH THE STEP-CALIBRATED MINICOMPUTER SYSTEM.

To insure that a smooth transition between these two measurement processes was made, five different type surfaces with roughness values covering the instrument's range and the two roughness areas of the NBS-1 master artifact were measured with both processes. Figures 10 and 11 give profiles of the specimens used for the study. Table 3 summarizes the results of the measurements.

The procedure for the study was to:

1. measure each of the specimens and record the values read from the roughness meter,

2. correct each of these roughness readings by the same fraction needed to bring the NBS-1 values to those established by planimetry and round-robin measurements,

3. calibrate the computerized system with an interferometrically measured step,

4. remeasure each specimen and record roughness values printed by the teletype.

TABLE 1: UNCERTAINTY BUDGET FOR MEASUREMENTS OF THE 0.5 μm (20 μin) PRECISION ROUGHNESS SPECIMEN

	UNCERTAINTY COMPONENT (e_i)	ANALYTICAL OR EXPERIMENTALLY BASED ANALYTICAL VALUES*		EXPERIMENTAL LONG-TERM STABILITY STUDY*	
		Systematic	Random	Systematic	Random
STEP CALIBRATION OF SYSTEM	Interferometric Measurement of Step Height	25 nm/step height = 0.013			
	Surface Finish of Calibrating Step		1.1 x 25 nm/ Step height = 0.014		
	Nonlinearities of LVDT and Interface Hardware		0.006		Normalized $3\sigma_B = 0.02$ includes these three components
	Computation		Total is < 0.001		
ROUGHNESS MEASUREMENTS	Uncertainty in Stylus Tip Radius	5 nm/500 nm = 0.01			
	Finite Record Length		0.0005 to 0.003		Normalized $3\sigma_W = 0.004$ includes these two components
	Computation		Total is < 0.0005		
	Nonlinearities of LVDT and Interface Hardware		0.006		Normalized $3\sigma = 0.014$ includes these components
Totals = $\sqrt{\Sigma e_i^2}$		0.0164	0.0167	0.00	0.0244

*computed three standard deviations

TABLE 2: UNCERTAINTY BUDGET FOR MEASUREMENTS OF THE 3.17 μm (125 μin) PRECISION ROUGHNESS SPECIMEN

	UNCERTAINTY COMPONENT (e_i)	ANALYTICAL OR EXPERIMENTALLY BASED ANALYTICAL VALUE*		EXPERIMENTAL LONG-TERM STABILITY STUDY*	
		Systematic	Random	Systematic	Random
STEP CALIBRATION	Interferometric Measurement of Step Height	25 nm/step height = 0.0013			
	Surface Finish of Calibrating Step		1.1 x 25 nm/step height = 0.0014		
	Nonlinearities of LVDT and Interface Hardware		0.006		Normalized $3\sigma_B = 0.0084$ includes these three components
	Computation		Total is < 0.001		
ROUGHNESS MEASUREMENTS	Uncertainty in Stylus Tip Radius	5 nm/3175 nm = 0.0015			
	Finite Record Length		0.003		Normalized $3\sigma_W = 0.008$ includes these two components
	Computation		0.001		
	Nonlinearities of LVDT and Interface Hardware		0.006		Normalized $3\sigma = 0.014$ includes these three components
Totals = $\sqrt{\Sigma e_i^2}$		0.0020	0.0092	0.00	0.016

*Computed three standard deviations

	Roughness Meter Reading				Value Corrected to NBS-1				Step-Calibration Value			
	Mean		3s*		Mean		3s*		Mean		3s*	
	μin	μm	μin	μm	μin	μm	μin	μm	μin	μm	μin	μm
NBS-1, 125μin Area	117.1	2.974	2.7	0.068	120.8	3.068	2.0	0.051	121.2	3.078	3.6	0.091
Milled Surface	86	2.18	33	0.83	89	2.25	34	0.86	84	2.13	37	0.93
Specimen A	51.3	1.303	2.9	0.074	52.9	1.344	3.0	0.076	56.8	1.443	2.5	0.033
NBS-1, 20μin Area	19.50	0.495	0.45	0.011	20.34	0.517	0.93	0.024	19.97	0.507	0.54	0.014
Specimen B	18.3	0.465	2.7	0.069	19.1	0.485	2.8	0.072	18.6	0.472	2.4	0.061
Ground Glass	16.2	0.41	6.3	0.16	16.9	0.43	6.6	0.17	20.5	0.52	8.0	0.20
Ground Metal	5.8	0.147	3.3	0.083	6.1	0.153	3.4	0.86	6.0	0.152	2.4	0.061

Table 3. Comparison of AA Values Obtained From Roughness Meter Corrected to NBS-1 With Values Obtained With the Step-Calibrated Stylus/Computer System.

*s^2 is the sample estimate of variance defined by the equation:

$$s^2 \equiv \frac{1}{n-1} \sum_{i=1}^{n} (X_i - \overline{X})^2$$

for n sample values, X_i with a sample mean $\overline{X} \equiv \frac{1}{n} \sum_{i=1}^{n} X_i$

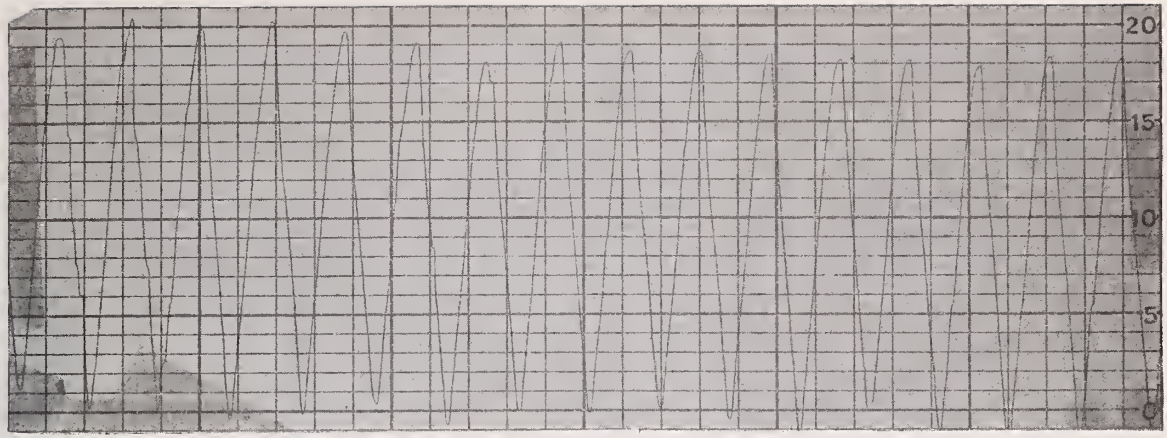

Figure 10a. NBS-1, 125 μin Patch; Vertical Magnification = 5,000

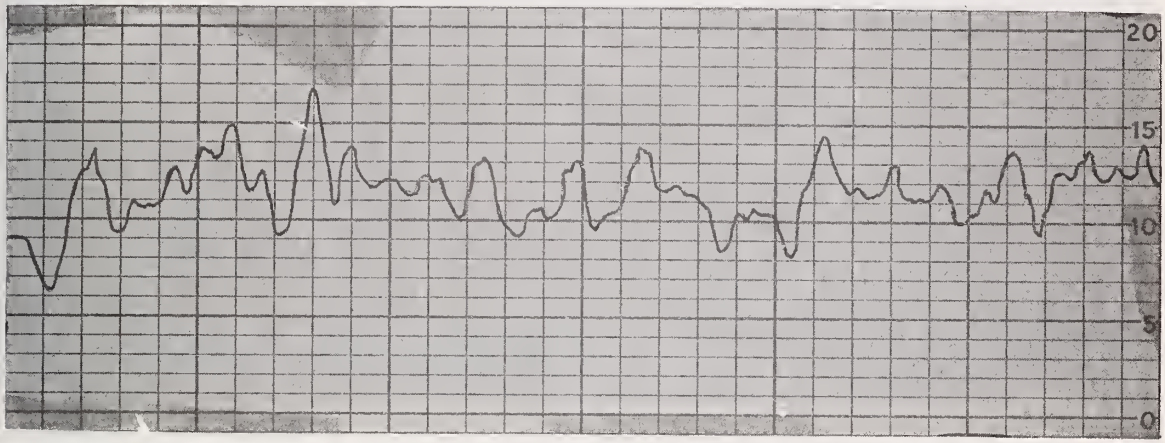

Figure 10b. Milled Surface; Vertical Magnification = 2,000

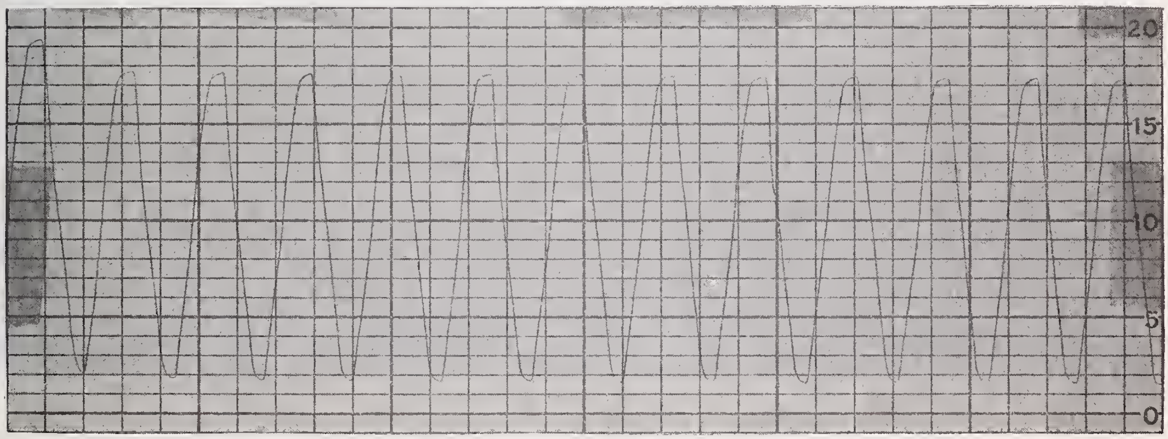

Figure 10c. Specimen A; Vertical Magnification = 10,000

Figure 10. Profiles of Specimens Used for Comparing Old and New Calibration Procedures. All Profiles are at a Horizontal Magnification = 100.

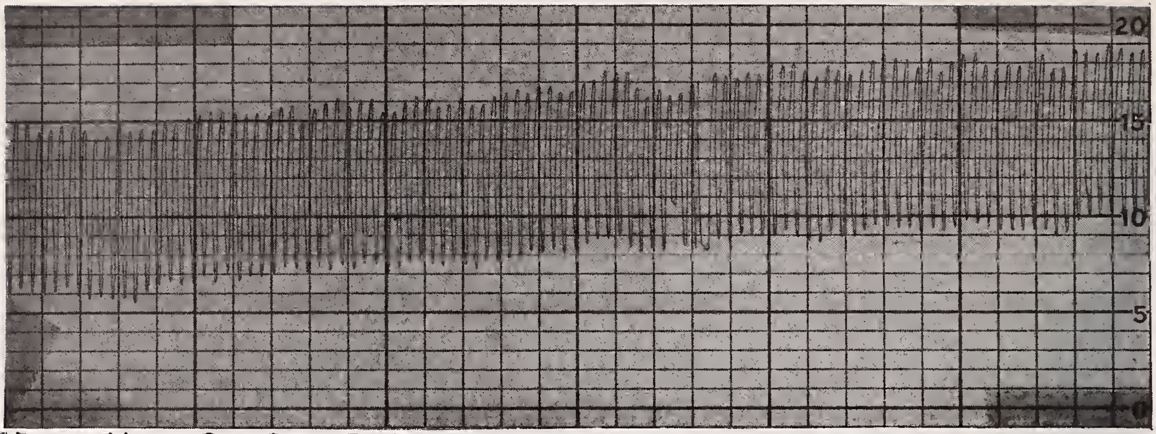

Figure 11a. Specimen B; Vertical Magnification = 20,000

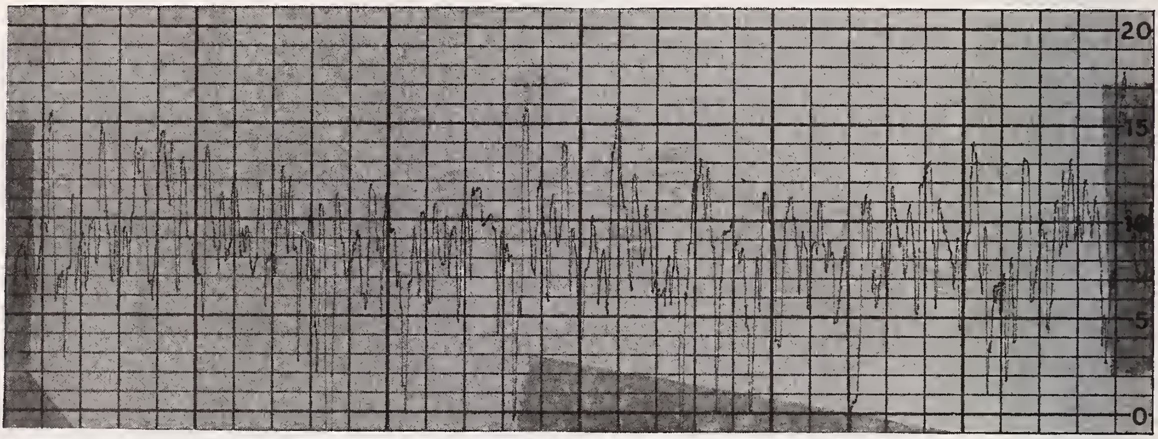

Figure 11b. Ground Glass; Vertical Magnification = 20,000

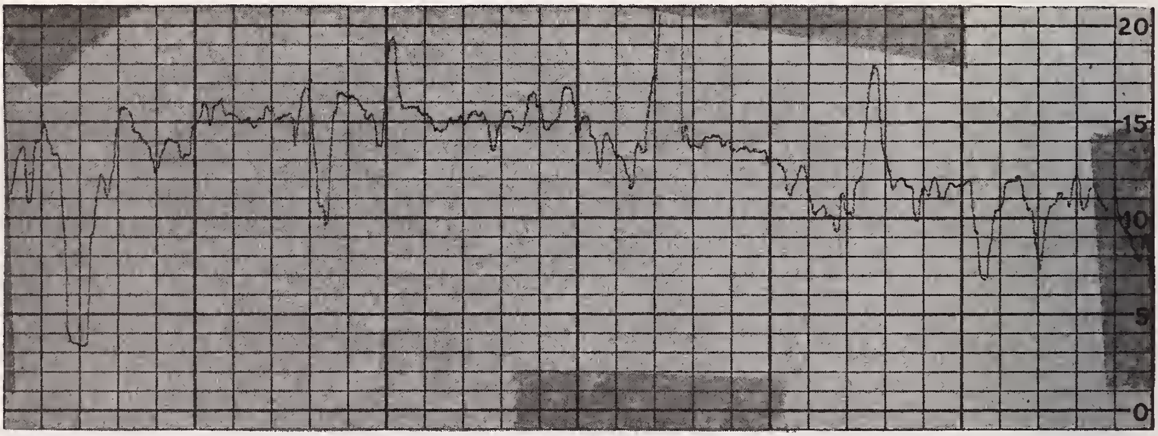

Figure 11c. Ground Metal; Vertical Magnification = 20,000

Figure 11. Profile of Specimens Used for Comparing Old and New Calibration Procedures. All Profiles are at a Horizontal Magnification = 100.

Only the two magnifications of the stylus instrument on which the two areas of NBS-1 could be conveniently measured were used for the measurements. The mean and 3s values were calculated according to the definitions given on page 32 from the data obtained in 3 traverses at each of 5 or more positions on each specimen.

Let R_i and δ_i represent the mean roughness value and the 3s limit respectively for the measurements on the i^{th} specimen. Then a statistically significant difference between the two measurement procedures is present only when:

$$R_i^A - R_i^C > \sqrt{(\delta_i^A)^2 + (\delta_i^C)^2}$$

where the superscripts A and C represent the artifact and computerized procedures respectively. This relation is not true for any of the data given in table 3. The relatively uniform specimens A and B impose the tightest constraints on the comparison between the two procedures.

Therefore, this study confirms that there is no significant difference between the roughness values obtained by the two measurement processes.

3.0 FURTHER UTILIZATION AND APPLICATION OF THE COMPUTERIZED ROUGHNESS MEASUREMENT SYSTEM

The capabilities of the minicomputer have facilitated the on-line implementation of many new statistical methods of characterizing surface topography. The following sections give a brief summary of the definitions and properties of the statistical parameters and functions which may be calculated on the NBS system or those for which off-line calculational capabilities have been developed. The reader should consult recent textbooks on statistical functions [5,9] or conference proceedings [10,11] for a more complete understanding of the new characterizations.

In addition to the AA value, the NBS system has the capability to calculate on line the average slope and average wavelength, the amplitude density function (ADF) and the autocorrelation function (ACF). Numerical results may be displayed at the teletype or in graphical form on a strip-chart recorder (for the functions). A by-product of the ACF calculation is the calculation of the profile's mean square value. A punched paper tape containing the ACF and ADF values may be punched from data stored in the minicomputer during their calculation. The ADF and ACF data may then be transfered to a larger computer to calculate the skewness and kurtosis of the profile from the ADF and the power spectral density from the ACF.

Because all these characterizations are readily calculated after a specimen profile has been stored in the minicomputer memory, they are available upon request as a standard test service.

3.1 MEAN SLOPE AND AVERAGE WAVELENGTH

Calculation of the mean slope and average wavelength of a profile is readily performed with routines from the AA calculations once the following observations have been made. Consider the profile as being represented in the computer memory by the equation:

$$y_n = f(n) \qquad n = 1,2,---,N.$$

Then as demonstrated in appendix B, the AA value of the profile is calculated by using the equations:

$$\bar{y} = \frac{1}{N} \sum_{1}^{N} f(n)$$

and

$$AA = \frac{1}{N} \sum_{1}^{N} |y_n - \bar{y}|$$

If now one calculates the differences,

$$\Delta y_n = f(n) - f(n-1),$$

stores the differences as a new "profile," and then performs the same AA calculation on the new profile, the result:

$$\text{AA of profile differences} = \frac{1}{N-1} \sum_{2}^{N} |\Delta y_n - \overline{\Delta y_n}|,$$

is obtained. Thus, if $\overline{\Delta y_n} = 0$ it follows that:

AA of profile differences = mean absolute differences,

$$\text{since mean absolute differences} = \frac{1}{N-1} \sum_{2}^{N} |\Delta y_n|.$$

This condition is very closely satisfied. Consider the y_n now as the original profile function, $y(n)$, where n is a multiple of the sample spacing along the profile. Then the following relations hold:

$$\overline{\Delta y_n} = \frac{1}{N-1} \int_{2}^{N} \frac{dy(n')}{dn'} \, dn'$$

$$= \frac{1}{N-1} \left[y(N) - y(2) \right].$$

The latter equation results from the fundamental theorem of integral calculus. Thus a worst case value for $\overline{\Delta y_n}$ would be:

$$\frac{1}{3.8\text{mm}} \left(2 \times \frac{2.54\text{cm}}{500}\right) = 0.0267,$$

which would occur using the lowest magnification of the stylus instrument. More commonly used magnifications are 2000 or greater such that worst case errors would be 0.0066 or less, which correspond to angular slopes of 0.38 degrees or less.

The mean slope program given in the listings therefore utilizes the AA routines as explained. The problem of having one less difference point than profile data points is solved by taking N+1 profile data points into the computer memory. Thus, profile data is stored from memory addresses 1000 through 3000, while the AA calculation uses only addresses 1002 through 3000.

A conservative range for the differences is taken as twice the profile data range, i.e., the profile data points; -X, +X, -X; give differences; 2X, -2X. The difference range of the profile data however is ultimately determined by the stylus tip shape and the sample spacing. The NBS stylus/computer system employs a 90° pyramidal tip with a radius of ∿3.4 μm and a sample spacing of ∿1 μm. Thus, profiles with peak to valley heights >4 μm would produce maximum data differences of approximately 1/3 the profile range. Profiles with peak to valley heights <4 μm produce data differences up to 1.25 of the profile range at a gain of 100,000. Both of these estimates may be obtained by considering the profiles produced as the stylus is traversed across a sharp edge with a height chosen to give an on scale trace.

The AA of the profile slope or the mean profile slope is then calculated by using the relation:

$$\text{AA of profile slope} = \frac{\text{mean absolute difference x KCAL}}{\text{mean sample spacing}}$$

The mean absolute difference is scaled to the same physical dimensions as the mean sample spacing by multiplying by KCAL and the necessary power of 10. The power of 10 is obtained from the computer memory by recalling the value entered at the teletype after the units query during step-calibration. Determination of the mean sample spacing is discussed in appendix O. Substituting the mean sample spacing, therefore, gives the final equation for the average slope:

$$\text{average slope} = \frac{\text{mean } \Delta y_n \text{ x KCAL}}{9300} \times 10^{7-p}$$

where p is power of ten entered for the calibrating step and the mean sample spacing is 9300×10^{-7} mm.

Spragg and Whitehouse [12] have shown that, for most profiles encountered in practice, the average wavelength of a profile may be calculated from the equation:

$$\text{average wavelength} = \lambda_{AA} = 2\pi \frac{\text{AA Value}}{\text{AA of profile slope.}}$$

The mean slope program also calculates and prints out at the teletype the value of this parameter. It is important to notice that the average wavelength is independent of KCAL and that it is a direct function of the sample spacing used for digitizing the profile. This point is demonstrated by the following equations:

$$\lambda_{AA} = 2\pi \times \frac{\text{AA} \quad \times \text{KCAL} \times 10^{-p}}{\left(\dfrac{\text{AA slope} \quad \times \text{KCAL} \times 10^{-p}}{9300 \times 10^{-7}\ \text{mm}}\right)}$$

$$= 2\pi \times \frac{\text{AA}}{\text{AA slope}} \times 93.0 \times 10^{-5}\ \text{mm}$$

The listing and flowchart of the mean slope program is given in appendix B.

3.2 AMPLITUDE DENSITY FUNCTION, SKEWNESS AND KURTOSIS

A functional characterization of the amplitude properties of a waveform or profile in a detailed statistical manner is given by the probability or amplitude density function, ADF, Figure 12. Numerically the ADF is defined as the probability that at a given ordinate value, the profile amplitude is within an interval Δy in a record length L. The probability is calculated using elementary geometrical ideas and is effectively a histogram of the profile as a function of the chosen interval's mean ordinate. The ADF is usually specified as a decimal fraction per unit interval length as a function of the interval's mean ordinate. Before computers, its calculation was very tedious, but the necessary bookkeeping procedures are very fast and efficient for a computer to perform.

Calculation of the ADF, as one may imply from the definition and the flowchart in appendix B, primarily involves sorting the profile data into the respective ordinate intervals. The present calculation employs 512 ordinate intervals each with a "width" of 8 units. The calculations performed by a computer to obtain the ADF are simpler and fewer in number than those in an AA computation. For a 512 interval ADF and 4000 profile data points only about 60,000 operations are needed. The AA calculation involves approximately twice this number of operations and double precision arithmetic to avoid overflow during summations. Computation time with the present minicomputer is 6 seconds but with recent generation minicomputers this time could be reduced to 0.1 second.

A slight alteration of the software for the ADF calculation enables the user to perform signal averaging on the ADFs obtained from one or a group of positions on a specimen surface.

Many of the traditionally used parameters are measures of the size of the ADF and may be easily obtained from it as various averages of the ordinate weighted by the ADF. Some examples are:

$$AA = \int_{-\infty}^{+\infty} |y| \, ADF(y) \, dy,$$

$$(RMS)^2 = \int_{-\infty}^{+\infty} y^2 \, ADF(y) \, dy.$$

In addition to these size dependent parameters several new parameters have been introduced which are measures of the ADF's shape. The skewness of the ADF is a measure of the symmetry of the profile about its mean, (figure 13). Skewness offers a convenient way to differentiate between the load carrying capacities of various surfaces. As one may conclude from the examples in figure 13, positively skewed surfaces are more suitable to carry loads than negatively skewed surfaces. A second shape dependent parameter the kurtosis, figure 14, is a measure of the amplitude density function's sharpness or the profiles fourth moment. In addition to characterizing this aspect of a profile, it has utility in quantitatively describing the randomness of a profile's shape relative to that of a perfectly random surface which has a kurtosis of 3. Skewness and kurtosis are calculated directly from the definitions given in the figures. The RMS is calculated from the ADF according to the relation given above.

3.3 AUTOCORRELATION FUNCTION, MEAN SQUARE VALUE AND POWER SPECTRAL DENSITY FUNCTION

The fundamental statistical function which characterizes the wavelength properties of a profile is the autocorrelation function, ACF. The ACF is a quantitative measure of the similarity between a laterally shifted and an unshifted version of the profile. Assuming the profile is specified by N ordinates Y_i, the ACF is defined by the

AMPLITUDE DENSITY FUNCTION

$$\text{AMPLITUDE PROB } (y) \equiv P[y, y + \Delta y] = \frac{\Sigma_i \Delta \ell_i}{L}$$

$$\text{AMPLITUDE DENSITY} \equiv p(y) = \frac{P(y, y + \Delta y)}{\Delta y}$$

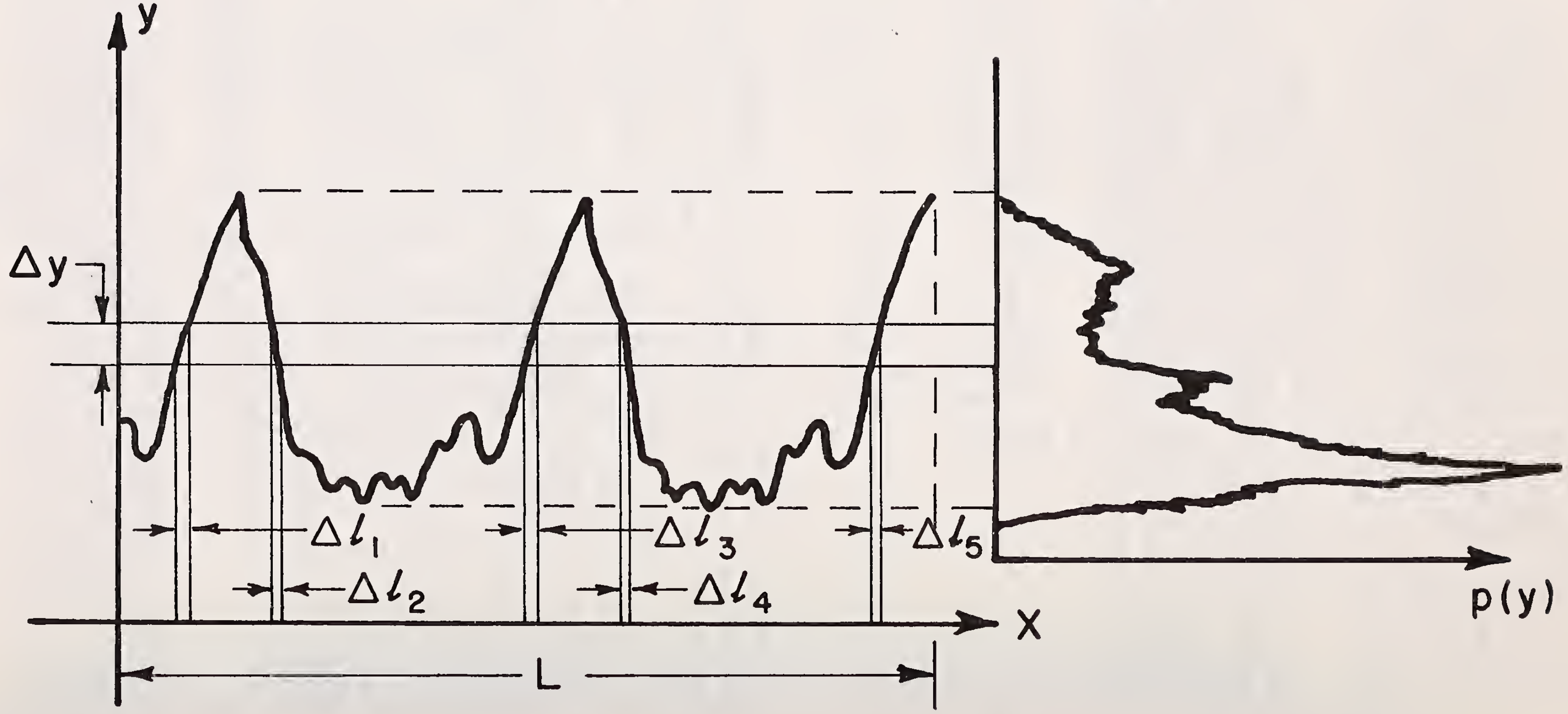

Figure 12

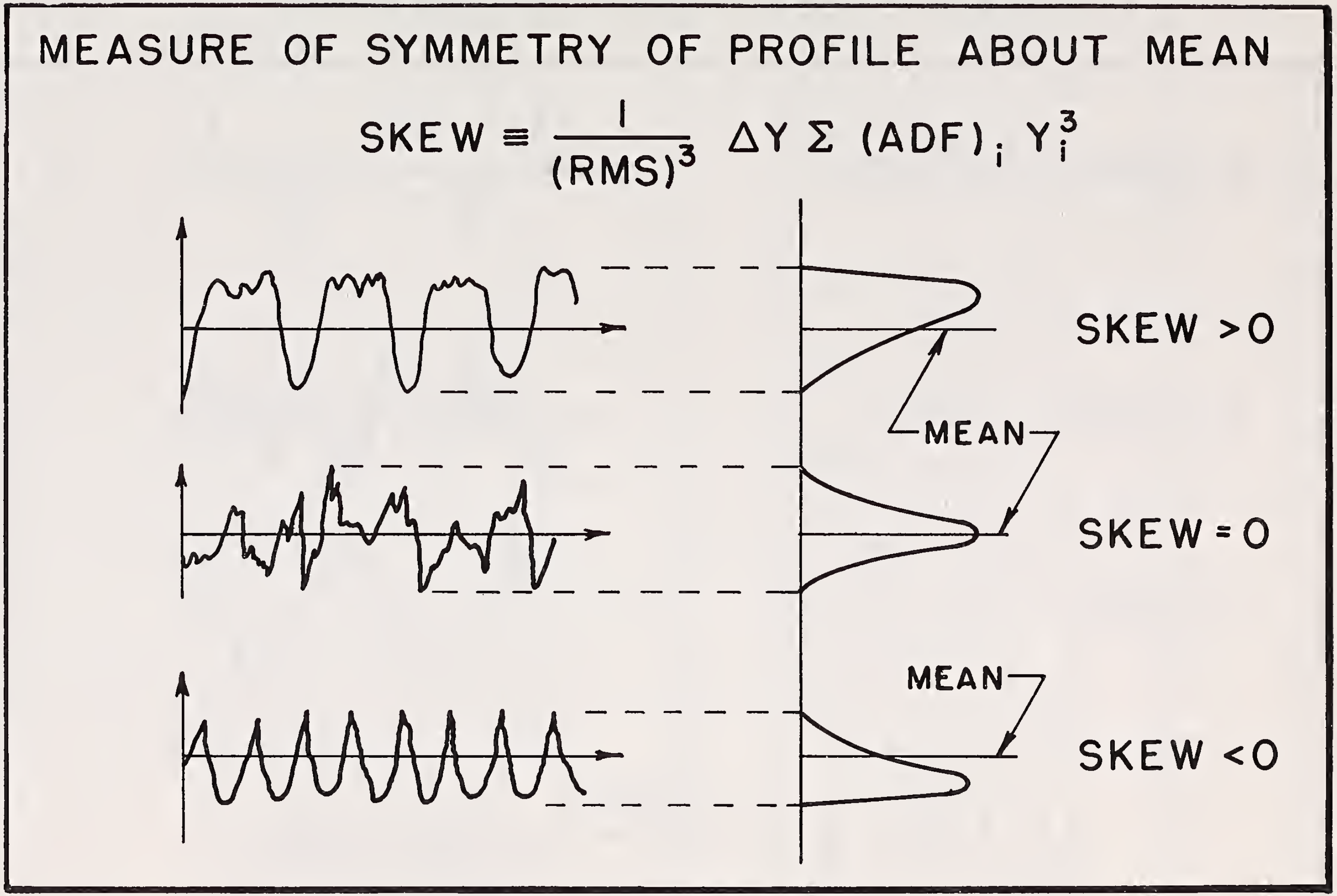
MEASURE OF SYMMETRY OF PROFILE ABOUT MEAN
$$SKEW \equiv \frac{1}{(RMS)^3} \Delta Y \Sigma (ADF)_i \, Y_i^3$$
MEAN
MEAN
SKEW >0
SKEW = 0
SKEW <0

Figure 13

MEASURE OF SHARPNESS OF ADF

$$\text{KURTOSIS} \equiv \frac{1}{(\text{RMS})^4} \, \Delta Y \sum_{1}^{N} (\text{ADF})_i \, Y_i^4$$

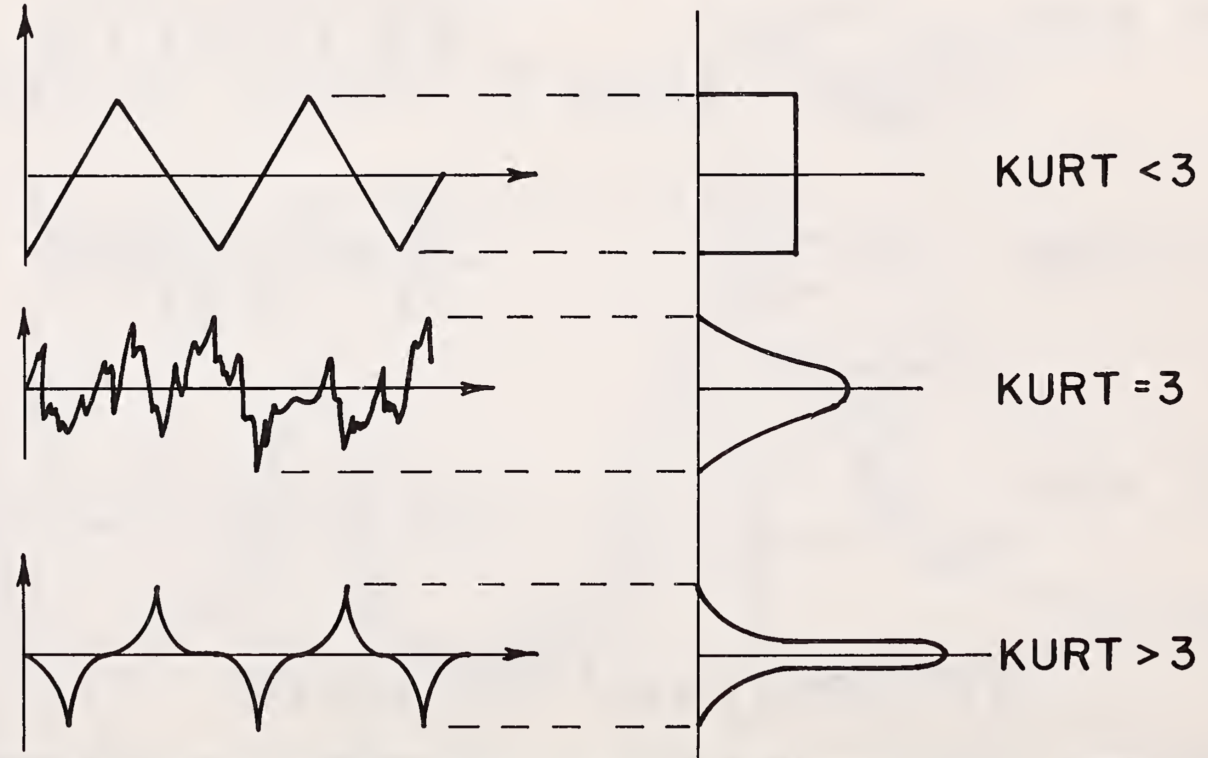

equation:

$$ACF(s) = \frac{1}{N-S} \sum_{i=1}^{N-S} Y_i \, Y_{i+S}.$$

Thus for a particular shift its value is obtained by multiplying the shifted and unshifted waveforms, over the overlapping length, ordinate by ordinate, then calculating the average product.

The ACF contains information about the characteristic lengths, short and long range, which describe a profile. The characteristic long range parameter is known as the correlation length; it is usually defined as the distance a profile must be shifted for the ACF or its envelope to drop to 10% of the zero shift value. Two points on the profile which are separated by more than a correlation length may be considered as uncorrelated or independent, i.e., portions of the surface represented by these points were produced by separate surface forming processes. Correlation lengths possible with a variety of waveforms may range from the infinite correlation length of a perfectly periodic waveform to zero for a completely random waveform.

If the profile has any periodic behavior the ACF will exhibit a periodicity with a wavelength equal to the mean wavelength present in the profile. The wavelength of the short range periodicity of the ACF is known as the correlation period.

The computations involved in the ACF calculation, are only slightly more complex than those for the AA calculation. However, since about 4000 multiplications are required for each shift, a total of 512 shifts results in at least 2×10^6 operations. The actual number is approximately 10^7 since summations, register initializations and data shifting are also involved in the computation. The number of programming instructions is smaller than the program required for the AA calculations. With the present NBS minicomputer approximately 13.5 minutes is required for an ACF calculation. The use of more recent minicomputers would reduce the time, with the same algorithm, to approximately 20 seconds. Readers who may feel that even this time is excessive will find that fast-Fourier-transform hardwired processors are available which can cut the time for an ACF calculation to less than 1 sec.

The ACF for a zero shift is:

$$ACF(o) = \frac{1}{N} \sum_{i=1}^{N} Y_i \, Y_{i+o}$$

Thus, the mean square value of the profile is easily obtained by simply taking ACF(o), converting the binary number to a decimal value and printing it at the teletype.

The power spectral density (PSD) function of a profile describes the general frequency composition of the waveform in terms of the mean square value of each component. For a narrow frequency band, Δf, about some frequency, f, the PSD(f) is defined by the equation:

$$PSD(f) = \frac{1}{\Delta f}\left[\frac{1}{L}\int_0^L y^2(x,f,\Delta f)\,dx\right]$$

Where L is the profile record length and $y^2(x,f,\Delta f)$ is the mean square value of the portion of y(x) in the frequency range from f to f + Δf. As a result of this definition, the PSD(f) is always a real valued, non-negative function and

$$(RMS)^2 = \int_0^\infty PSD(f)\,df.$$

The PSD is closely related to the autocorrelation function as expressed by the equation:

$$PSD(f) = 4\int_0^L ACF(s)\cos 2\pi fs\,ds. \qquad (7)$$

Put in mathematical terminology the PSD and the ACF are Fourier pairs, namely, one is the Fourier transform of the other. The ACF expresses the length properties of a profile while the PSD expresses the frequency properties of a profile. The PSD representation of a profile is useful when one wishes to put a machine into a process loop where a knowledge of the transfer function of the machining process is required. A normalized form of the PSD is usually given:

$$PSD_n(f) = \frac{PSD(f)}{(RMS)^2},$$

such that one obtains the PSD(f) as a fractional value plotted versus frequency in cycles/mm or cycles/μm. Equation 7 is presently employed for all PSD calculations since it only involves the transfer of 512 data points. Calculations directly from the profile would require the transfer on paper tape of 4096 points. At standard teletype punching speeds the transfer of 4096 points requires approximately 70 minutes.

3.4 APPLICATIONS

Since the development of the software for the calculation of statistical parameters and functions in January 1974, NBS has performed 10 studies involving the use of this capability. A test report which contain calculations of the ADF, average wavelength and average slope is given in appendix P.

Two other examples will be given here to demonstrate the results of employing the stylus instrument/minicomputer system's capabilities and the improved measurements provided by the statistical characterizations. The first study is an example of how more controlled surface generation may be possible by comparing the statistical characterizations of a fabricated specimen's roughness profile with those of an ideal roughness profile. This approach was used in work to evaluate how closely typical precision roughness specimens (PRS) conformed to the specifications in American National Standard B46.1. The procedure for test was to obtain a specimen profile and then to calculate its AA, mean slope, ACF, and ADF. This was followed by adjusting the simulation waveform such that its AA and frequency were the theoretical values, then to calculate the simulation waveform's ADF and ACF. Results for a typical specimen are summarized in figures 15 and 16.

Some conclusions are:

1. the dominant peak to valley heights of the PRS are 13% and 29% lower than the theoretical peak-to-valley heights of the 125 μin and 20 μin areas, respectively;

2. both areas have significant amplitude and frequency modulation of their waveforms so that the correlation lengths are less than the record length used for AA calculations, 3.8 mm (0.15 in); and

3. the mean spacing of the rulings as observed in the correlation periods is equal to the theoretical period to within the system's uncertainty.

The second study is an example of how one may gain knowledge about the relationship between part function and surface texture by experimentally taking bad, medium and good parts and then searching for correlation between one of the parameters and part quality. A summary of the measurements for three surfaces (a polished steel substrate, a cloudy nickel electroplated surface, and a bright nickel electroplated surface) is presented in figure 17. Some qualitative conclusions which may be drawn from this limited data are;

1. brighter surfaces produce longer correlation lengths and Gaussian ADFs (skewness approaches) and kurtosis approaches 3),

and

2. increasingly bright surfaces produce ADFs which, for a fixed ordinate range, approach a Dirac-delta function.

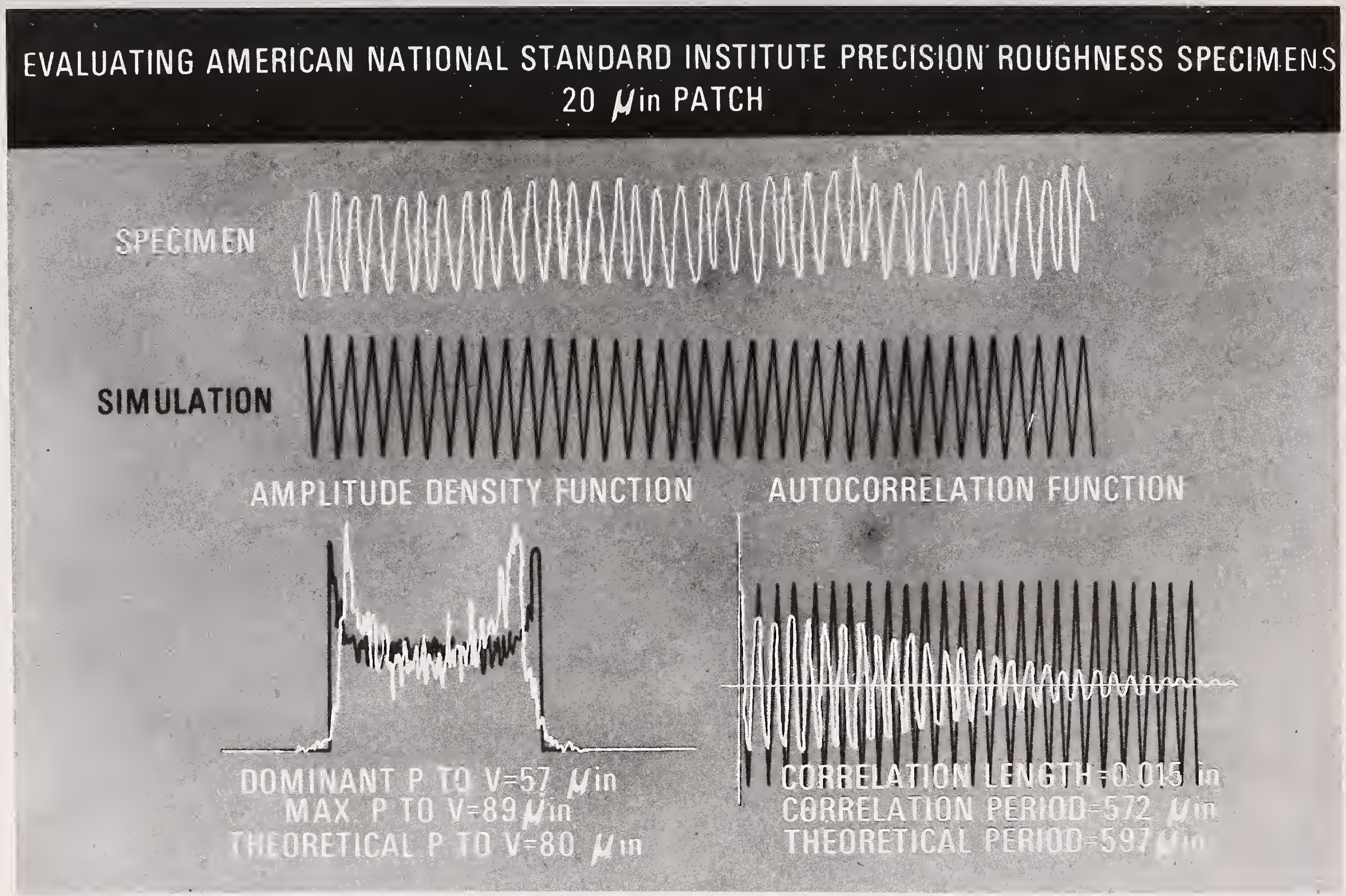
EVALUATING AMERICAN NATIONAL STANDARD INSTITUTE PRECISION ROUGHNESS SPECIMENS
20 μin PATCH
SPECIMEN
SIMULATION
AMPLITUDE DENSITY FUNCTION
AUTOCORRELATION FUNCTION
DOMINANT P TO V=57 μin
MAX. P TO V=89 μin
THEORETICAL P TO V=80 μin
CORRELATION LENGTH=0.015 in
CORRELATION PERIOD=572 μin
THEORETICAL PERIOD=597 μin

Figure 15

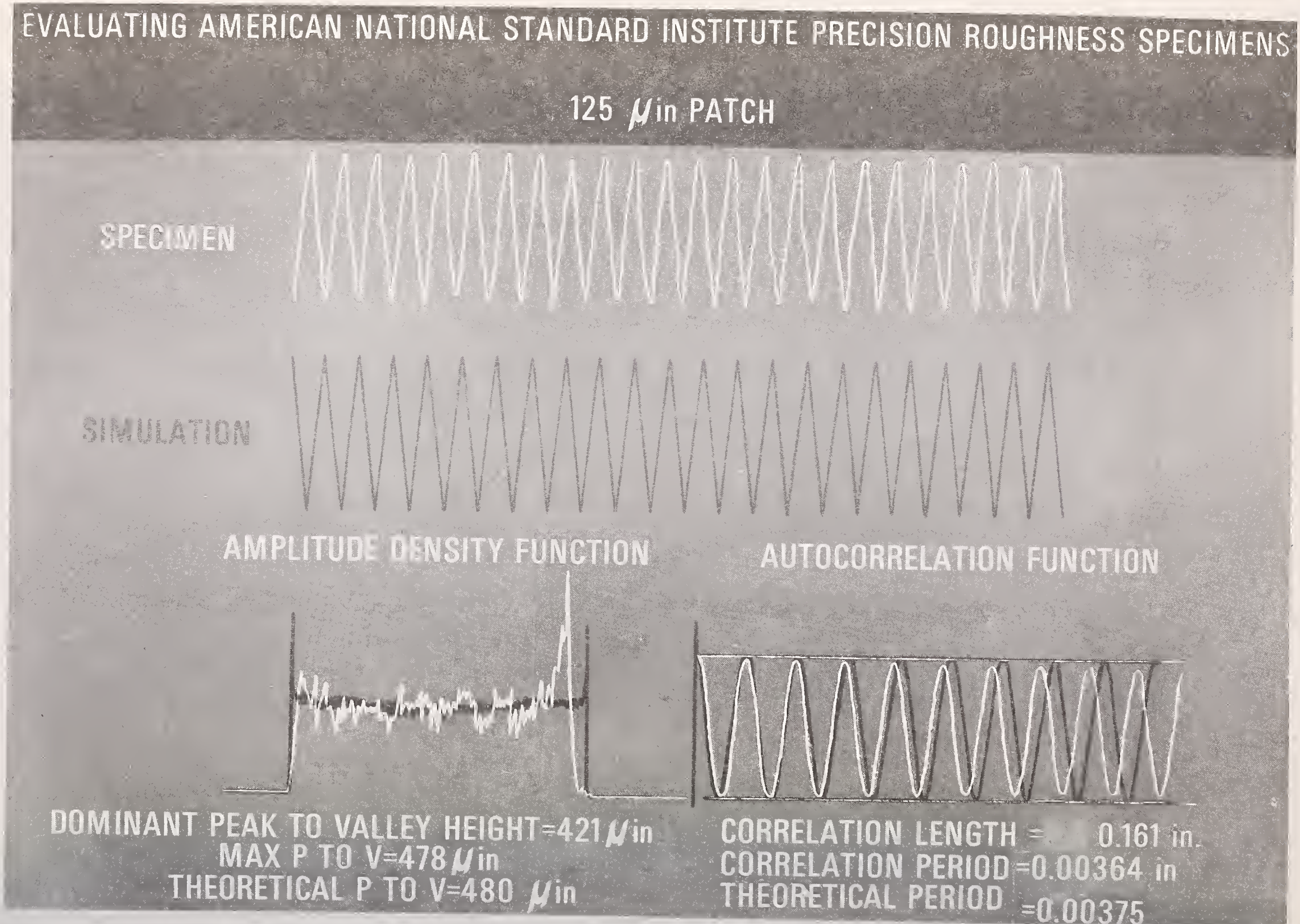
EVALUATING AMERICAN NATIONAL STANDARD INSTITUTE PRECISION ROUGHNESS SPECIMENS
125 μin PATCH
SPECIMEN
SIMULATION
AMPLITUDE DENSITY FUNCTION
AUTOCORRELATION FUNCTION
DOMINANT PEAK TO VALLEY HEIGHT=421 μin
MAX P TO V=478 μin
THEORETICAL P TO V=480 μin
CORRELATION LENGTH = 0.161 in.
CORRELATION PERIOD=0.00364 in
THEORETICAL PERIOD =0.00375

Figure 16

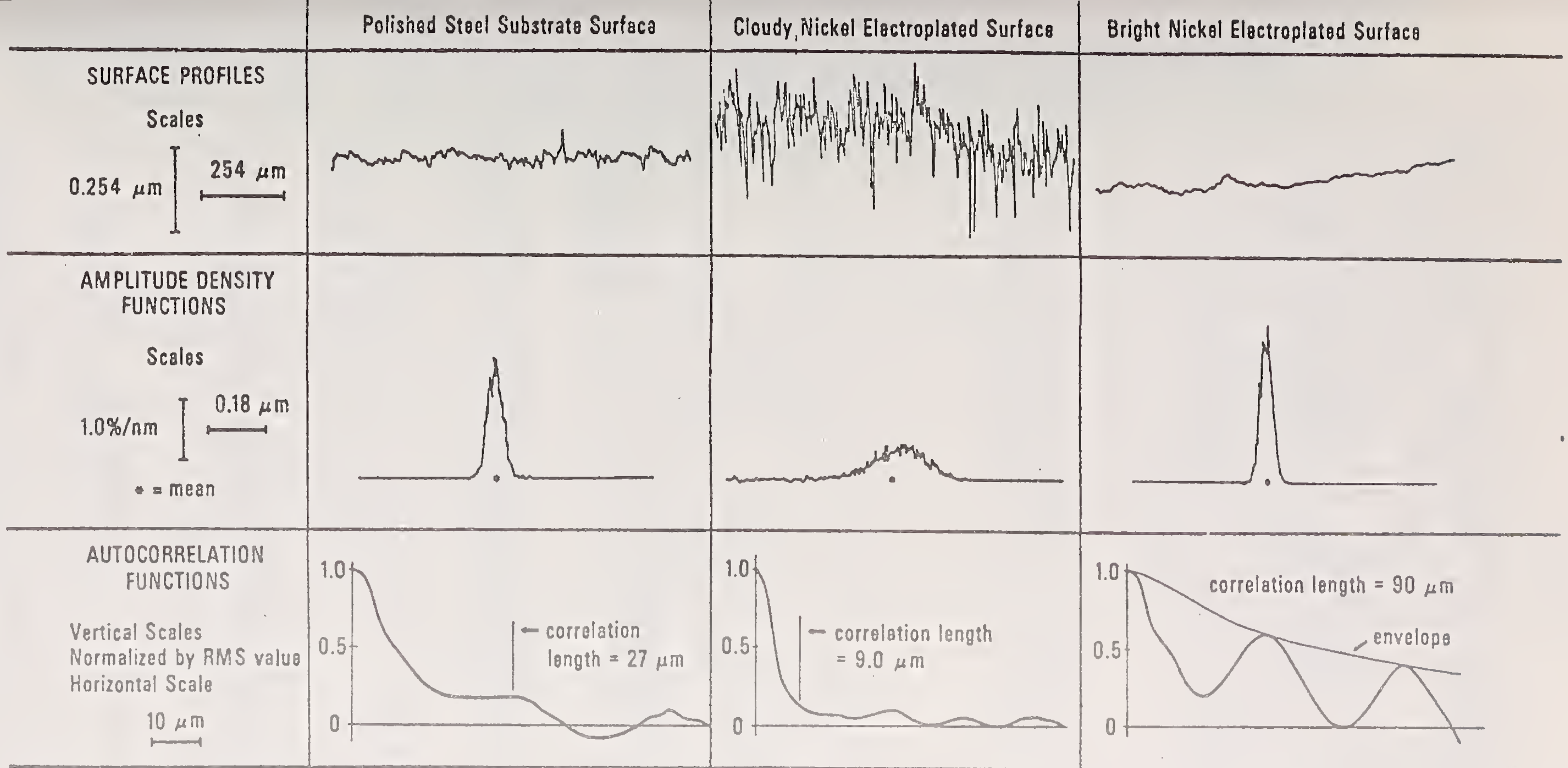

	Polished Steel Substrate Surface	Cloudy Nickel Electroplated Surface	Bright Nickel Electroplated Surface
AA (μm)	0.11	0.51	0.07
RMS (μm)	0.18	0.79	0.10
Average Slope	0.033	0.21	0.023
Average Wavelength (μm)	20.9	15.2	19.1
Skewness	+0.15	–1.7	+0.058
Kurtosis	3.36	8.8	2.84

Figure 17: Eight Characterizations of a Polished Steel Substrate, a Cloudy Nickel Electroplated Surface and a Bright Nickel Electroplated Surface.

ACKNOWLEDGEMENTS

Many people have contributed significantly to the development of this system and to the preparation of this report. Those I would especially like to thank are Dennis A. Swyt for helping me to understand his programs and the minicomputer's operation and for working co-operatively with me during the early stages of system evaluation, Margie Johnson for carefully and patiently typing the report, Fredric Scire for taking much of the data required for statistical evaluation, and Joseph M. Cameron for thoroughly analyzing the calibration data. Other contributors to the software are acknowledged in appendix B.

REFERENCE

[1] D. J. Whitehouse, Theoretical Analysis of Stylus Integration, Annals of the International Institution for Production Engineering Research (CIRP) Volume 23, pp. 181-2 (1974).

[2] Mary Gibbons Natrella, Experimental Statistics, National Bureau of Standards Handbook 91, 1963, pp. 4-6, U.S. Government Printing Office, Superintendent of Documents.

[3] D. J. Whitehouse and J. F. Archard, The Properties of Random Surface of Significance in Their Contact, Proceeding of the Royal Society of London A316, 97-121 (1970).

[4] Natrella, op cit p. 5-15.

[5] Julian S. Bendat and Allan G. Piersol, Random Data: Analysis and Measurement Procedures, Wiley Interscience, 1971, pages 129f.

[6] Ibid, p. 232.

[7] Ibid, p. 60.

[8] R. K. Otnes and L. Enochsen, Digital Time Series Analysis, John Wiley and Sons, 1972.

[9] D. C. Champeney, Fourier Transforms and Their Physical Applications, Academic Press, 1973.

[10] Proceedings of the International Conference on Surface Technology, 1973 Society of Manufacturing Engineers Conference in Pittsburgh, Pa.

[11] Properties and Metrology of Surfaces, Proceedings of the International Conference organized by The Institution of Mechanical Engineers, Volume 182, part 3K, 1968.

[12] R. C. Spragg and D. J. Whitehouse, A New Unified Approach to Surface Metrology, Proceedings of the Institution of Mechanical Engineers 185, 47-71 (1970).

[13] R. D. Deslattes, Optical and X-ray Interferometry of a Silicon Lattice Spacing, Applied Physics Letters 15 386 (1969).

[14] Bendat and Piersol, op cit Chapters 3 and 6.

[15] D. K. Cheng, Analysis of Linear Systems, Addison Wesley Publishing Co., 1959, p. 244.

[16] R. C. Spragg, The Interdisciplinary Nature of Surface Measurement, Joint Measurement Conference, Boulder, Colorado, June 1972.

[17] Precision Measurement and Calibration, Edited by H. H. Ku; pp. 331-342, NBS Special Publication 300, Volume 1, U.S. Government Printing Office, Superintendent of Documents, 1969.

[18] Teletype Waveform Receiving System, NBS Report 9887 by Louis J. Palombo, National Bureau of Standards, Washington, D.C. 20234, 1967.

[19] Private Communication; Mr. Frank Flaherty, Director of Advanced Process and Control; The Gillette Company; Boston Research and Development Laboratory; Gillette Park; S. Boston, Massachusetts 02106.

APPENDIX A*

SYSTEM ELECTRONICS AND INTERFACING

The system components as shown schematically in figure 2 are:

1. An Interdata Model 3 Minicomputer
2. A teletype Model 33
3. A Talysurf Model 4 stylus instrument
4. A 12 bit analog to digital converter, A/D
5. An 8 bit digital to analog converter, D/A
6. Two strip chart recorders,

and

7. An electronic filter.

The minicomputer, teletype and A/D were interfaced by the minicomputer manufacturer; one of the chart recorders is also a standard accessory for the Talysurf 4. Thus, the only interfacing needed was between the stylus instrument and the minicomputer-A/D subsystem, and between the minicomputer and an output strip chart recorder.

The latter was accomplished with a system designed by Louis J. Palombo [18] of NBS to transform the digital teletype output to an analog signal. With this system two modes of output from the minicomputer's teletype interface are available. In a normal mode, the usual keyboard-teleprinter operations are provided. In a plot mode, the binary value of each 8-bit character is converted to an analog voltage with the D/A and input to the second strip chart recorder. Several commercial systems are available which will perform the same operations; the Palombo system was employed because of its availability. A block diagram of the waveform receiver is shown in figure 18. In addition to an analog signal output proportional to the 8-bit character input of the teletype data line, the receiver controls a set of relays which, when energized by the plot character, lower the pen (to the paper) and start the chart motor of the recorder. They also disable the keyboard and paper tape punch on the teletype. In the block diagram S1 is the teletype enabling line.

The electronics for the analog filter and interfacing are shown schematically in figures 19 and 20. The gain-bandpass characteristics of the filter circuits, shown in figure 21, have been designed to conform with ANSI Standards when the device is used in conjunction with a Talysurf 4. The filter 3 db down points are related to the conventional wavelength cut-off through the stylus speed:

$$f(\text{Hz}) = .06 \text{ in/sec} \div \lambda_c \text{ (in)}.$$

The filters are active 2-pole Butterworths with selectable high-pass cut-off frequencies as indicated by figure 19. Roughness measurements are made with one of three high-pass filters in series with the single low-pass filter. Step height measurements are made with only the X10 amplifier in the circuit.

The conformity of the filters to specified operation is indicated by the bandpass curves in figure 21 and the observed phase delay of the low-pass filter in figure 22. Components of the filter-amplifier circuits are listed in Table 4.

An additional part of the interfacing, interrupt circuitry, is shown in figure 20. This circuitry generates at a signal from the Talysurf 4 an appropriate pulse to the A/D converter and a pulse to serve as an event marker on step profile data. Both pulses have the standard TTL voltage levels; the event maker pulse is one second long; the A/D pulse is fifty microseconds long. As shown in appendix Q the signal from the Talysurf 4 is produced from a relay actuated by motion of the stylus driving mechanism.

Block diagrams of the system component interconnections are given in appendix Q.

A compilation of characteristic parameters of the entire system is given in Table 5.

Table 4

Components List for Filter-Amplifier

F.6	Frequency Devices, Inc. (FDI) 0.6 Hz high-pass filter Model Number 708H2B
F2	FDI 2.0 Hz high-pass filter Model Number 710H2B
F6	FDI 6.0 Hz high-pass filter Model Number 710H2B
F300	FDI 300 Hz low-pass filter Model Number 706L2B
ASIG and AREC	Analog Devices Model 40J Operational Amplifiers

Table 5

Characteristic Parameters

Talysurf 4

Profile Output (nominal)	$\pm$ 1 V
Relay Output (nominal)	- 4V
Magnification (vertical, Max.)	10^5
Stylus Speed (4X)	3.6 in
(20X)	0.72 in
(100X)	0.14 in
Scan Distance (.030 in cutoff, 4X)	.150 in
Chart Speed	14.4 in

Filter-Amplifier

Input (limited)	$\pm$ 1 V
Input Impedance	100 kΩ
Gain (nominal)	10X
High Frequency Cut-off	300 Hz
Low Frequency Cut-off	6 Hz
	2 Hz
	.6 Hz
Filter Roll-off	-12 db/octave
Flatness	$\pm$ .02 db
Overall Linearity	.02%
Output (nominal)	$\pm$ 10V
Noise Output	$\leq$ 5 mV.

Table 5 (continued)

Interface Circuitry

Pulse Output	+ 4V
Event Marker Output	+ 1.0 V (1 s)
Interrupt Signal Output	+ 3V (50 μs)

Data Input: Step Mode

Record Length (time)	25 s
(chart)	5.9 in
(surface, 100X)	.060 in
(surface, 20X)	.300 in
Number of data points	512
Time per data point	50 ms
Horizontal Resolution (100X)	120 μin
(20X)	600 μin
Vertical Resolution (A/D resolution at highst Talysurf gain).	.005 μin

Data Input: AA Mode

Record Length (time)	2.5 s
(chart)	.6 in
(surface, 4X)	.150 in
Number of data points	4096
Time per data point	600 μs
Horizontal resolution (4X)	37 μin
Vertical resolution (at 10^5 X)	.005 μin
Short Wavelength cut-off	200 μin
Long Wavelength cut-off	.010 in, .030 in, and .100 in

A/D Converter

Input Voltage	$\pm$ 10V
Input Impedance	100 MΩ
Output (including sign)	12 bit
Resolution (voltage)	5 mv
(relative)	.025% FS
Linearity	.010%

Waveform Receiving System

Input (including sign)	8 bit (Teletype logic levels)
Output	0-10 volt

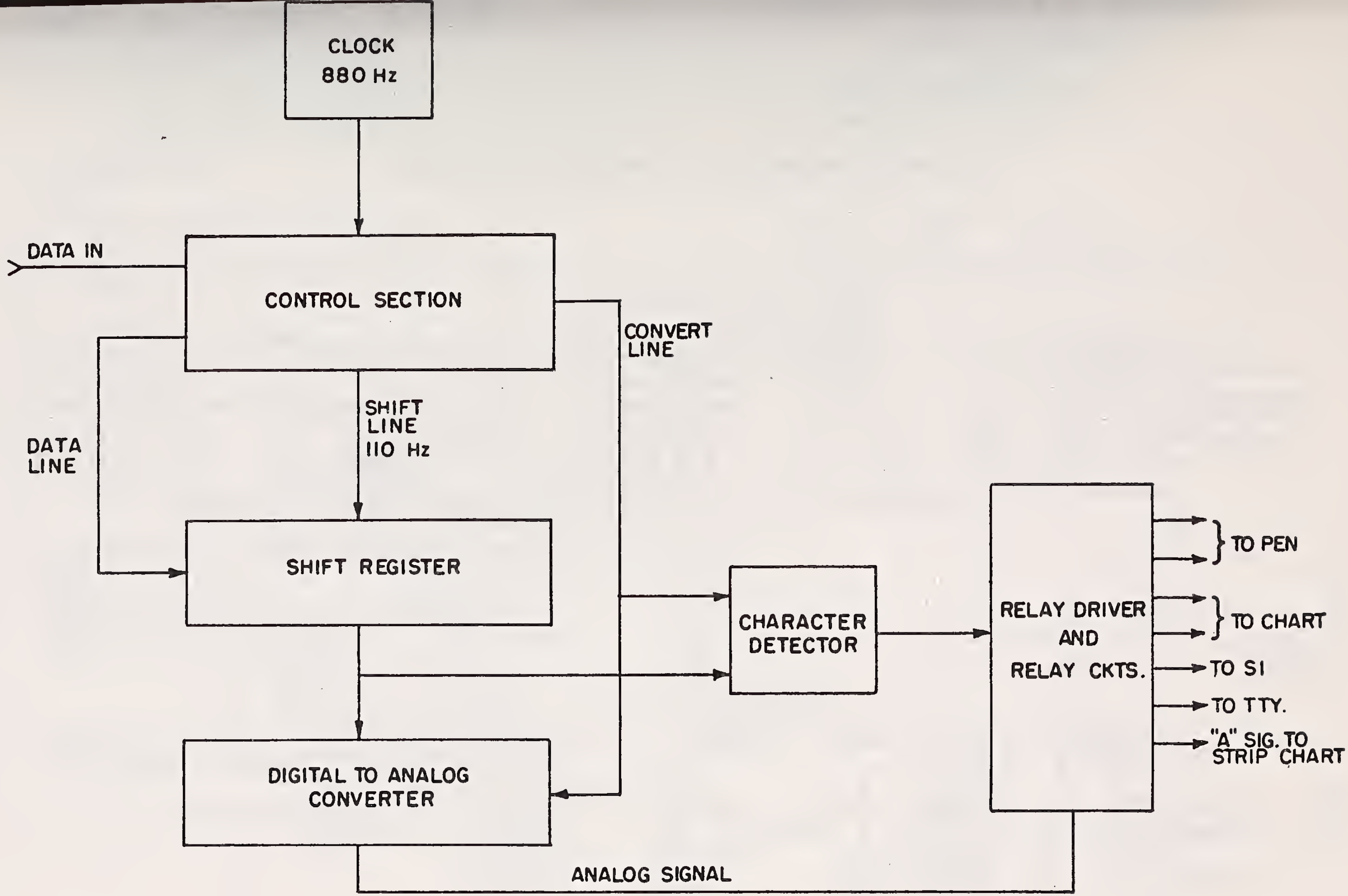

BLOCK DIAGRAM OF WAVEFORM RECEIVER

Figure 18

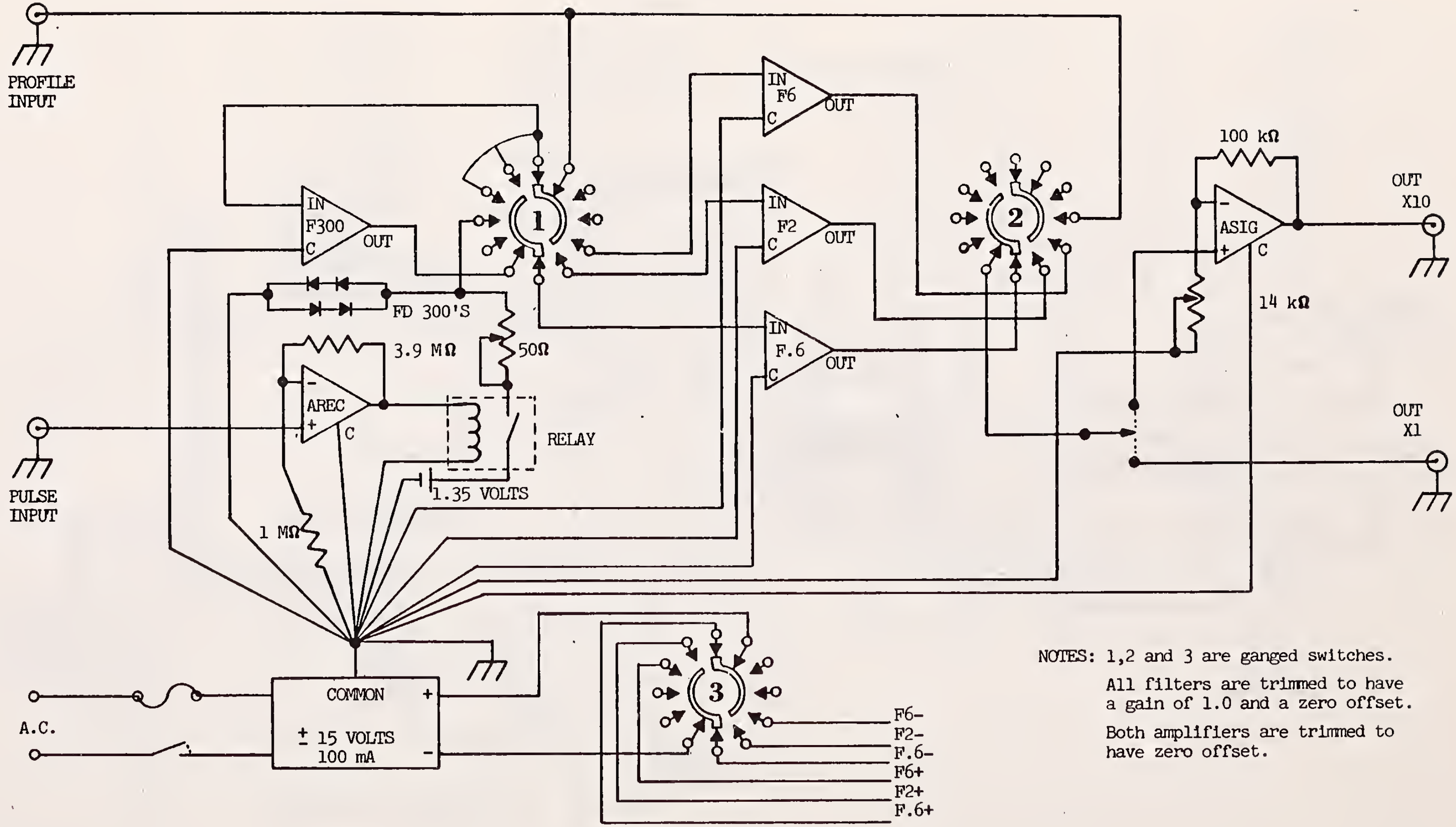

Figure 19: Schematic of Interface Electronics

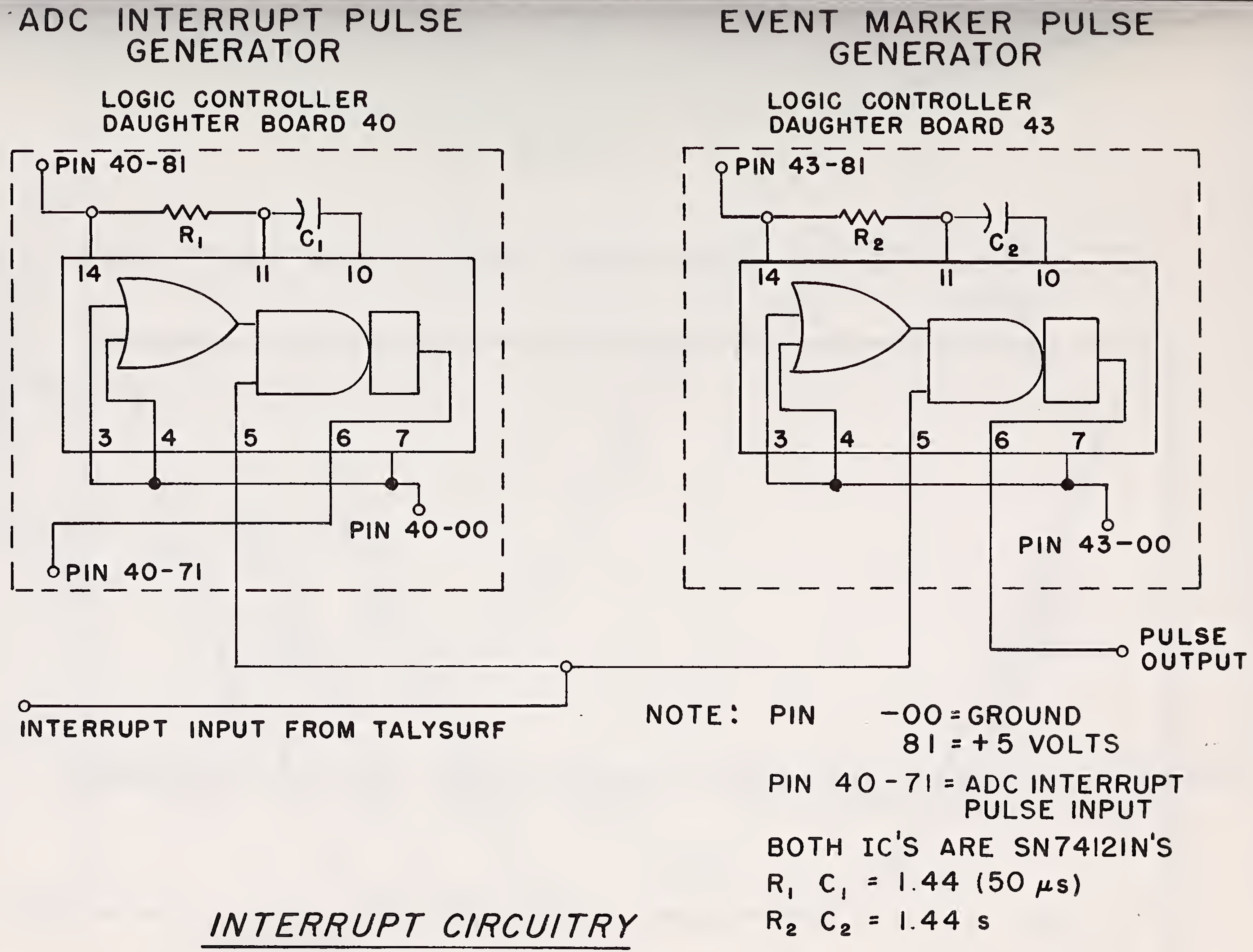
ADC INTERRUPT PULSE GENERATOR
LOGIC CONTROLLER DAUGHTER BOARD 40
PIN 40-81
R_1
C_1
14
11
10
3
4
5
6
7
PIN 40-00
PIN 40-71
EVENT MARKER PULSE GENERATOR
LOGIC CONTROLLER DAUGHTER BOARD 43
PIN 43-81
R_2
C_2
14
11
10
3
4
5
6
7
PIN 43-00
PULSE OUTPUT
INTERRUPT INPUT FROM TALYSURF
NOTE: PIN -00 = GROUND
81 = +5 VOLTS
PIN 40-71 = ADC INTERRUPT PULSE INPUT
BOTH IC'S ARE SN74121N'S
R_1 C_1 = 1.44 (50 μs)
R_2 C_2 = 1.44 s
INTERRUPT CIRCUITRY

Figure 20

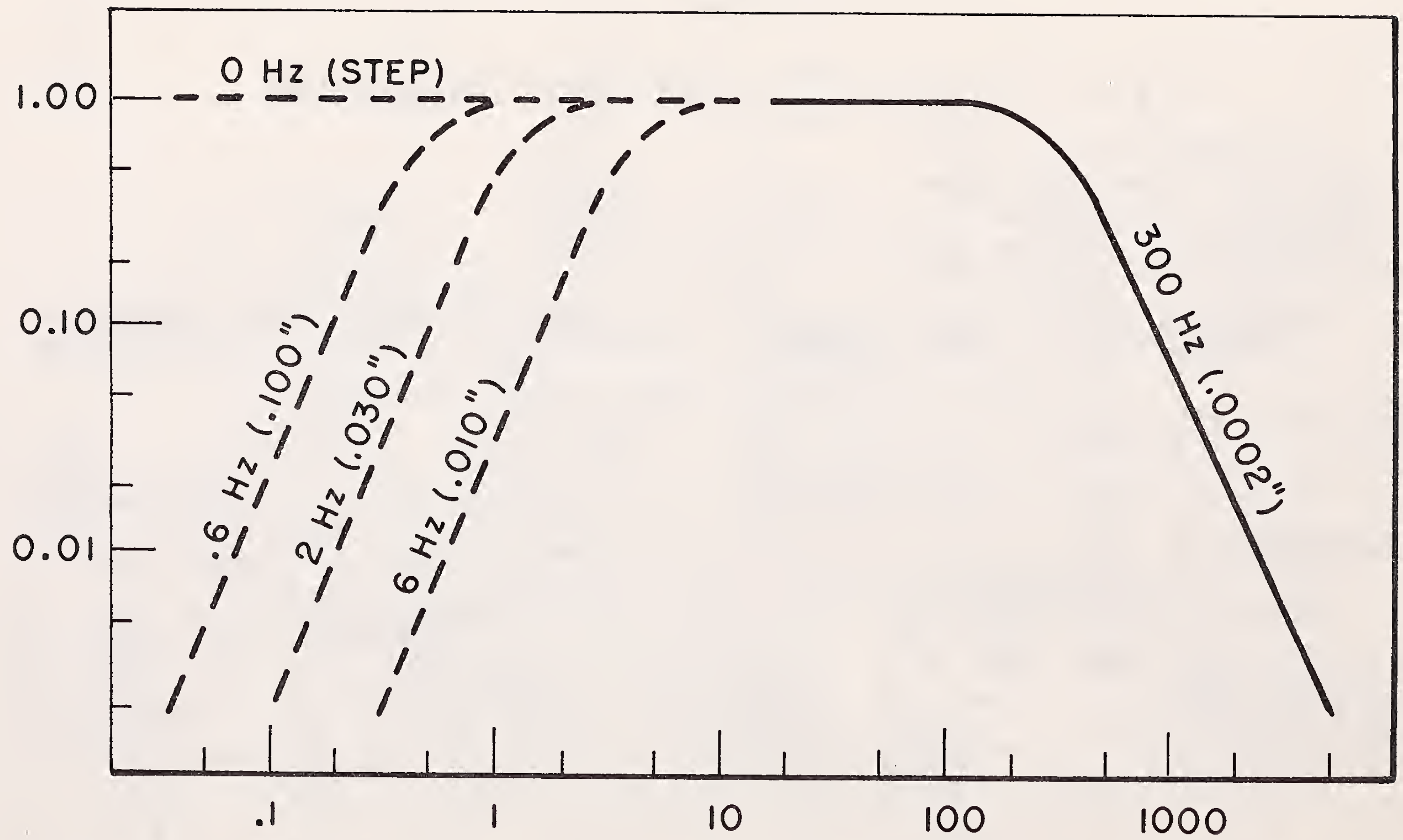

FILTER-AMPLIFIER GAIN-BANDPASS CHARACTERISTICS

FIGURE 21

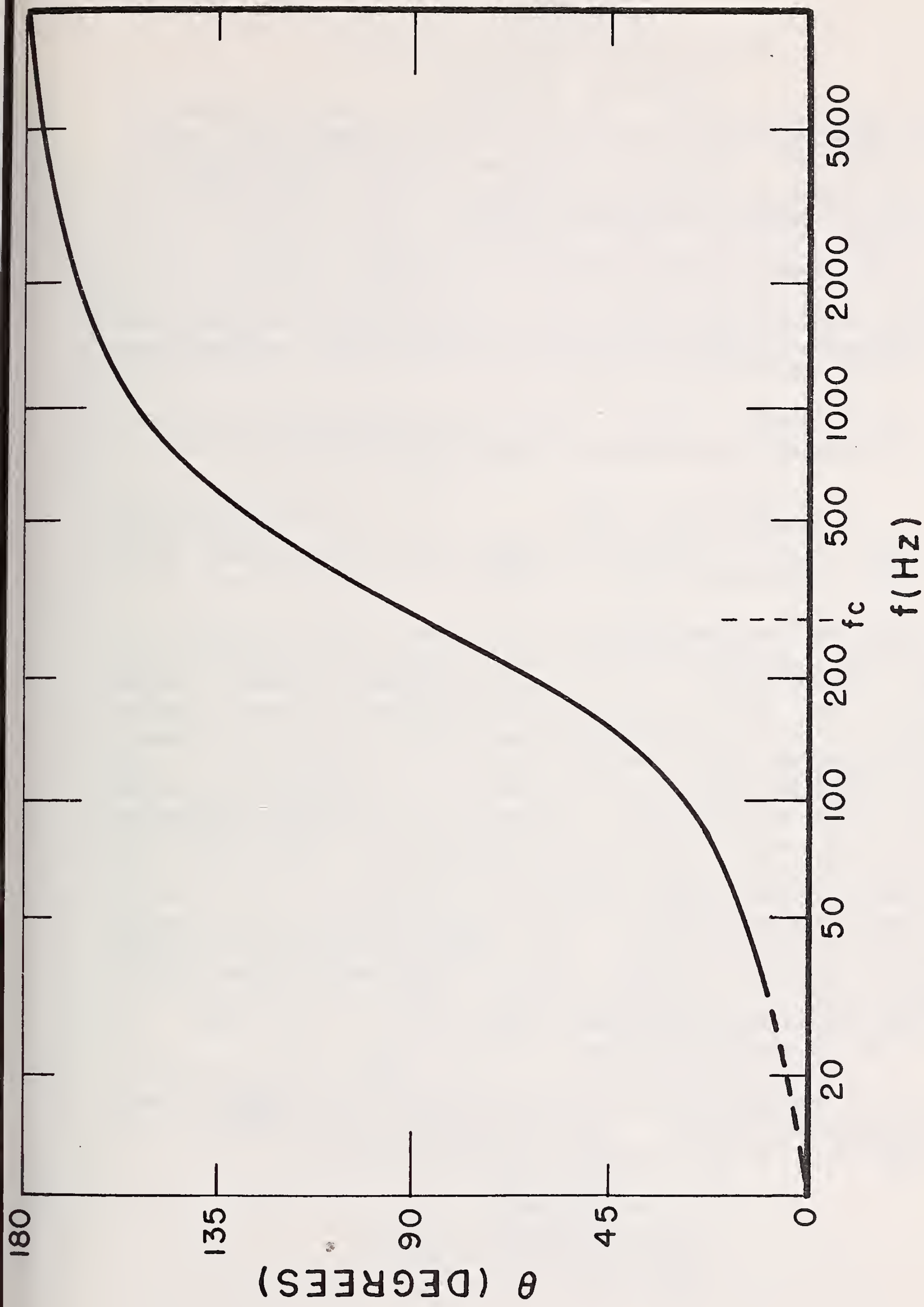

OBSERVED AMPLIFIER-FILTER PHASE DELAY

FIGURE 22

APPENDIX B

COMPUTER SOFTWARE

This appendix contains the following information about the computer software used with the minicomputer/stylus instrument system:

A. Allocation of the Interdata Model 3 memory during use by the step/roughness measurement software,

B. Flow diagrams of major programs or routines,

C. A memorandum by Philip G. Stein which describes the properties and the use of an operating system he developed for the Interdata Model 3,

D. An annotated listing of all the step/roughness measurement software and of the monitor system designed by Philip Stein,

and

E. An instruction set listed by Op-code, for the interdata model 3 with an excerpt on instruction word formats taken from the Interdata Model 3 manual.

The detailed information about the computer software which is given herein is presented so that the reader will have available a concrete implementation of a total software system. Such documentation of computer programs is impossible without making reference to specific equipment and instruction sets by brand name. However, no judgement as to the quality or suitability of the equipment discussed here has been made by the National Bureau of Standards, and no recommendation, favorable or other wise, should be implied by this report. Listings of the software in machine language should be of use to the reader whose minicomputer memory size is limited and thus, is unable to support a compiler and to the reader considering the implementation of parts of the software system on a recent generation microcomputer. For those with either assemblers or compilers, the flow diagrams and listings should enable the efficient writing of necessary programs. The incorporation of this appendix was motivated by the desire that one or all three of these routes be encouraged in every possible way.

Due to the length of this appendix (approximately 70 pages) it was issued as a separate volume. Interested readers may obtain a copy of the appendix by sending a request for NBSIR 75-924 to:

E. Clayton Teague
National Bureau of Standards
Met. Bldg., Room A-123
Washington, D. C. 20234

APPENDIX C

TIME STUDY OF THE FOUR MOST COMMON MEASUREMENT PROCEDURES

The times given in the following charts assume that only one step or roughness value is measured and calculated. Statistics on the input-calibrating step or roughness measurements would add to these times multipes of only the times for data acquisition and computation since realignment at different positions is not required for a good quality artifact. Times for the autocorrelation and amplitude density function calculations (and all other calculations), are determined by the Interdata 3 computation times; the use of recent generation minicomputers would reduce the calculation times to between 1/10th to 1/100th the values given. The symbols are those described in section 1.0.

Time Study of Measurement Procedure Step

Operator Function:	Machine Function
Align Calibration Artifact; Begin Program (5 min.)	
	Input Step Data (0.5 min.)
Select A1 and A2 from Chart & Scale, enter (1 min.)	
	Computer Step Height (0.25 min.)
Align Unknown Step (5 min.)	
	Input Step Data (0.5 min.)
Select A1 and A2 from Chart & Scale, enter (1 min.)	
	Computer Unknown: Exit (0.5 min.)
Operator Function Time (12 min.)	Machine Function Time (1.5 min.)

Total Time

13.5 min.

Time Study of Measurement Procedure: Roughness

Operator Function	Machine Function
Align Calibration Artifact; Begin Program (5 min.)	
	Input Step Data (0.5 min.)
Select A1 and A2 from Chart Scale; Enter (1 min.)	
	Compute Step Height (0.25 min.)
Allign Unknown Roughness (5 min.)	
	Input Roughness Data (0.05 min.)
	Compute AA; Exit (0.25 min.)
Operator Function Time (11 min.)	Machine Function Time (1 min.)

Total Time
12 min.

Time Study of Measurement Procedure: Statistical Parameters
(continuing from Roughness)

Operation Function	Machine Function
Enter "J" at teletype (0.1 min.)	
	Calculate and Plot Amplitude Density Function (0.5 min.)
Enter "V" at teletype (0.1 min.)	
	Calculate and Plot Autocorrelation Function (13.5 min.)
Enter "Y" at teletype (0.1 min.)	
	Calculate and Print Average Wavelength and Slope (0.25 min.)
Operator Function Time (11.3 min.)	Machine Function Time (14.8 min.)

Total Time
26.1 min.

Time Study of Measurement Procedure: Step Calibrated Amplitude Density Function

Operator Function	Machine Function
Align Calibration Artifact; Begin Program (5 min.)	
	Input Step Data (0.5 min.)
Select A1 and A2 from Chart and Scale; Enter (1 min.)	
	Compute Step Height (0.25 min.)
Enter "J" at teletype (0.1 min.)	
	Compute and Plot Amplitude Density Function
Align Roughness Unknown (5 min.)	
	Input Roughness Data (0.05 min.)
Enter "J" at teletype (0.1 min.)	
	Compute and Plot Amplitude Density Function (0.5 min.)
Operator Function Time (11.2 min.)	Machine Function Time (2.0 min.)

Total Time

13.2 min.

Appendix D*

THE LINEAR LEAST SQUARES CURVE FIT

For the general case of a linear least squares (LSQ) curve fit of the form:

$$y = a\,x + b,$$

where y is the dependent variable, x the independent variable, a the slope, and b the intercept, the following formulae apply.

$$(1)\quad b = \frac{1}{N}\,\Sigma\, y_i - \frac{a}{N}\,\Sigma\, x_i$$

$$(2)\quad a = \frac{N\,\Sigma\, x_i\, y_i - (\Sigma\, x_i)\,(\Sigma\, y_i)}{N\,\Sigma\, x_i^2 - (\Sigma\, x_i)^2}$$

where Σ indicates the summation over the n index from 1 to N.

For the special case of equally spaced x increments, x_i may be replaced by an integer n corresponding to the value of i and the summations over x_i and x_i^2 evaluated as standard series.

$$(3)\quad \Sigma\, x_i = \Sigma\, n = \frac{N}{2}\,(N + 1)$$

$$(4)\quad \Sigma\, x_i^2 = \Sigma\, n^2 = \frac{N}{6}\,(N + 1)\,(2\,N + 1)$$

Substitution of equations (3) and (4) into equations (1) and (2), with some simplification, leads to:

$$(5)\quad b = \frac{1}{N}\sum y_i - \frac{a}{2}\,(N + 1)$$

$$(6)\quad a = \frac{12\,\Sigma\, i\, y_i - 6\,(N + 1)\,\Sigma\, y_i}{N(N + 1)(N - 1)}$$

A flowchart and listing of the program for the least squares calculation is given in appendix B.

*From DASR.

Appendix E*

STEP LOCATION

At the interrupt signal generated near the beginning of the stylus stroke, a one second delay is executed by the computer and data is read into memory for twenty-five seconds at the rate of approximately twenty points per second. Since the event marker is in the information channel, the delay is necessary to avoid reading the event maker as data. The signal which is recorded in those twenty-five seconds is thus entered as 512 data points in memory locations 1000_{16} to 1400_{16}. The memory locations of selected points and the corresponding positions on the strip chart are indicated in figure 23. These data are measured in mm relative to the trailing edge of the event marker as illustrated in figure 24.

Figure 24a illustrates a properly positioned step-one which is approximately centered within the 40 mm - 110 mm region. A representation of the data recorded in memory is given in figure 24b.

The length of the segment on the chart, corresponding to the 128 points over which a least-squares straight line is computed, is 37.5 mm. The address A_1 (input during program execution) must correspond to a location in the region between the 40 mm position and the step edge; similarly, A_2 must correspond to a location in the region between the step edge and the 110 mm position. These positions are illustrated in figure 25. The line segments corresponding to the A_1 and A_2 selected are indicated in figure 25b. Choices for A_1 and A_2 are limited to pairs of points situated equally distant to the left and right of the step location, S, such that:

$$S(\text{mm}) - A_1(\text{mm}) = A_2(\text{mm}) - S(\text{mm}).$$

A_1 and A_2 determine individually over which segments the lines are to be computed by least squares fitting; the mean of A_1 and A_2 determines the location at which a step height is to be computed from the two lines. The effects on the calculations of the step height of proper and improper selections of A_1 and A_2 may be significant; these effects are illustrated in figures 26a and 26b, respectively.

*From DASR.

Distance on Strip Chart From Event Marker to Step in MM	Hexadecimal Address	Distance on Strip Chart From Event Marker to Step in MM	Hexadecimal Address
0040	1116	0075	1206
0041	111E	0076	120E
0042	1124	0077	1214
0043	112A	0078	121A
0044	1132	0079	1222
0045	1138	0080	1228
0046	1140	0081	1230
0047	1146	0082	1236
0048	114E	0083	123E
0049	1154	0084	1244
0050	115A	0085	124A
0051	1162	0086	1252
0052	1168	0087	1258
0053	1170	0088	1260
0054	1176	0089	1266
0055	117E	0090	126E
0056	1184	0091	1274
0057	118A	0092	127A
0058	1192	0093	1282
0059	1198	0094	1288
0060	11A0	0095	1290
0061	11A6	0096	1296
0062	11AE	0097	129E
0063	11B4	0098	12A4
0064	11BA	0099	12AA
0065	11C2	0100	12B2
0066	11C8	0101	12B8
0067	11D0	0102	12C0
0068	11D6	0103	12C6
0069	11DE	0104	12CE
0070	11E4	0105	12D4
0071	11EA	0106	12DA
0072	11F2	0107	12E2
0073	11F8	0108	12E8
0074	1200	0109	12F0

Figure 23: Step Locator Chart

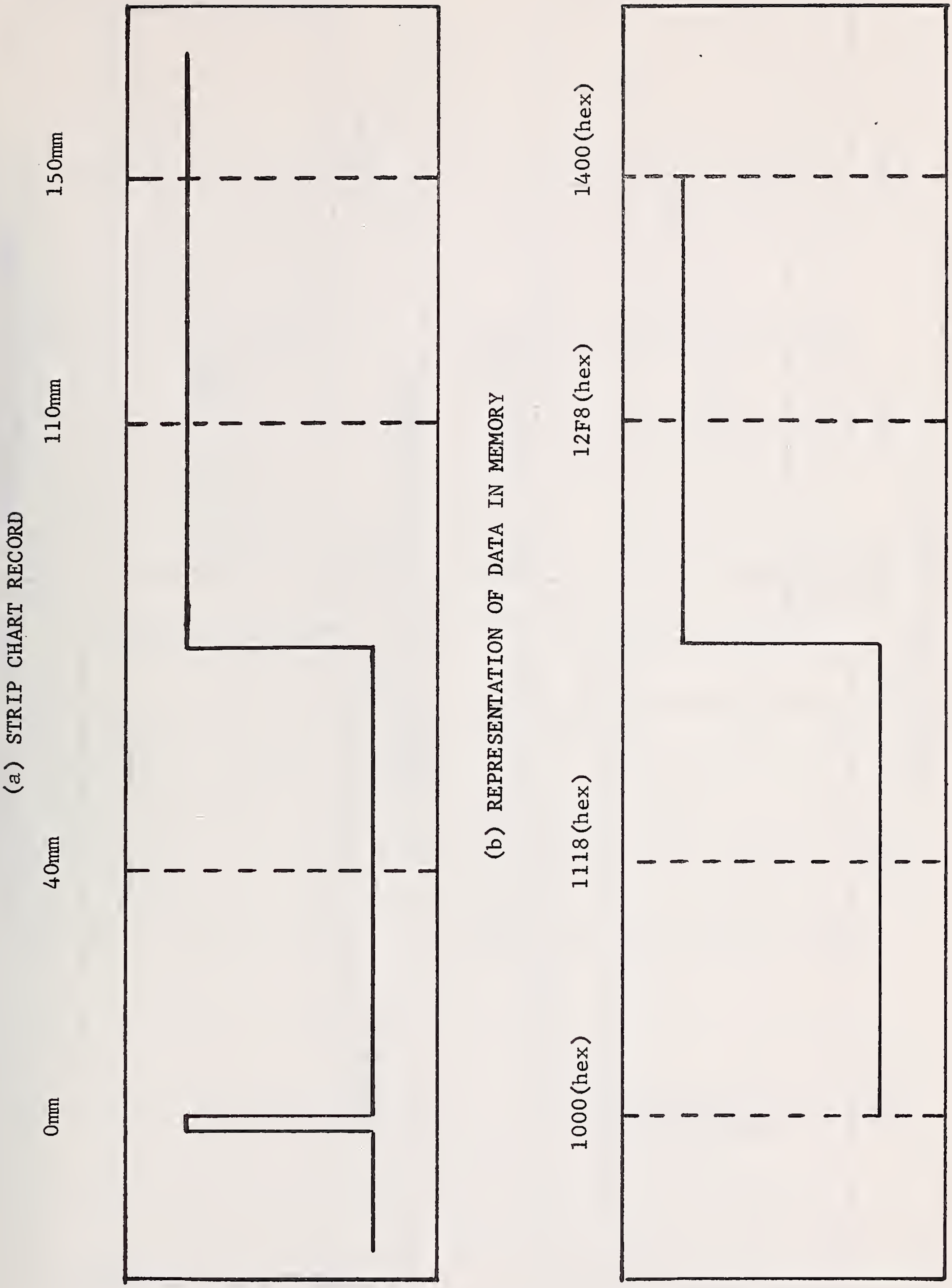

FIGURE 24. PROPER LOCATION OF STEP RELATIVE TO EVENT MARKER

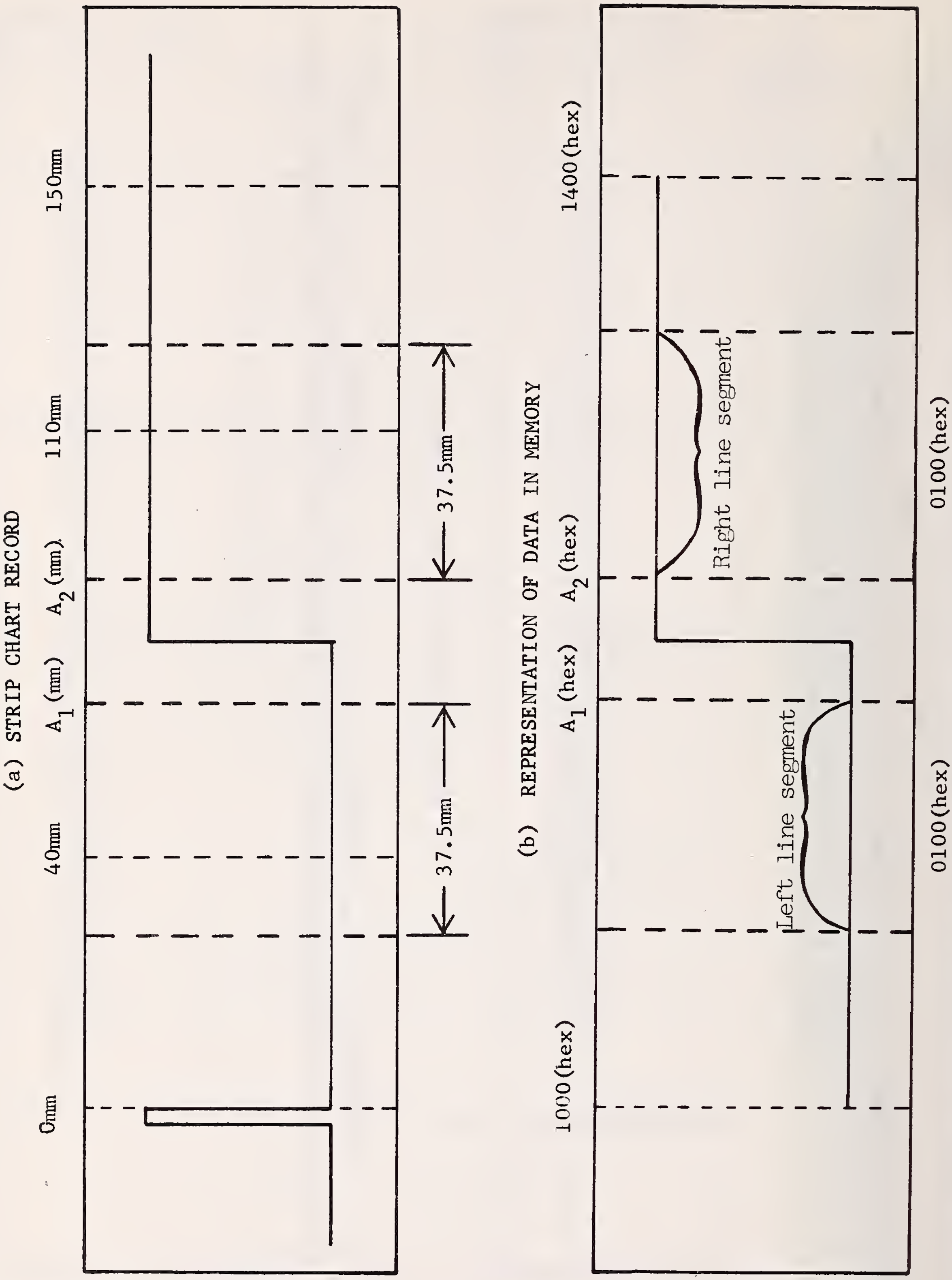

FIGURE 25. SELECTION OF A1 AND A2 LOCATIONS

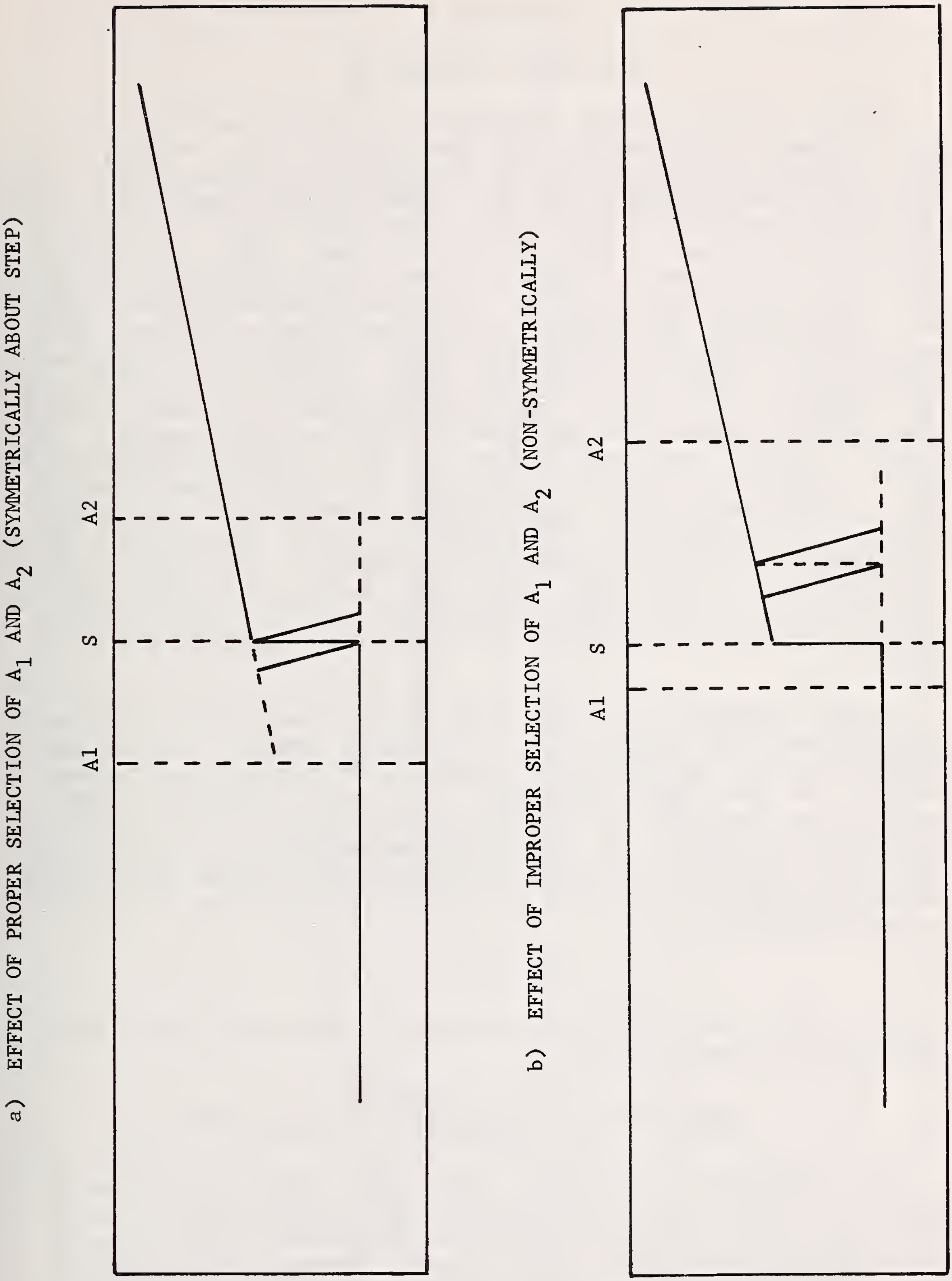

FIGURE 26. PROPER AND IMPROPER SELECTION OF A1 AND A2.

APPENDIX F

STEP HEIGHT CALCULATION

From the two lines determined by a least squares fit to the profile data from the two opposite sides of the step profile, the step height is calculated as the mean ordinate difference along the horizontal distance between the line segment ends, selected by the operator as described in appendix E. Thus, calculations as presently implemented in the system software assume that the errors introduced by non-parallel sides of a step and non-parallelism of the step relative to the reference datum (the reference surface plane) are insignificant with respect to the overall system accuracy. This assumption is valid because the large vertical to horizontal magnification ratios used with the stylus instrument allow only very small angles to be on scale. Two extreme examples for a step height approximately equal to one-fourth of full scale are presented in figure 27, as they would appear on the stylus instrument's chart recorder; figure 27a also shows, by a dashed line the output for a step height of approximately one-tenth full scale. Vertical to horizontal magnification ratios employed with the stylus instrument are 50 or greater for inputs to the step height calculations. Thus, even though the angles on the strip chart recorder, in the extreme cases illustrated, are 15° and 30°, the true angles are 0.31° and 0.66°, respectively, for a magnification ratio of 50.

Errors introduced by this approach are most obvious from the examples shown in figure 27a. For these examples the natural definition of the specimen's step height is the perpendicular distance between the two lines defining the step's opposite sides. Measurements performed in this manner directly from the strip chart recorder output would be in error unless corrected for the vertical to horizontal magnification ratio. The true error between calculating the step height as the ordinate difference and calculating it as the perpendicular distance is:

$$\Delta h = y - \sqrt{y^2 + x^2},$$

where y and x are as shown in figure 27a. For a magnification ratio of 50 the fractional error is:

$$\frac{\Delta h}{y} = \left| 1 - \left[1 + \frac{\tan 15^\circ}{2500} \right]^{\frac{1}{2}} \right| = 1.4 \times 10^{-5}.$$

The definition of the step height whose profile is as shown in figure 27b is not obvious. The approach taken in DASR was to define the step height as the "mean perpendicular distance" between the two least-squares fitted lines. This mean perpendicular distance, h_{MPD}, was calculated as the arithmetic mean of the two distances between the point A located on the bottom of the step and the points of

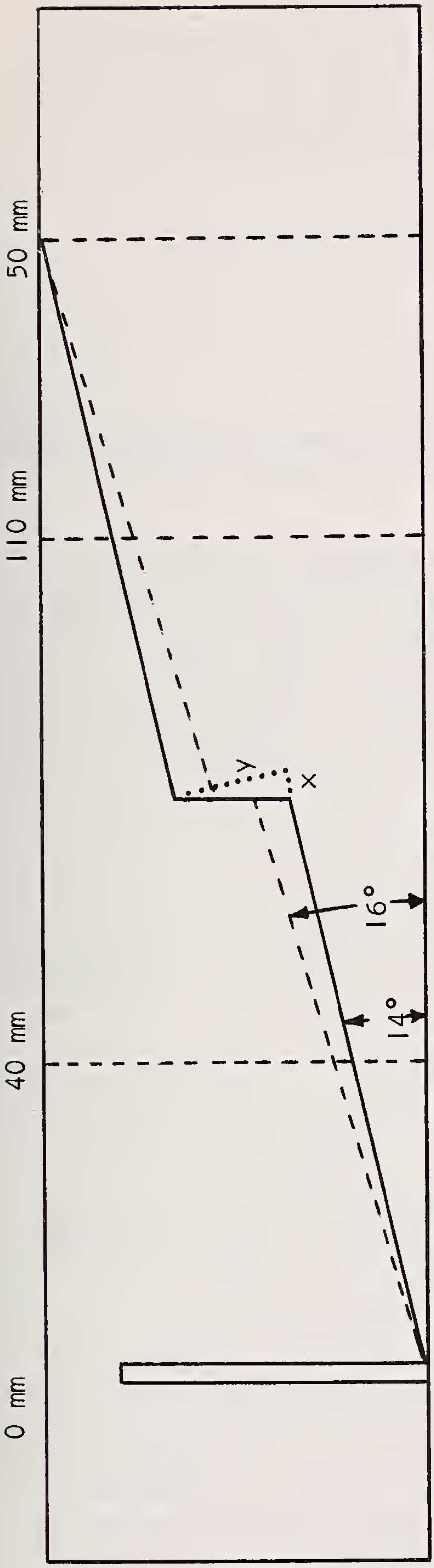

Figure 27a. Record of Step with Maximum Slope Relative to Datum.

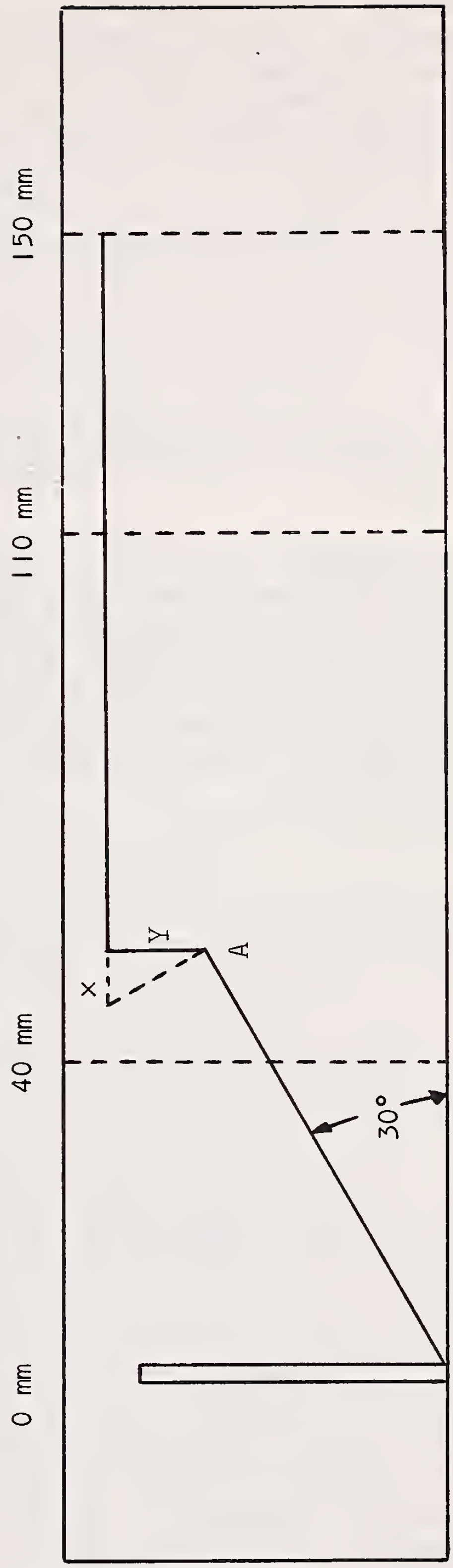

Figure 27b. Record of Step with Large Slope Difference between Opposite Sides.

Figure 27. Schematic Strip Chart Records of Highly Sloped Profiles.

intersection of the perpendicular lines with the top of step as shown in figure 27b. The line perpendicular to the right hand side of the step is coincident with the step profile and is defined as the ordinate difference, h_{OD}. The difference between the "mean perpendicular distance", h_{MPD}, and the ordinate difference, h_{OD}, for this example is:

$$h_{MPD} - h_{OD} = \tfrac{1}{2}\,[y + \sqrt{y^2 + x^2}\,] - y$$

$$\text{or} \quad |h_{MPD} - h_{OD}| = \tfrac{1}{2}\,|\Delta h|.$$

For an angle of 30° on the strip chart recording and a magnification ratio of 50, the fractional difference between the two definitions is 3.4×10^{-5}.

Implementing the ordinate difference definition of step height requires only that the two lines fitted by the least squares procedure be transformed to a common co-ordinate system. In figure 28, the line fitted to the step's low side, S_L, is referenced to the primed system and the line fitted to the high side S_H, is in the unprimed system; A_1 and A_2 are the step locator points entered by the operator. From the least squares fitting operation one has for the representations of lines S_L and S_H:

$$y_L' = a_L\,x' + b_L$$

and

$$y_H = a_H\,x + b_H.$$

The co-ordinate transformations are:

$$y' = y$$

$$x' = x + c + z,$$

where $c = 128 = 80$ (hexadecimal) and $Z = A_2 - A_1$. By transforming both lines to the unprimed system, the result:

$$y_L = a_L\,(x + c + z) + b_L$$

and

$$y_H = a_H\,x + b_H,$$

is obtained. The step height, H, at a particular abscissa, x, is therefore:

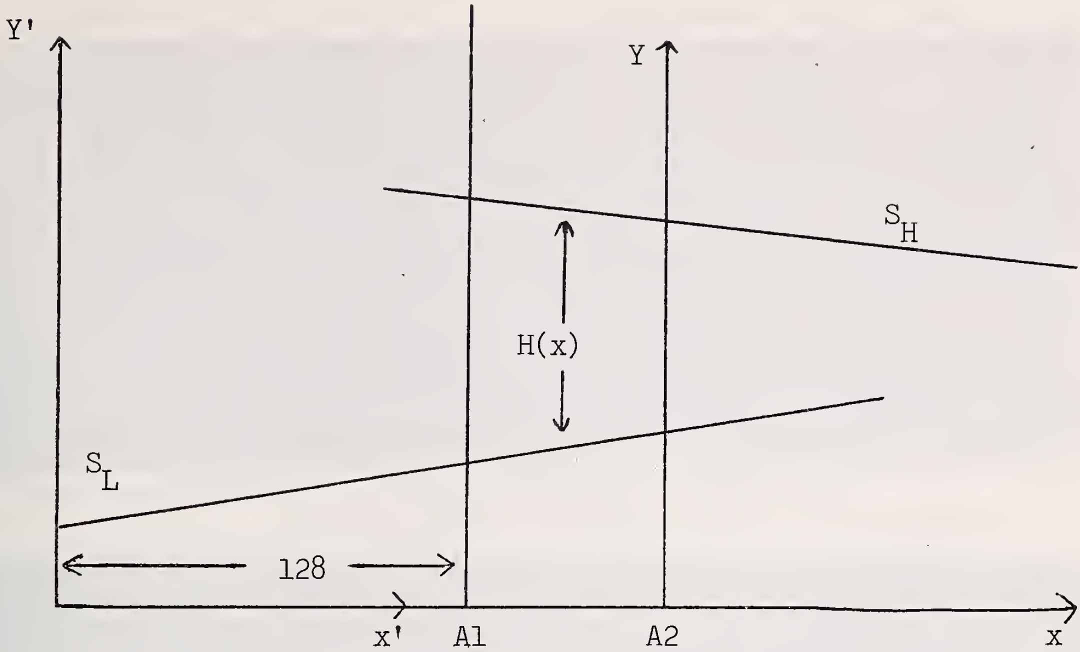

Figure 28: Co-ordinate System for Step Height Calculation.

$$H = y_H - y_L = (a_H - a_L)\ x + (b_H - b_L) - (Z + c)\ a_L.$$

The step height routine given in appendix B calculates H for values of X from -Z to 0 in increments of Z/8.

To confirm that the step height calculation was insensitive to changes in the slope of the step profile with parallel horizontal surfaces, a sequence of measurements at the slopes shown in figure 29 was made. The slopes of the profiles in figures 29b and 29c are the maximum possible positive and negative slopes for which on scale profile data may be obtained. Results of 10 measurements at each of these cases is given in table 6. The format of the data is explained in appendix K. These results show that the maximum difference between the mean step height calculated from a level profile and one from a highly sloped profile is 0.2%. The 3s value (see page 32) of this calculated step height is 0.2% and is primarily due to surface finish (section 2.2). Thus the uncertainty, 3s, in the difference between step height calculated for the two cases would be 0.3%. The difference between unsloped and sloped profile calculations being less than its 3s uncertainty therefore verifies that to within the limits imposed by surface finish effects no statistically significant relationship between calculated step height and input profile slope is present. The uncertainties of these measurements are larger than the expected 0.2% found experimentally in appendix K. This increased uncertainty is produced by the scratches or pits which were unfortunately present in the right side of the step.

Figure 29a. Slope ≈ 0.

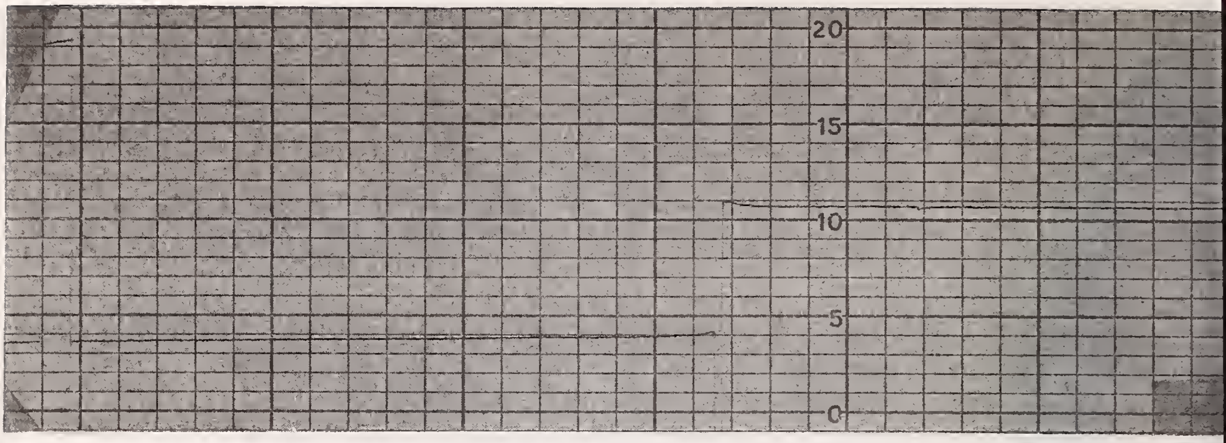

Figure 29b. Slope = Maximum Positive Value

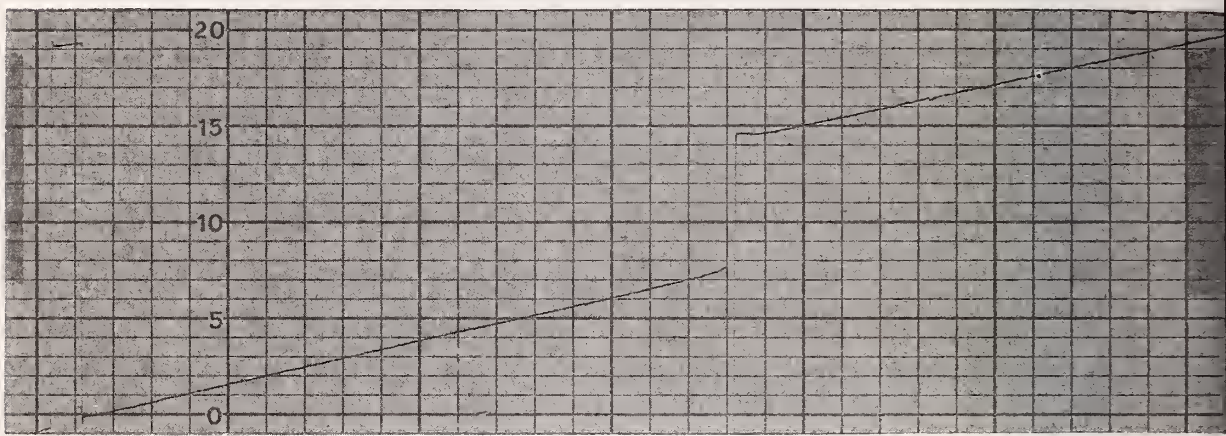

Figure 29c. Slope = Maximum Negative Value.

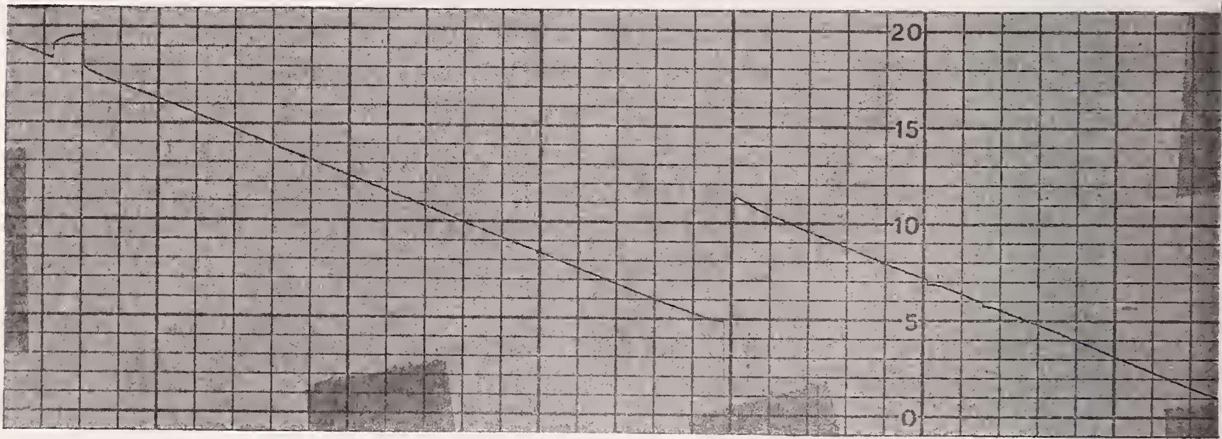

Figure 29. Profiles of 12.8 μm Step Used to Obtain Statistical Data on Possible Variation of Calculated Step Height with Changes in Slope. Horizontal Magnification X20; Vertical Magnification ≈ 1000.

```
 2500G
IN00002920 FB1F1800 FFFFECA0 00905800 00001756 055B5B30
H1         H3         H5         H7         HM
00001004 00001002 00001000 00000997 00001000
IN
00002820 FB1E9800 FFFFE920 008EB800 00001756 055B2F00
H1         H3         H5         H7         HM
00001004 00001002 00000999 00000997 00001000
IN
000028E0 FB1C0800 FFFFEF60 008B4800 00001756 05593680
H1         H3         H5         H7         HM
00001002 00001000 00000998 00000996 00000998
IN
00002F60 FB1BA800 FFFFE7A0 008B1800 00001756 05566F40
H1         H3         H5         H7         HM
00001001 00000998 00000996 00000993 00000996
IN
000035A0 FB135800 FFFFF620 00833800 00001756 0551B480
H1         H3         H5         H7         HM
00000997 00000995 00000992 00000990 00000993
IN
00003020 FB13F800 FFFFEB20 00883800 00001756 055A7100
H1         H3         H5         H7         HM
00001004 00001001 00000999 00000996 00000999
IN
00003060 FB0B0800 FFFFEE60 007B0800 00001756 0555B400
H1         H3         H5         H7         HM
00001000 00000998 00000995 00000993 00000996
IN
00002C20 FB0ED800 FFFFEEE0 007F6800 00001756 0558AFC0
H1         H3         H5         H7         HM
00001002 00001000 00000998 00000995 00000998
IN
000039A0 FB0EB800 FFFFF600 00838000 00001756 05594BE0
H1         H3         H5         H7         HM
00001003 00001000 00000998 00000996 00000999
IN
000031A0 FB103800 FFFFECE0 00876800 00001756 055C5240
H1         H3         H5         H7         HM
00001005 00001003 00001000 00000998 00001001
```

Mean = 998 3 Standard Deviation =7

Table 6a. Statistical Data for Height Measurement of 12.8 μm Step with Surface Finish of 13 nm AA. Slope Relative to Datum ≈ 0.

```
IN
00052F60 FB576800 0004FE80 043E0000 00001756 055B2DA0
H1       H3       H5       H7       HM
00001003 00001001 00001000 00000998 00001000
IN
000540A0 FB53D800 0004FD60 043E2800 00001756 0554F9C0
H1       H3       H5       H7       HM
00000999 00000997 00000995 00000993 00000995
IN
000529E0 FB0A8800 0004F3C0 03EF5000 00001756 055DB360
H1       H3       H5       H7       HM
00001005 00001003 00001001 00000999 00001002
IN
00052F80 FB0A4000 0004EEC0 03F17000 00001756 055D5C40
H1       H3       H5       H7       HM
00001005 00001003 00001001 00000999 00001002
IN
00052840 FAFFB000 0004F8C0 03E31000 00001756 055CB680
H1       H3       H5       H7       HM
00001004 00001002 00001001 00000999 00001001
IN
000532C0 FAFA1000 0004FC60 03DFA800 00001756 05587020
H1       H3       H5       H7       HM
00001001 00000999 00000997 00000996 00000998
IN
00052BA0 FAFED800 0004F240 03E59000 00001756 055EC720
H1       H3       H5       H7       HM
00001006 00001004 00001002 00001000 00001003
IN
00052E20 FAF8D800 0004EE40 03E0D000 00001756 055EFEA0
H1       H3       H5       H7       HM
00001007 00001004 00001002 00001000 00001003
IN
00053220 FAFA3800 0004F500 03DF8000 00001756 05594460
H1       H3       H5       H7       HM
00001002 00001000 00000998 00000996 00000999
IN
00052CA0 FAFAF800 0004F540 03DED000 00001756 055B0120
H1       H3       H5       H7       HM
00001003 00001001 00000999 00000997 00001000
```

Mean = 1000   3 Standard Deviations = 7

Table 6b. Statistical Data for Height Measurement of 12.8 μm Step with Surface Finish of 13 nm AA. Slope Relative to Datum = Maximum Positive Value

```
IN
00000000 07FF0000 00000000 07FF0000 00001756 00000000
H1       H3       H5       H7       HM
00000000 00000000 00000000 00000000 00000000
IN
FFF6F8E0 01F20800 FFF6C600 01130000 00001756 055B3BA0
H1       H3       H5       H7       HM
00001003 00001001 00001000 00000998 00001000
IN
FFF70180 01F3E000 FFF6C380 01174000 00001756 0558E200
H1       H3       H5       H7       HM
00001002 00001000 00000998 00000996 00000998
IN
FFF707A0 01F01800 FFF6CDC0 01117000 00001756 055234A0
H1       H3       H5       H7       HM
00000997 00000995 00000993 00000991 00000993
IN
FFF70400 01F48000 FFF6DC20 01133800 00001756 05502CA0
H1       H3       H5       H7       HM
00000994 00000993 00000992 00000990 00000992
IN
FFF70360 01DEC800 FFF6D760 00FEE800 00001756 05527200
H1       H3       H5       H7       HM
00000996 00000995 00000993 00000992 00000994
IN
FFF6FCC0 008F7000 FFF6C1C0 FFB21000 00001756 055B1500
H1       H3       H5       H7       HM
00001003 00001001 00000999 00000997 00001000
IN
FFF6F480 0091A000 FFF6C700 FFB24000 00001756 055D5480
H1       H3       H5       H7       HM
00001004 00001003 00001001 00001000 00001001
IN
FFF6FFA0 0090D800 FFF6C640 FFB29000 00001756 05580720
H1       H3       H5       H7       HM
00001001 00000999 00000997 00000995 00000998
IN
FFF70920 008AF800 FFF6C880 FFB0A000 00001756 055632E0
H1       H3       H5       H7       HM
00001000 00000998 00000996 00000994 00000996
IN
FFF6FC60 00920800 FFF6CF40 FFB13000 00001756 05566860
H1       H3       H5       H7       HM
00000999 00000998 00000996 00000995 00000996

>
  Mean = 997      3 Standard Deviations = 9
```

Table 6c. Statistical Data for Height Measurement of 12.8 μm Step with Surface Finish of 13 nm AA. Slope Relative to Datum = Maximum Negative Value

APPENDIX G*

THE AA CALCULATION AND AMERICAN NATIONAL STANDARD B46.1

The AA roughness value of a surface profile is defined as the arithmetic average deviation of the surface profile from its center line; this center line in turn is defined by American National Standard B46.1 as "the line parallel to the general direction of the profile within the limits of the roughness width cut-off, such that the sums of the areas contained between it and those parts which lie on either side of it are equal".

The specific details involved in the implementation of these definitions in the operation of analog or digital devices are not delineated in the standard. While band-pass characteristics in terms of half-power points and roll-off rates are specified, the exact nature of center-line, to which a profile is instantaneously referenced, is not clearly specified (again see appendix A for filter characteristics).

In the operation of an integrating-meter stylus instrument, the filtered signal represents the surface profile with wavelength cut-off restriction imposed. The continuous analog computations of the center line and average deviation from the center line are made by integrating circuitry. Specifically, the stylus instrument stroke is begun at time T_1 and the resulting signal averaged up to time t to establish a center-line; beginning at a particular point, T_2, in the stroke, the instantaneous signal is compared to the established center line and the magnitude of the difference is averaged over a further length of the stroke to time T_3. Mathematically, the operation corresponds to the integral:

$$AA = \frac{1}{T_3 - T_2} \int_{T_2}^{T_3} \left[\text{Abs} \left\{ f(t) - \frac{1}{t - T_1} \int_{T_1}^{t} f(t')dt' \right\} \right] dt.$$

This equation reflects the necessity in an analog device of comparing the instantaneous signal to a center line which does not bracket the signal, but rather represents a segment of the profile of which the signal is the trailing edge.

In the operation of the present digital system, the filtered signal is digitized and stored in the computer memory; the conversion rate (1.64 kHZ) is sufficiently high to reproduce the analog information in the filter bandpass (-3dB frequency is 300 HZ) with no loss of fidelity. The record length of the data corresponds to five wavelength cut-off widths. Since wavelength cut-off restrictions have

*From DASR (Revised).

been imposed on the signal by filtering, the center line is computed over the record length. Mathematically, the operation corresponds to the integral:

$$AA = \frac{1}{T} \int_0^T \left[\mathrm{Abs} \left(f(t) - \frac{1}{T} \int_0^T f(t')dt' \right) \right] dt.$$

Although the mathematical descriptions of the analog and digital computations differ, it is believed that the digital computations are in accord with the present American National Standard B46.1 on surface texture, in terms of the fundamental definitions of AA and the center line. Since the effective center line is computed as the mean over the record length and the record width is five times the cut-off width, the effect of a fractional roughness wavelength in the record length is greatly diminished.

APPENDIX H

STATISTICAL EVALUATION OF THE LONG TERM STABILITY OF STEP CALIBRATED ROUGHNESS MEASUREMENTS

In cooperation with Joseph M. Cameron of the Office of Measurement Services at NBS, a statistical evaluation of the procedure for measuring surface roughness was performed. The measurements for this study were made over the period extending from November 9, 1973 to January 30, 1974. The specific days of measurement were: operator 1; November 9 and 12, 1973; operator 2; November 12, 13 and 14, 1973 and January 4, 21, 25, 28 and 30, 1974. Each day the procedure consisted of calibrating the system at two magnifications with an interferometrically measured step then measuring the specimen roughness for three traverses at the number of positions indicated in the enclosed memorandum. The specimen used for the evaluation was a precision roughness specimen conforming to American National Standard B46.1-1962. Only a small area of each patch, approximately 3 mm by 25 mm, was used for the study to minimize the effect of positional variations on the resultant data. Random positions within this area were used for the indiated measurements.

The following memorandum presents Joseph M. Cameron's analysis of the data.

U.S. DEPARTMENT OF COMMERCE
National Bureau of Standards
Washington, D.C. 20234

Date: July 19, 1974

To: Clayton Teague
Dimensional Technology Section
Optical Physics Division

From: J. M. Cameron, Chief
Office of Measurement Services

Subject: Analysis of Roughness Data

A. Structure of the Data

Two patterns of observations were made.

1. Triplicate measurements were made on each of 6 positions on 5 different days.
2. Triplicate measurements were made on each of 10 positions on 5 different days subsequent to those in (1).

Both patterns were carried out on specimens of nominal value 20(AA) and 120(AA). For each day a new correction factor was used to normalize the results.

Table I and Table II give the triplicate values and their average and standard deviation based on the differences among the triplicate (d.f. = 2) for 20(AA) and 120(AA) respectively.

B. Variability Within Triplicate

Figure 1 and figure 2 plot the deviations of the triplicate measurements from their averages and show quite clearly that triplicate numbers 4, 56, and 68 on the 20(AA) data and number 61 on the 120(AA) data are not consistent with the remainder of the data. If these triplicates are omitted, then the "within triplicate" standard deviations are:

Nominal	d.f.	s.d.	s.d. of Average of Three
20(AA)	151	.0486	.0280
120(AA)	157	.5320	.3070

These values of standard deviation would serve as "accepted" values for control of the measurement process. Because the other components of variation are much larger (as will be seen later), the addition of more runs with only duplicates instead of triplicates would be the better partition of a fixed number of observations.

C. Day-to-Day Component of Variation

Let y denote the average of the triplicate measurements, then its value on the i^{th} day on the j^{th} position can be written as

$$y = \mu_j + \delta_i + \varepsilon_{ij}$$

where μ_j is the value for the j^{th} position; δ_i is the random error due to day-to-day variations--$Var(\delta_i) = \sigma_B^2$; ε_{ij} is the random error of the average about the value for the position and day $V(\varepsilon_{ij}) = \sigma^2$.

The variance of y can be represented as

$$Var(y) = \sigma_B^2 + \sigma^2$$

The daily average of n positions will have the structure

$$\text{average for the } i^{th} \text{ day} = \bar{y}_i = \bar{\mu} + \delta_i + \Sigma\varepsilon_{ij}/n$$

$$V(\bar{y}_i) = \sigma_B^2 + \sigma^2/n$$

Table III gives the daily averages for the two nominal roughness specimens and table IV shows the estimates of the variance component.

TABLE III: Deviation of Daily Average From Overall Average

		20 AA		120 AA
6 positions	Day 1	.1674	6 positions	-.047
Overall	2	-.1526	Overall	.009
Average 1888.64	3	-.0209	Average 1196.35	-.297
	4	-.1064		.081
	5	.1124		.253
10 positions	Day 1	.1036	10 positions	.349
Overall	2	-.2297	Overall	.003
Average 1887.78	3	.0383	Average 1194.94	.629
	4	.0066		-.474
	5	.0813		-.507

TABLE IV: Estimation of Variance Components

20 AA	s.d. of Daily Averages (d.f. = 4)	Between Day Component σ_B^2	$\hat{\sigma}^2$	$\hat{\sigma}_B$	$\hat{\sigma}$
6 positions	.1376	.017956	.0058	.1340	.0764
10 positions	.1338	.016824	.0108	.1297	.1040
Combined	.1350 (10 days)	.017390	.0083	.1319	.0912
120 AA					
6 positions	.237	*	.3367	*	.5800
10 positions	.500	.2238	.2624	.4730	.5120
Combined	.368 (10 days)	.1138	.2930	.3370	.5470

*Between component not present.

The standard deviation of the daily averages* would have to be taken as the appropriate variability for assessing the uncertainty of the roughness measurements. This leads to a 3 s.d. limit of .40 AA on a mean of 18.88 (or a percentage uncertainty of 2.1%) for the 20 AA specimen and to a 3 s.d. limit of 1.1 AA on a mean of 119.5 for a percentage uncertainty of 0.9% for the 120 AA specimen.

Figures 3 and 4 plot the deviations of the daily values from the averages for the positions for the 20 AA specimen and 120 AA specimen respectively. Figures 5 and 6 show the values for the specimens on successive days.

For the 20 AA specimen, statistically significant position-to-position variation exists whereas it does not for the 120 AA specimen. These are shown in Table V as deviations from the grand average.

*s.d. of average of ten values = $\sqrt{\sigma_B^2 + \sigma^2/10}$ give combined value of .135 for 20 AA and .368 for 120 AA.

TABLE V: Deviations of Position Averages From Overall Average*

	20 AA	120 AA
Position 1	.1469	.411
2	-.0798	-.069
3	-.0244	-.002
4	-.0364	-.249
5	.0176	-.169
6	-.0238	.078
Position 1	.2209	.213
2	-.0664	.153
3	-.0984	-.107
4	-.0677	.139
5	.0363	-.094
6	.0443	-.001
7	-.0391	-.001
8	.0703	-.121
9	-.0437	-.081
10	-.0564	-.101

*s.d. of position average = $\frac{1}{\sqrt{5}}$ s.d. (avg. of three) is .064 for 20 AA and .210 for 120 AA.

D. Correction Factor

Each day a correction factor was determined and used with the results of that day. Table 6 shows these correction factors along with the daily averages and their corresponding rankings. Figure 6 is a plot of the rankings of the daily averages as a function of the rankings of the correction factor. No significant dependence of the results on the magnitude of the correction factors is apparent.

TABLE VI: Correction Factors

	20 AA				120 AA			
Day	Correction Factors	RANK	Daily Average	RANK	Correction Factors	RANK	Daily Average	RANK
			6 Positions					
1	45778	3	.167	5	44184	3	-.047	2
2	46070	5	-.153	1	44230	4	.009	3
3	45680	2	-.021	3	44142	2	-.297	1
4	45394	1	-.106	2	44052	1	.081	4
5	45834	4	.112	4	44290	5	.253	5
			10 Positions					
6	45148	3	.104	5	43902	5	.349	4
7	45032	2	-.230	1	43856	4	.003	3
8	45164	4	.038	3	43630	2	.629	5
9	45016	1	.007	2	43316	1	-.474	2
10	45732	5	.081	4	43664	3	-.507	1

Figure 5: Ranking of Daily Average as a Function of the Ranking of Correction Factors

```
5      *             *                 *       *
4        *               *     *                     *
3    *                 *             *             *
2  *             *                 *         *
1          *       *             *               *
   1 2 3 4 5     1 2 3 4 5     1 2 3 4 5     1 2 3 4 5
    6 pos.        10 pos.       6 pos.       10 pos.
          20 AA                        120 AA
```

Conclusions: The following conclusions emerge from the analysis.

(1) The standard deviation of the average of k values is $0.0486/\sqrt{k}$-μin for the 20 μin AA and $0.5320/\sqrt{k}$-μin for the 120-μin AA specimens which turns out to be 0.028 μin and 0.31 μin respectively for k=3. One would use these values to establish process control on the range of duplicate or triplicate measurements.

(2) If an average of values from 10 positions is used to establish a value for a test specimen, then the standard deviation associated with such averages is .135 for 20 AA and .378 for 120 AA ignoring position-to-position (i.e., if one could return to the same 10 positions).

(3) If there are significant position-to-position variations, then the question as to how well the average of 10 positions represents the specimen is brought into focus. The value for a single position will have standard deviation $\sqrt{\sigma_\beta^2 + \sigma^2}$ which turns out to be .427 for 20 AA and .6378 for 120 AA. If one regards the position variation as having a variance component σ_p^2, then the standard deviation based on ten positions has the long-run value $\sqrt{\sigma_p^2 + \sigma_\beta^2 + \sigma^2}$.

Thus if the 10 positions are selected at random, the average, $\bar{y}$, will have a standard deviation that can be estimated by $s = \sqrt{\sum_1^{10} (y-\bar{y})^2/9}$.

(It would not be proper to use the triplicate values and compute s using 30 values and with divisor 29 because of the correlation of the triplicate values with each other.)

ROUGHNESS = 20 (AA)

TABLE I: Summary of Roughness Data

Pos.	DAY	NUMBER	X(1)	X(2)	X(3)	AVERAGE	S.D.(DF=2)	S.D.(DF=160)
1	1	1.0000	19.2800	19.1900	19.1700	19.2133	.0586	.0651
	2	2.0000	18.9800	19.0500	19.0400	19.0233	.0379	.0651
	3	3.0000	18.9800	19.0100	18.9300	18.9733	.0404	.0651
	4	4.0000	19.0500	18.8000	18.7800	18.8767	.1504	.0651
	5	5.0000	19.1100	19.0300	19.1000	19.0800	.0436	.0651
2	1	6.0000	18.9100	18.9200	18.9700	18.9333	.0321	.0651
	2	7.0000	18.6300	18.6600	18.6600	18.6500	.0173	.0651
	3	8.0000	18.7100	18.6300	18.6400	18.6600	.0436	.0651
	4	9.0000	18.7700	18.7400	18.7200	18.7433	.0252	.0651
	5	10.0000	19.0300	19.0400	19.0700	19.0467	.0208	.0651
3	1	11.0000	19.0200	19.0400	19.0600	19.0400	.0200	.0651
	2	12.0000	18.7100	18.7600	18.7300	18.7333	.0252	.0651
	3	13.0000	18.8500	18.8500	18.7100	18.8033	.0308	.0651
	4	14.0000	18.7800	18.7000	18.7400	18.7400	.0400	.0651
	5	15.0000	18.9800	18.9700	19.0300	18.9933	.0321	.0651
4	1	16.0000	18.9800	19.0000	19.0200	19.0000	.0200	.0651
	2	17.0000	18.6000	18.6800	18.7000	18.6600	.0529	.0651
	3	18.0000	19.0100	18.8900	18.8500	18.9167	.0833	.0651
	4	19.0000	18.7900	18.7100	18.7200	18.7400	.0436	.0651
	5	20.0000	18.9800	18.9400	18.8800	18.9333	.0503	.0651
5	1	21.0000	19.0700	19.0600	19.0700	19.0667	.0058	.0651
	2	22.0000	18.6200	18.6700	18.7400	18.6767	.0603	.0651
	3	23.0000	19.0400	18.9800	18.9900	19.0033	.0321	.0651
	4	24.0000	18.8600	18.9000	18.8000	18.8533	.0503	.0651
	5	25.0000	18.9200	18.8900	18.9500	18.9200	.0300	.0651
6	1	26.0000	19.1200	19.0500	19.0400	19.0700	.0436	.0651
	2	27.0000	18.6600	18.6500	18.6700	18.6600	.0100	.0651
	3	28.0000	18.8400	18.8300	18.8400	18.8367	.0058	.0651
	4	29.0000	18.7300	18.7700	18.6800	18.7267	.0451	.0651
	5	30.0000	19.0800	19.0600	18.9200	19.0200	.0872	.0651
1	6	31.0000	19.1800	19.2000	19.1800	19.1867	.0115	.0651
	7	32.0000	18.8600	18.8400	18.8200	18.8400	.0200	.0651
	8	33.0000	19.2700	19.1200	19.1400	19.1767	.0814	.0651
	9	34.0000	19.3300	19.2600	19.1100	19.2333	.1124	.0651
	10	35.0000	19.0200	19.0800	19.0700	19.0567	.0321	.0651
2	6	36.0000	19.0300	19.0700	19.1200	19.0733	.0451	.0651
	7	37.0000	18.7600	18.6300	18.6200	18.6700	.0781	.0651
	8	38.0000	18.5300	18.6200	18.6500	18.6000	.0624	.0651
	9	39.0000	18.7800	18.7800	18.8000	18.7867	.0115	.0651
	10	40.0000	18.9100	18.9200	18.9500	18.9267	.0208	.0651
3	6	41.0000	18.7300	18.7600	18.7400	18.7433	.0153	.0651
	7	42.0000	18.5200	18.5000	18.3900	18.4700	.0700	.0651
	8	43.0000	18.9200	18.9800	18.9200	18.9400	.0346	.0651
	9	44.0000	18.7900	18.8000	18.8500	18.8133	.0321	.0651
	10	45.0000	18.9600	18.8700	18.9600	18.9300	.0520	.0651
4	6	46.0000	18.8800	18.8500	18.8300	18.8533	.0252	.0651
	7	47.0000	18.6500	18.6100	18.7200	18.6600	.0557	.0651
	8	48.0000	18.7400	18.8000	18.7400	18.7600	.0346	.0651
	9	49.0000	18.8100	18.8900	18.8900	18.8633	.0462	.0651
	10	50.0000	18.9600	18.9200	18.8600	18.9133	.0503	.0651

OMNITAB CLAYTON TEAGUE (2181) == ROUGHNESS DATA (1 JULY)

ROUGHNESS = 20 (AA)

TABLE I (cont.)

Pos.	Day	NUMBER	X(1)	X(2)	X(3)	AVERAGE	S.D.(DF=2)	S.D.(DF=160)
5	6	51.0000	18.9700	18.9400	18.9400	18.9500	.0173	.0651
	7	52.0000	18.7200	18.7000	18.7000	18.7067	.0115	.0651
	8	53.0000	18.9300	18.9600	19.0700	18.9867	.0737	.0651
	9	54.0000	18.9200	18.9500	18.9000	18.9233	.0252	.0651
	10	55.0000	19.0100	18.9400	19.0600	19.0033	.0603	.0651
6	6	56.0000	18.9300	19.1800	19.4700	19.1933	.2702	.0651
	7	57.0000	18.7700	18.7000	18.7300	18.7333	.0351	.0651
	8	58.0000	18.8300	18.7600	18.8700	18.8200	.0557	.0651
	9	59.0000	18.8200	18.8100	18.8300	18.8200	.0100	.0651
	10	60.0000	19.1100	19.1000	18.9200	19.0433	.1069	.0651
7	6	61.0000	18.8300	18.8700	18.7700	18.8233	.0503	.0651
	7	62.0000	18.6300	18.6300	18.5300	18.5967	.0577	.0651
	8	63.0000	18.8900	18.3700	18.9800	18.9133	.0586	.0651
	9	64.0000	18.8700	18.8900	18.8400	18.8667	.0252	.0651
	10	65.0000	18.9900	18.9300	19.0600	18.9933	.0651	.0651
8	6	66.0000	19.0900	19.1400	18.9800	19.0700	.0819	.0651
	7	67.0000	18.5800	18.7000	18.6200	18.6333	.0611	.0651
	8	68.0000	18.9600	18.9800	19.4000	19.1133	.2435	.0651
	9	69.0000	18.8500	18.8500	18.8900	18.8633	.0231	.0651
	10	70.0000	19.1000	19.0500	19.0300	19.0600	.0351	.0651
9	6	71.0000	19.0700	19.0500	19.1600	19.0933	.0586	.0651
	7	72.0000	18.6300	18.5400	18.6200	18.5967	.0493	.0651
	8	73.0000	18.9200	18.8500	18.8700	18.8800	.0361	.0651
	9	74.0000	18.8700	18.8000	18.8100	18.8267	.0379	.0651
	10	75.0000	18.7600	18.7800	18.7600	18.7733	.0115	.0651
10	6	76.0000	18.8300	18.8100	18.8400	18.8267	.0153	.0651
	7	77.0000	18.5800	18.6100	18.5300	18.5733	.0404	.0651
	8	78.0000	18.9400	18.9400	19.0300	18.9700	.0520	.0651
	9	79.0000	18.8300	18.7900	18.9200	18.8467	.0666	.0651
	10	80.0000	18.8900	18.8600	18.9200	18.8900	.0300	.0651

ROW/COL	37	38	39	40	41	42	43
1	19.2133	18.9333	19.0400	19.0000	19.0667	19.0700	-1000.0000
2	19.0233	18.6500	18.7333	18.6600	18.6767	18.6600	-1000.0000
3	18.9733	18.6600	18.8033	18.9167	19.0033	18.8367	-1000.0000
4	18.8767	18.7433	18.7400	18.7400	18.8533	18.7267	-1000.0000
5	19.0800	19.0467	18.9933	18.9333	18.9200	19.0200	-1000.0000
6	19.1867	19.0733	18.7433	18.8533	18.9500	19.1933	18.8233
7	18.6400	18.6700	18.4700	18.6600	18.7067	18.7333	18.5967
8	19.1767	18.6000	18.9400	18.7600	18.9867	18.8200	18.9133
9	19.2333	18.7867	18.8133	18.8633	18.9233	18.8200	18.8667
10	19.0567	18.9267	18.9300	18.9133	19.0033	19.0433	18.9933

ROW/COL	44	45	46
1	-1000.0000	-1000.0000	-1000.0000
2	-1000.0000	-1000.0000	-1000.0000
3	-1000.0000	-1000.0000	-1000.0000
4	-1000.0000	-1000.0000	-1000.0000
5	-1000.0000	-1000.0000	-1000.0000
6	19.0700	19.0933	18.8267
7	18.6333	18.5967	18.5733
8	19.1133	18.8800	18.9700
9	18.8633	18.8267	18.8467
10	19.0600	18.7733	18.8900

OMNITAB CLAYTON TEAGUE (2181) == ROUGHNESS DATA (1 JULY)

ROUGHNESS = 120

TABLE II: Summary of Roughness Data

Pos.	Day	NUMBER	X(1)	X(2)	X(3)	AVERAGE	S.D.(DF=2)	S.D.(DF=160)
1	1	1.000	119.200	119.400	119.000	119.200	.200	.571
	2	2.000	119.600	119.900	120.200	119.900	.300	.571
	3	3.000	120.000	119.500	118.500	119.333	.764	.571
	4	4.000	120.500	122.100	121.300	121.300	.800	.571
	5	5.000	120.300	120.500	120.700	120.500	.200	.571
2	1	6.000	120.300	119.600	119.700	119.867	.379	.571
	2	7.000	119.300	119.200	118.200	118.900	.608	.571
	3	8.000	120.300	119.600	119.500	119.800	.436	.571
	4	9.000	118.700	119.500	119.200	119.133	.404	.571
	5	10.000	120.000	121.200	119.200	120.133	1.007	.571
3	1	11.000	119.700	120.200	120.500	120.133	.404	.571
	2	12.000	120.200	119.600	120.200	120.000	.346	.571
	3	13.000	118.900	119.200	119.400	119.167	.252	.571
	4	14.000	119.600	119.900	119.500	119.667	.208	.571
	5	15.000	119.500	119.000	119.100	119.200	.265	.571
4	1	16.000	118.900	118.800	118.700	118.800	.100	.571
	2	17.000	119.600	120.200	119.600	119.800	.346	.571
	3	18.000	118.500	118.900	118.900	118.767	.231	.571
	4	19.000	119.600	119.600	119.800	119.667	.115	.571
	5	20.000	120.000	119.800	119.900	119.900	.100	.571
5	1	21.000	118.600	119.900	119.500	119.333	.666	.571
	2	22.000	120.200	119.800	119.900	119.967	.208	.571
	3	23.000	119.100	119.300	120.800	119.733	.929	.571
	4	24.000	118.400	119.400	118.900	118.900	.500	.571
	5	25.000	119.700	118.900	119.600	119.400	.436	.571
6	1	26.000	119.300	120.400	120.900	120.200	.819	.571
	2	27.000	119.300	120.000	118.600	119.300	.700	.571
	3	28.000	119.900	118.700	119.100	119.233	.611	.571
	4	29.000	119.800	118.800	120.300	119.633	.764	.571
	5	30.000	121.000	119.000	120.600	120.200	1.058	.571
1	6	31.000	119.700	121.200	120.100	120.333	.777	.571
	7	32.000	119.500	119.400	120.000	119.633	.321	.571
	8	33.000	119.800	120.900	119.700	120.133	.666	.571
	9	34.000	119.200	119.400	119.100	119.233	.153	.571
	10	35.000	119.700	118.500	119.400	119.200	.624	.571
2	6	36.000	120.200	119.500	119.400	119.700	.435	.571
	7	37.000	118.800	119.500	119.600	119.300	.436	.571
	8	38.000	120.600	119.800	120.100	120.167	.404	.571
	9	39.000	120.100	119.900	120.100	120.033	.115	.571
	10	40.000	119.800	118.500	118.800	119.033	.681	.571
3	6	41.000	119.600	118.600	120.100	119.433	.764	.571
	7	42.000	119.200	118.400	118.000	118.533	.611	.571
	8	43.000	120.200	119.800	120.400	120.133	.306	.571
	9	44.000	118.500	119.200	119.900	119.200	.700	.571
	10	45.000	119.500	119.400	120.000	119.633	.321	.571
4	6	46.000	120.600	121.500	121.400	121.167	.493	.571
	7	47.000	118.800	119.500	119.900	119.400	.557	.571
	8	48.000	120.500	120.800	120.500	120.600	.173	.571
	9	49.000	118.700	118.400	118.400	118.500	.173	.571
	10	50.000	119.300	118.600	117.600	118.500	.854	.571

OMNITAB CLAYTON TEAGUE (2181) == ROUGHNESS DATA (1 JULY)

ROUGHNESS = 120

TABLE II (cont.)

Pos.	Day	NUMBER	X(1)	X(2)	X(3)	AVERAGE	S.D.(DF=2)	S.D.(DF=160)
5	6	51.000	119.600	119.900	120.700	120.067	.569	.571
	7	52.000	118.500	119.600	119.500	119.200	.608	.571
	8	53.000	121.000	119.900	119.100	120.000	.954	.571
	9	54.000	119.000	118.400	118.600	118.667	.306	.571
	10	55.000	119.200	118.400	119.600	119.067	.611	.571
6	6	56.000	119.400	120.000	120.200	119.867	.416	.571
	7	57.000	120.000	118.900	120.000	119.633	.635	.571
	8	58.000	119.900	120.000	120.300	120.067	.208	.571
	9	59.000	119.500	119.200	118.800	119.167	.351	.571
	10	60.000	118.800	118.600	118.800	118.733	.115	.571
7	6	61.000	116.800	119.800	120.400	119.000	1.929	.571
	7	62.000	118.900	119.600	120.300	119.600	.700	.571
	8	63.000	119.300	121.400	120.500	120.400	1.054	.571
	9	64.000	119.500	119.700	118.800	119.333	.473	.571
	10	65.000	119.000	119.100	119.300	119.133	.153	.571
8	6	66.000	119.600	119.000	119.000	119.200	.346	.571
	7	67.000	119.000	119.400	119.900	119.433	.451	.571
	8	68.000	120.600	120.500	120.700	120.600	.100	.571
	9	69.000	119.200	118.800	117.600	118.533	.833	.571
	10	70.000	119.000	119.000	119.300	119.100	.173	.571
9	6	71.000	119.400	120.000	118.800	119.400	.600	.571
	7	72.000	119.000	120.700	120.100	119.933	.862	.571
	8	73.000	119.100	119.600	120.300	119.667	.603	.571
	9	74.000	118.700	118.700	119.500	118.967	.462	.571
	10	75.000	118.800	119.400	119.100	119.100	.300	.571
10	6	76.000	120.200	120.400	120.200	120.267	.115	.571
	7	77.000	120.300	120.700	119.900	120.300	.400	.571
	8	78.000	119.600	119.400	119.400	119.467	.115	.571
	9	79.000	118.500	118.700	118.500	118.567	.115	.571
	10	80.000	118.500	118.000	118.600	118.367	.321	.571

ROW/COL	37	38	39	40	41	42	43
1	119.200	119.367	120.133	118.800	119.333	120.200	-1000.000
2	119.900	118.900	120.000	119.800	119.967	119.300	-1000.000
3	119.333	119.800	119.167	118.767	119.733	119.233	-1000.000
4	121.300	119.133	119.667	119.667	118.900	119.633	-1000.000
5	120.500	120.133	119.200	119.900	119.400	120.200	-1000.000
6	120.333	119.700	119.433	121.167	120.067	119.867	119.000
7	119.633	119.300	118.533	119.400	119.200	119.633	119.600
8	120.133	120.167	120.133	120.600	120.000	120.067	120.400
9	119.233	120.033	119.200	118.500	118.667	119.167	119.333
10	119.200	119.033	119.633	118.500	119.067	118.733	119.133

ROW/COL	44	45	46
1	-1000.000	-1000.000	-1000.000
2	-1000.000	-1000.000	-1000.000
3	-1000.000	-1000.000	-1000.000
4	-1000.000	-1000.000	-1000.000
5	-1000.000	-1000.000	-1000.000
6	119.200	119.400	120.267
7	119.433	119.933	120.300
8	120.600	119.667	119.467
9	118.533	118.967	118.567
10	119.100	119.100	118.367

OMNITAB CLAYTON TEAGUE (2181) == ROUGHNESS DATA (1 JULY) PAGE 2

ROUGHNESS = 20 (AA)

ABS- NUMBER,ORD- COLUMN 25 (.), COLUMN 26 (*), COLUMN 27 (+),
TOTAL NO. OF PTS. PLOTTED IS 240 AND NO. NOT PLOTTED BECAUSE THEY FALL OUTSIDE OF BOUNDS IS 0

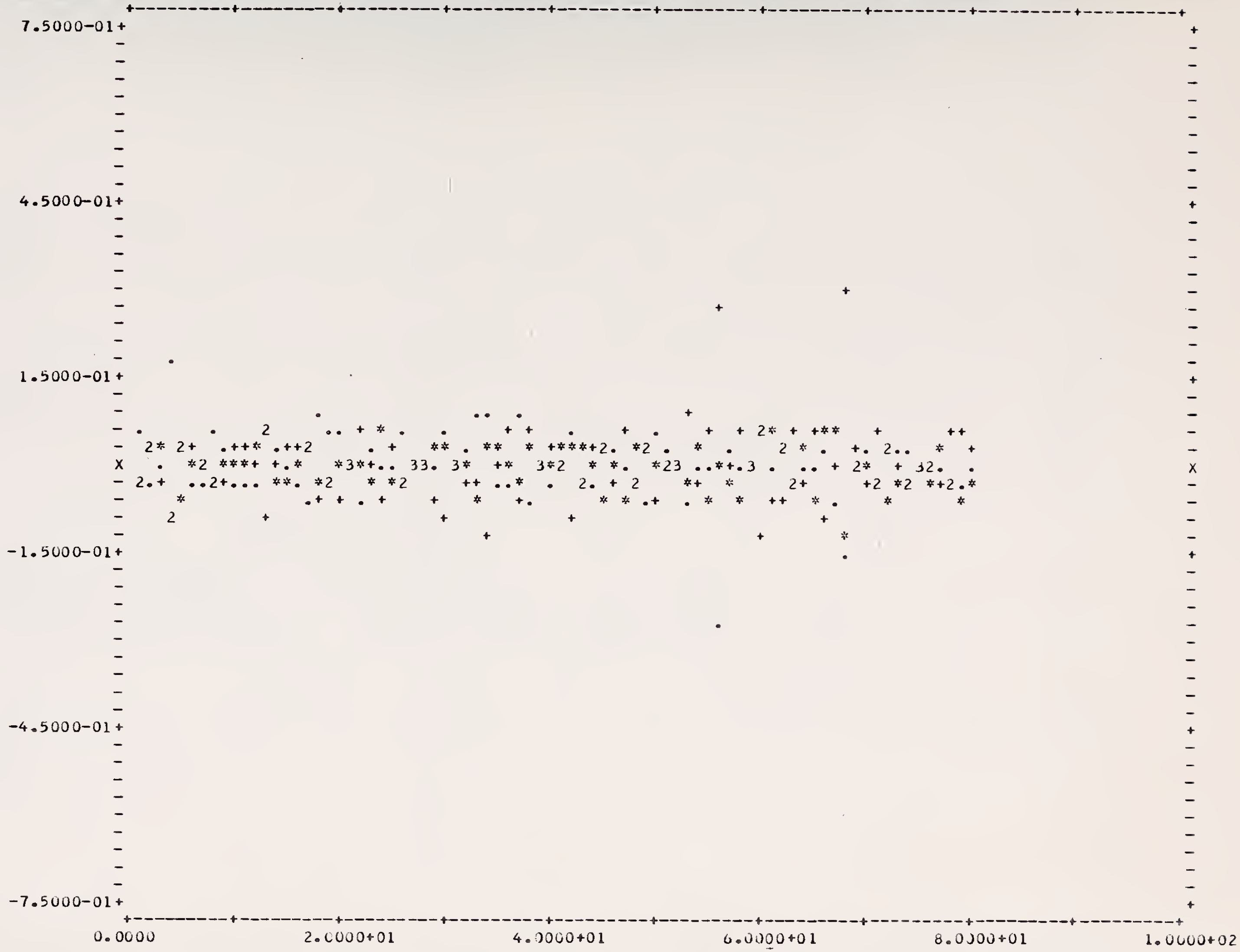

FIGURE 1: Deviation of Triplicate Measurements From Their Own Average
(Data in same order as in table I)

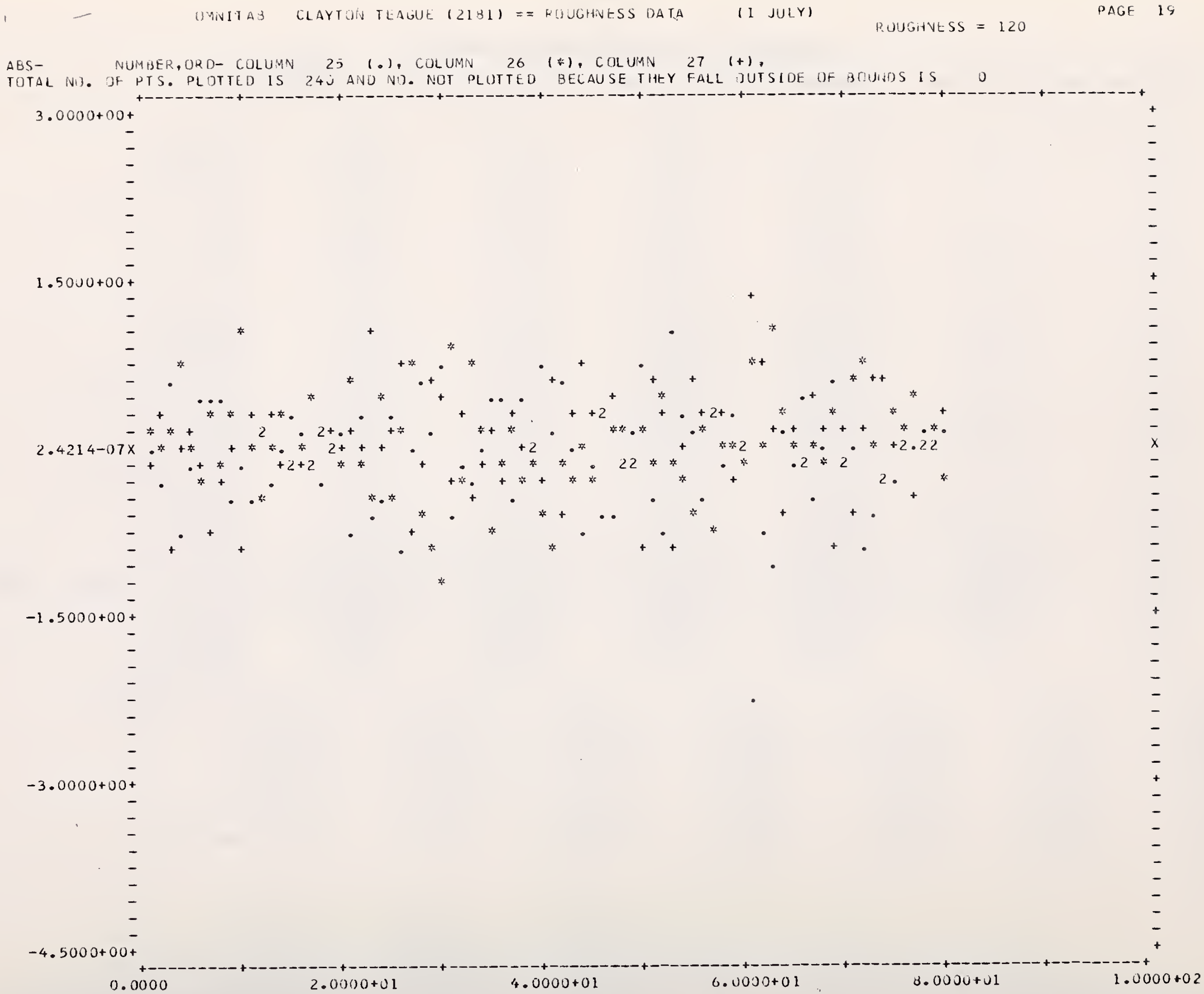

FIGURE 2: Deviation of Triplicate Measurements From Their Own Average (Data in same order as in table II)

OMNITAB CLAYTON TEAGUE (2131) == ROUGHNESS DATA (1 JULY) PAGE 6
ROUGHNESS = 20 (AA)

ABS- COLUMN 47 ,ORD- COLUMN 37 (.), COLUMN 38 (*), COLUMN 39 (+), COLUMN 40 (,), COLUMN 41 (-),
TOTAL NO. OF PTS. PLOTTED IS 80 AND NO. NOT PLOTTED BECAUSE THEY FALL OUTSIDE OF BOUNDS IS 0

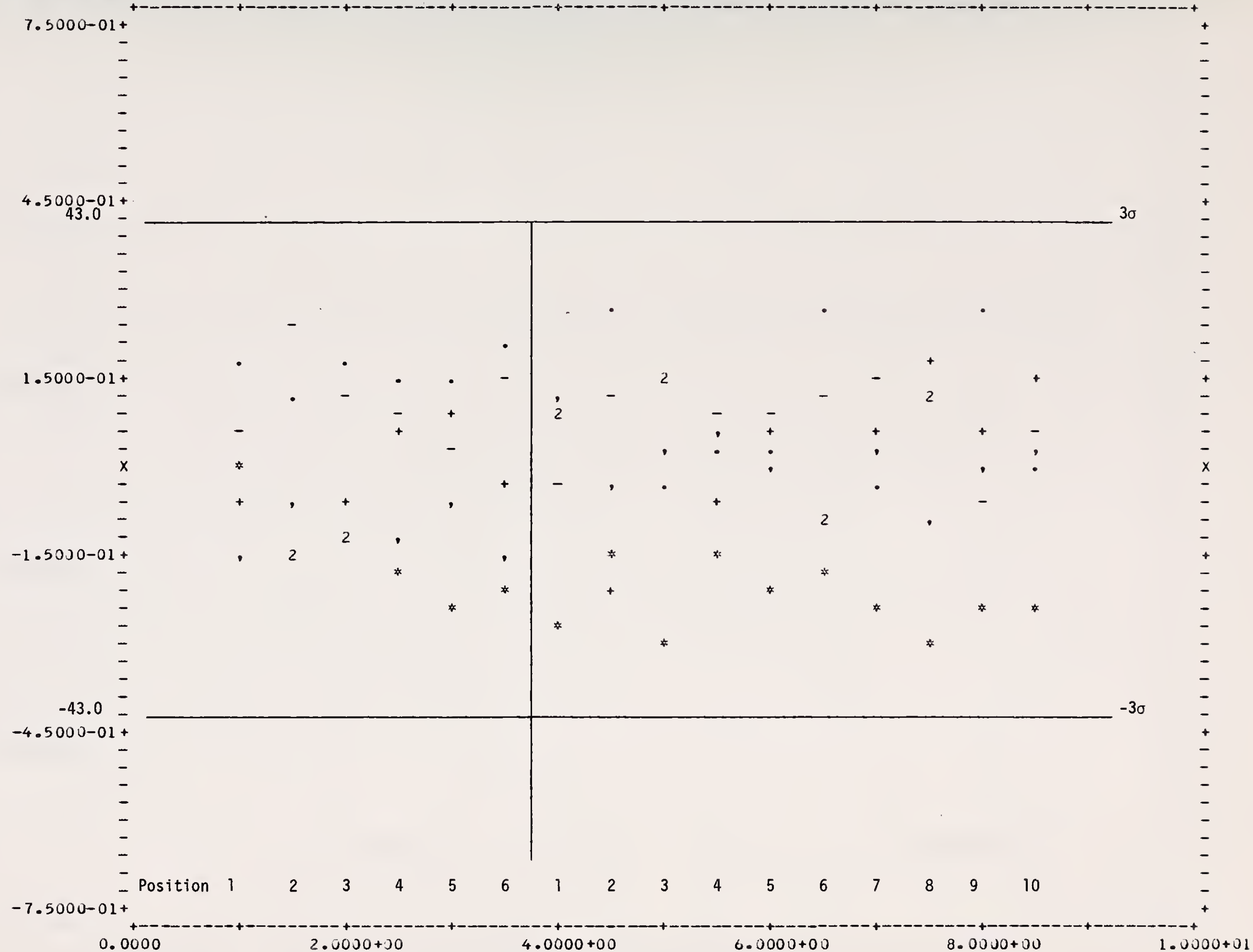

FIGURE 3: Variation of Values From 5 Days For Each Position About the Average for the Position (20 AA)

OMNITAB CLAYTON TEAGUE (2181) == ROUGHNESS DATA (1 JULY) PAGE 23

ROUGHNESS = 120

ABS- COLUMN 47 ,ORD- COLUMN 37 (.), COLUMN 38 (*), COLUMN 39 (+), COLUMN 40 (,), COLUMN 41 (-),
TOTAL NO. OF PTS. PLOTTED IS 80 AND NO. NOT PLOTTED BECAUSE THEY FALL OUTSIDE OF BOUNDS IS 0

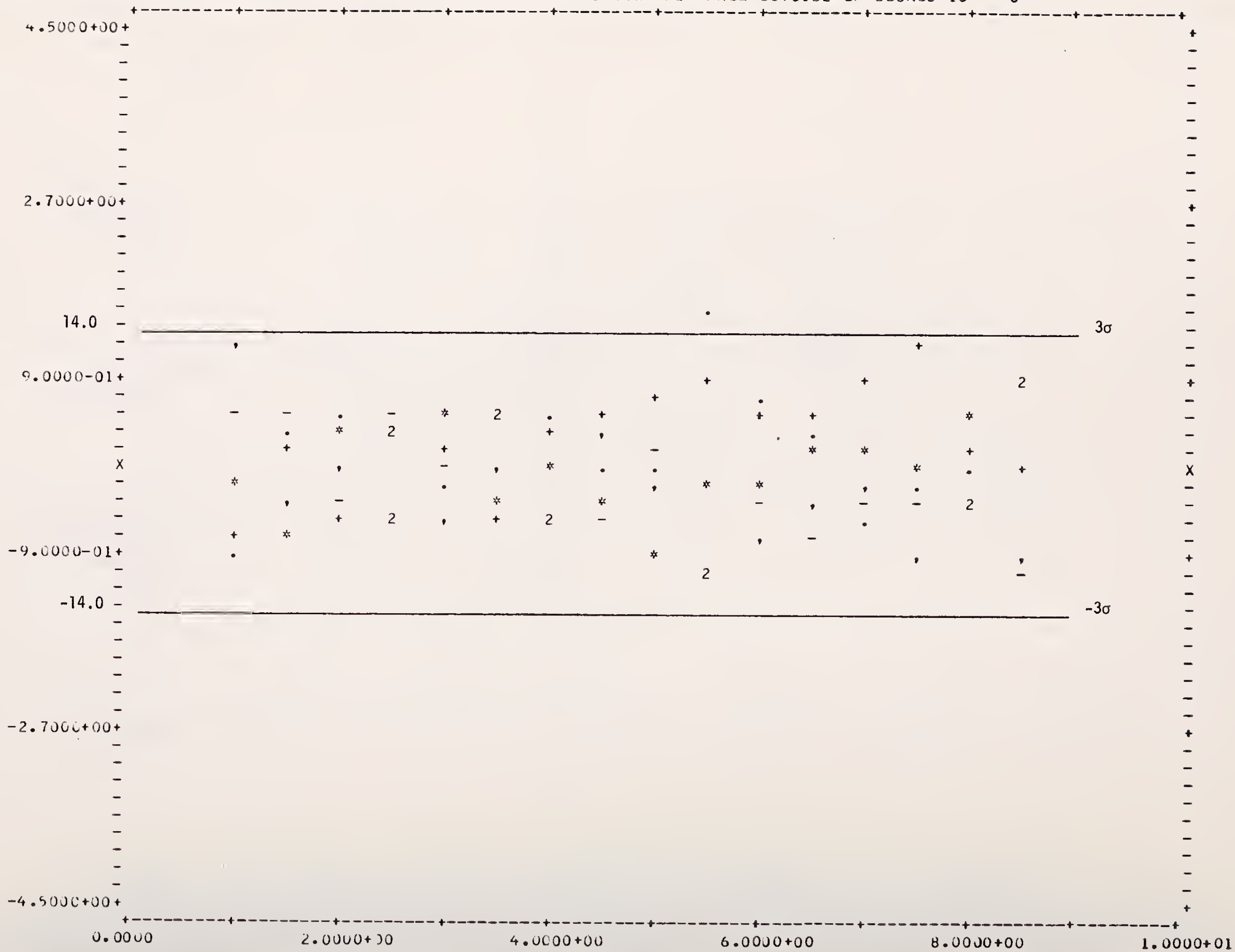

FIGURE 4: Variation of Values From 5 Days For Each Position About Average for the Position (120 AA)

OMNITAB CLAYTON TEAGUE (2181) == ROUGHNESS DATA (1 JULY) PAGE 5

ROUGHNESS = 20 (AA)

ABS- COLUMN 47 ,ORD- COLUMN 37 (.), COLUMN 38 (*), COLUMN 39 (+), COLUMN 40 (,), COLUMN 41 (-),

TOTAL NO. OF PTS. PLOTTED IS 80 AND NO. NOT PLOTTED BECAUSE THEY FALL OUTSIDE OF BOUNDS IS 20

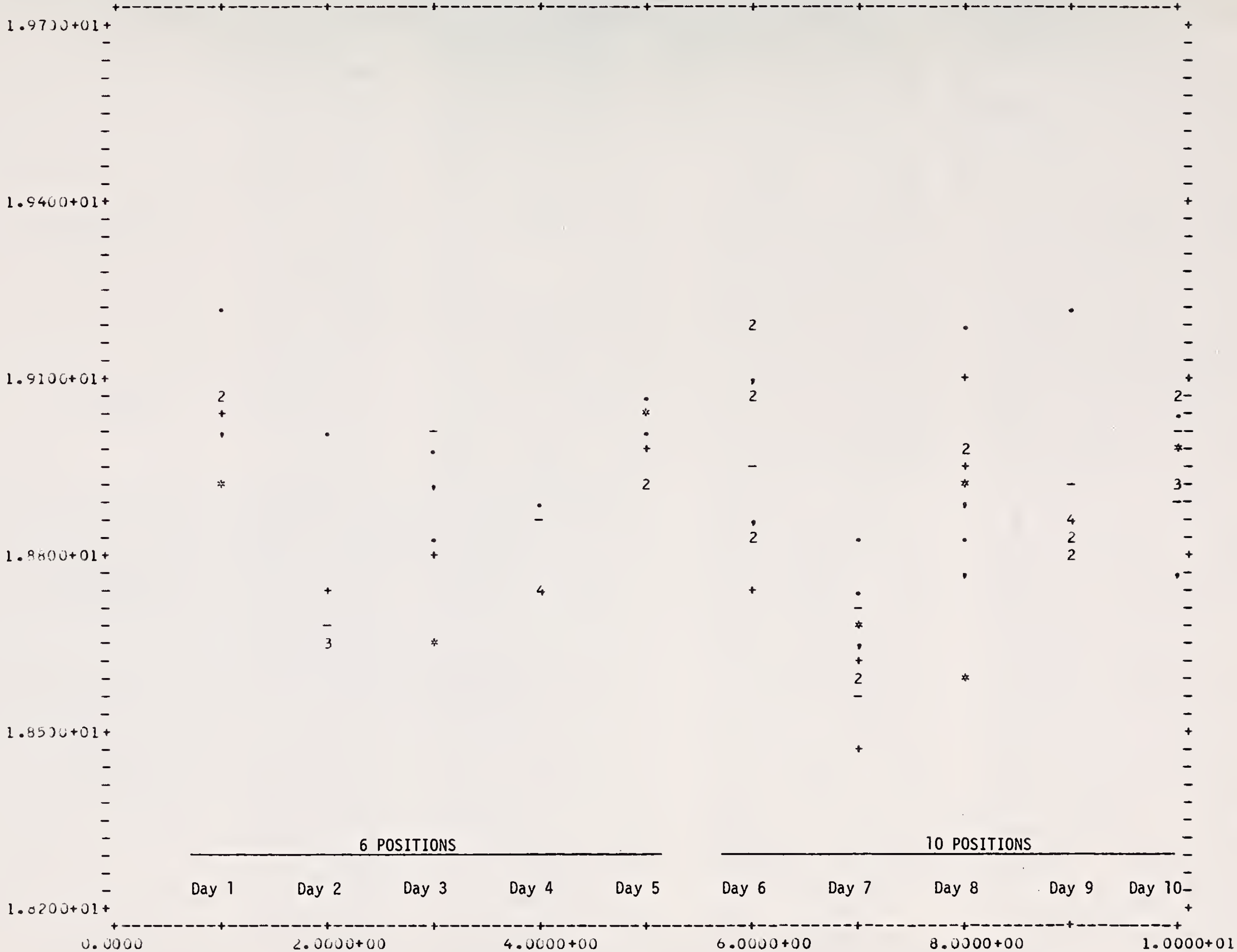

FIGURE 5: Variation of Position Values on Different Days

OMNITAB   CLAYTON TEAGUE (2181) == ROUGHNESS DATA   (1 JULY)   PAGE 22

ROUGHNESS = 120

ABS- COLUMN 47 ,ORD- COLUMN 37 (.), COLUMN 38 (*), COLUMN 39 (+), COLUMN 40 (,), COLUMN 41 (-),
TOTAL NO. OF PTS. PLOTTED IS 80 AND NO. NOT PLOTTED BECAUSE THEY FALL OUTSIDE OF BOUNDS IS 20

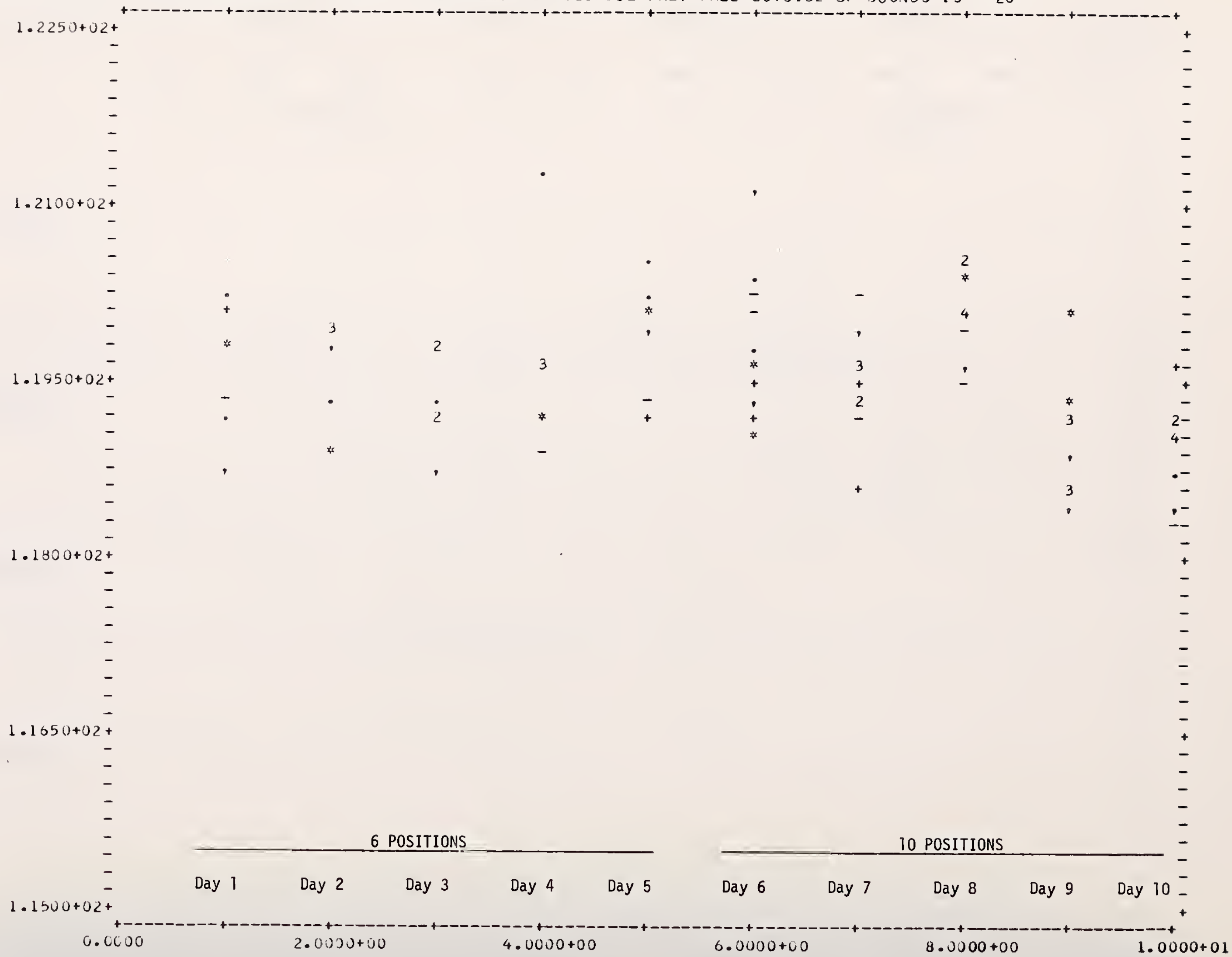

FIGURE 6: Variation of Position Values on Different Days

APPENDIX I

STYLUS TIP RADIUS MEASUREMENTS

Periodically the stylus tip radius used in the NBS roughness measurement system is measured by obtaining a profile of the tip as it is traversed across an edge whose radius of curvature is very small compared to that of the stylus tip. Most razor-blades manufactured after about 1960 have edges whose radii of curvature are less than 0.1 µm [19]. The radius of curvature observed in the profile obtained from the motion of a stylus tip across a razor-blade edge is equal to the sum of the tip radius and any curvature present in the razor-blade edge. Thus, the observed radius of curvature is an upper bound on the tip radius i.e., the tip radius is less than or equal to that observed in the profile.

For graphical determinations of the tip radius large, equal vertical and horizontal magnifications should be used. The profile in figure 30 was obtained in the most recent measurements of the stylus's tip radius. A convenient method for estimating the radii of inscribed and circumscribed circles for tips with a 90° included angle is to measure the distance from the point of intersection of lines drawn along the tip sides to the estimated points of tangency with the measured profile. The results of this procedure are illustrated in figure 30.

Based on the two radii values shown in figure 30, an estimated tip radius would be (3.4 ± 0.6 µm). This estimate does not include any uncertainty due to elastic or plastic motion of the razor-blade edge during the motion. However, profiles of the tip were obtained at several different positions along the razor-blade edge and by traversing the tip across the same position several times. All the profiles measured were very similar in shape and had approximately the same radii of curvature as the one shown in figure 30.

A further confirmation of this radius value and of the measurement technique was obtained by making a photomicrograph of one face of the pyramidal tip. The photomicrograph is shown as an insert in figure 30; the included angle is approximately 70° which is the angle expected when looking in a direction perpendicular to one face of a 90° pyramid.

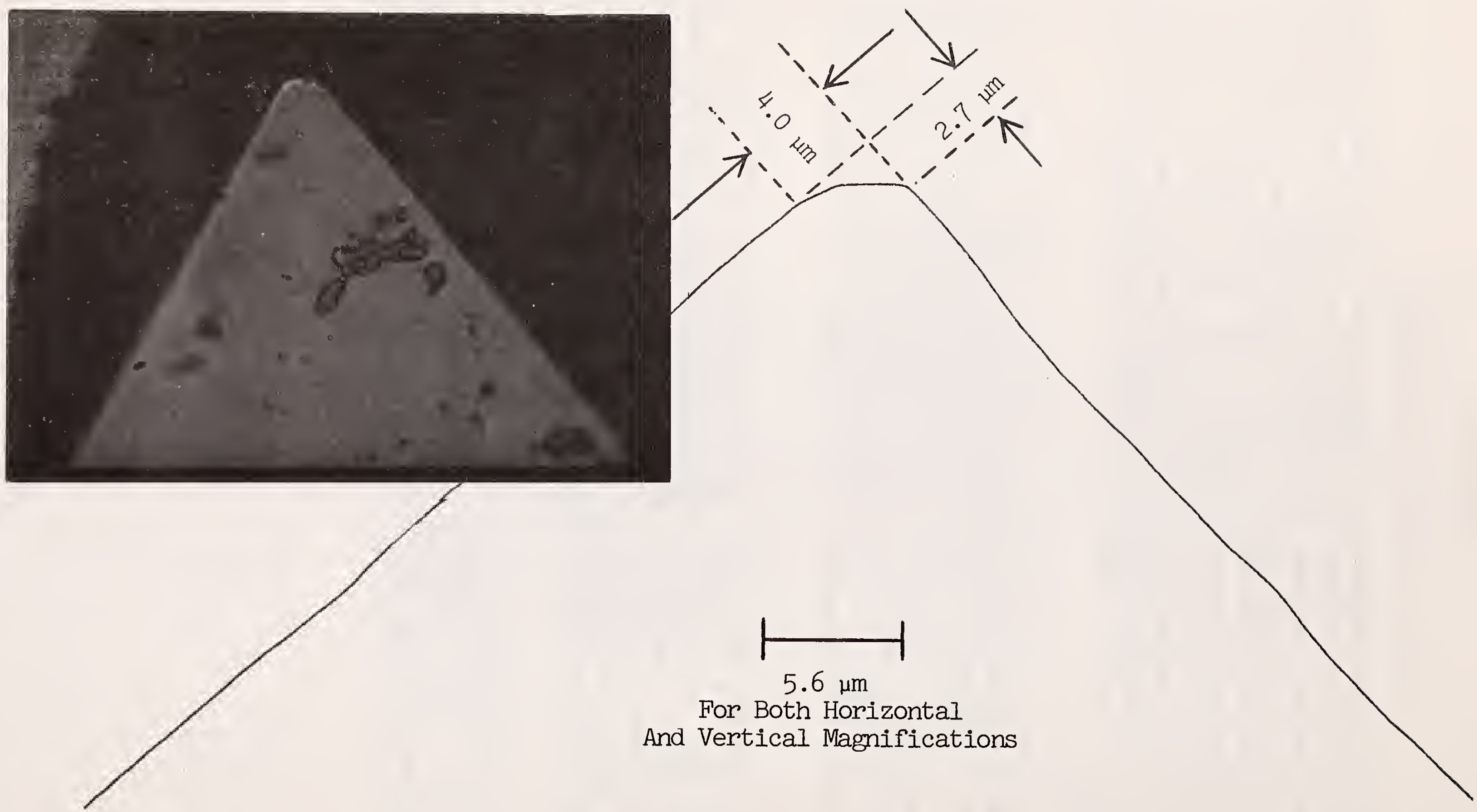

Figure 30. Profile of Stylus Tip
(Photographic insert is a photomicrograph of one face of the pyramidal tip at a magnification of approximately 1500X.)

APPENDIX J*

NOISE EFFECT IN AA MEASUREMENT

It is known that measurements of ultrafine finishes are limited in accuracy by the inherent noise level of the stylus instrument itself. The specific effect of this noise has been established by a study of the computer calculated AA values as a function of the signal-to-noise ratio. The experimental set-up is shown in figure 31. An operational amplifier was employed as an inverting adder without weighting. The apparatus allowed the stylus instrument output to be measured separately and combined with a known signal. Measurements were made of the inherent electronic noise in the system (with the stylus stationary), the mechanical and electronic noise (stylus resting on a plane which traversed with the stylus), and the stylus output while traversing an ultrafine surface (a float-formed glass substrate). The results for each case, normalized to the zero signal input level, are indicated in figure 32. The smooth curve represents the equation:

$$\text{Signal Output} - [(\text{Signal Input})^2 + (\text{Noise})^2]^{1/2}.$$

The actual "noise" levels associated with the three cases above indicated: (1) an electronic noise equivalent to .13 μin. AA, (2) a mechanical and electronic noise equivalent to .16 μin. AA, and (3) a probable minimum AA reading of .25 μin. It has not been determined what portion of the minimum AA reading is due to the highly polished surface. Therefore, if is assumed that the full minumum reading is due to the instrument; thus; the total inherent noise is taken to be .25 μin.

---

*From DASR

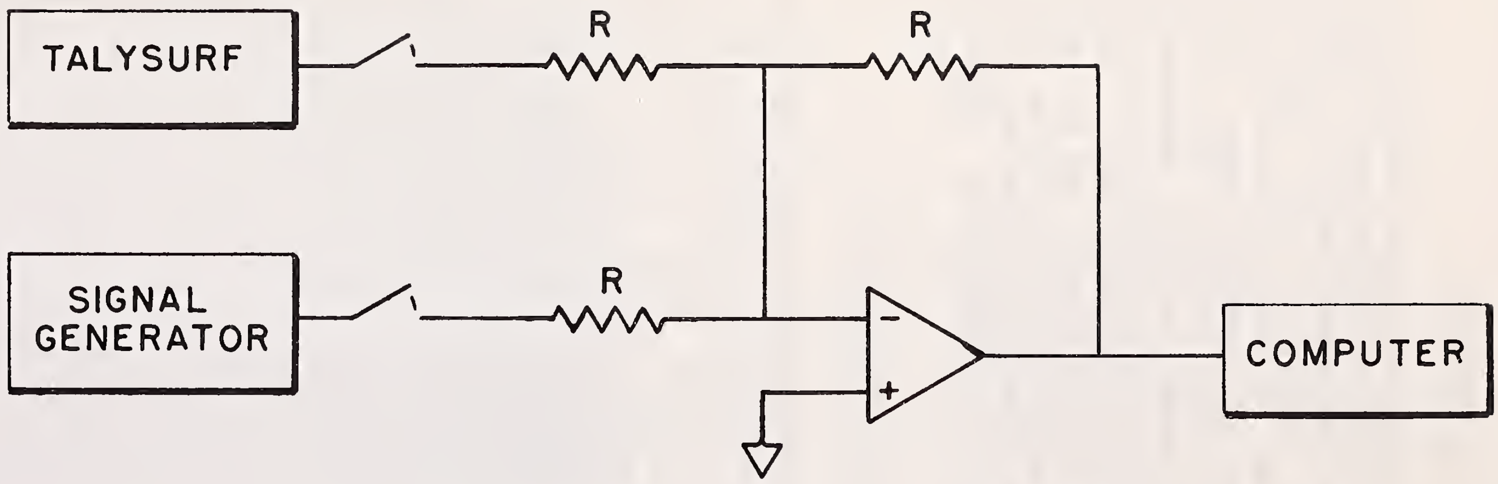

NOISE EFFECT MEASUREMENT

FIGURE 31

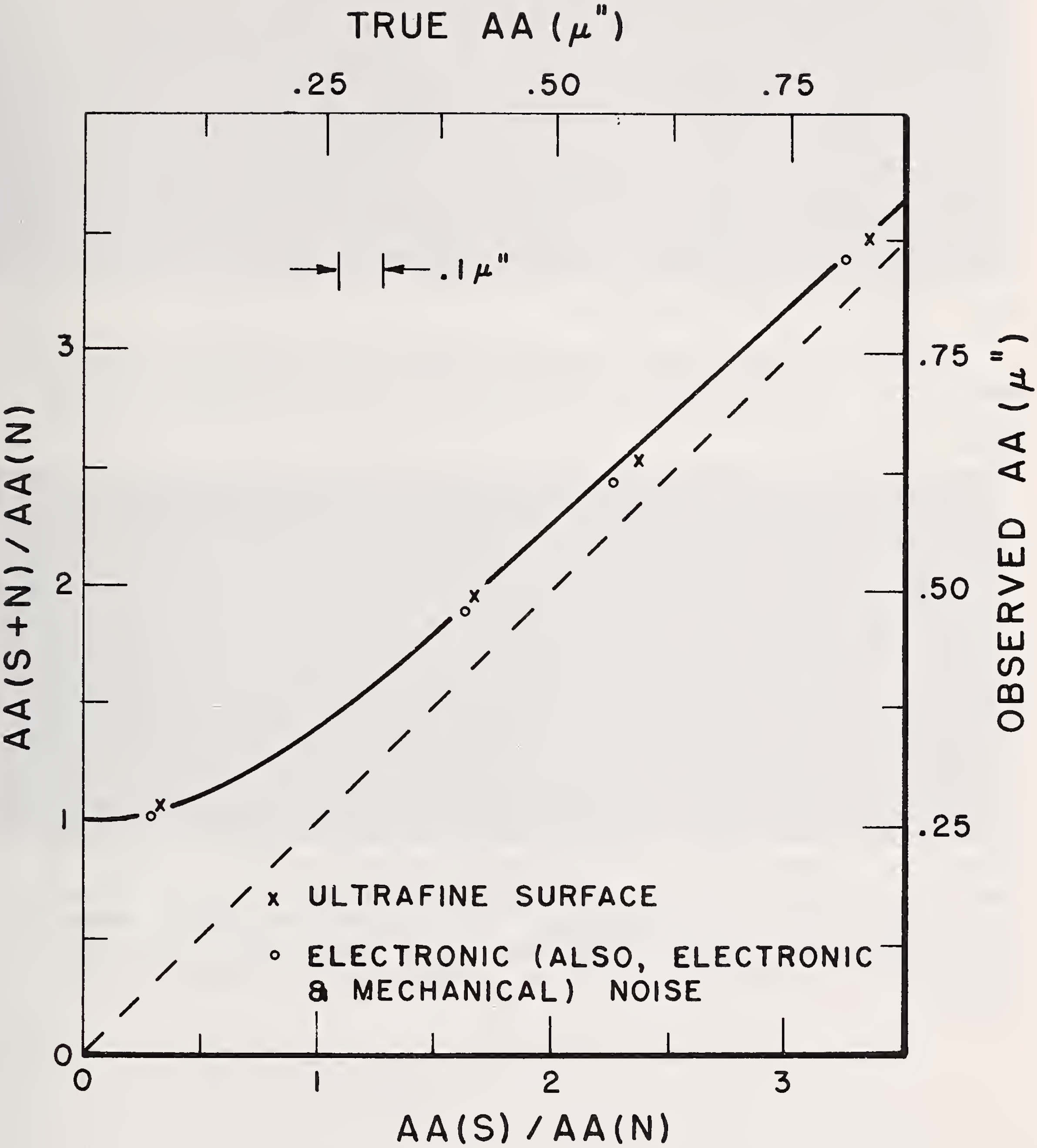

Results of Noise Measurement
Figure 32

APPENDIX K

EFFECTS OF SURFACE FINISH ON STEP HEIGHT MEASUREMENTS FROM STYLUS PROFILES

To check the analytical predictions of section 2.2, measurements on two step-specimens were performed. Profiles of the two specimens used in the measurements are shown in figure 33. Twenty-eight (28) measurements of each specimen in approximately the same location were made to obtain a sufficient amount of data to statistically characterize the relationship between surface finish and calculated step height. The procedure for the measurements was to employ each of the steps as a calibrating step, labelling its height as 10,000, then to repetitively remeasure its height using the calibration constant, KCAL, from the first measurement.

Analysis of the profile data followed the procedure outlined in section 1.2. Computer printouts of the analysis are given in tables 7 and 8. In each of the 56 printouts the following results are given after the word IN:

line 1; left slope - left intercept - right slope - right intercept - KCAL - step height (all in hexadecimal),

line 2; step height headings,

line 3; calculated step heights.

For the 12.8 μm step with a surface finish of 13 nm AA, the 3s value* of the data was $\pm$ 0.16% of the mean step height. For the 503 nm step with a surface finish of 8 nm AA, the 3s value* of the data was $\pm$ 2.0% of the mean step height. Expected values, based on the predictions of section 2.2, for the two specimens were 0.11% and 1.7%, respectively. The predicted 3s values* would be slightly larger if system noise and quantization were included, but not by the amount needed to give exact agreement with the measured values. Agreement between the analytical and measured values is however sufficient to confirm that the major source of statistical variation in calculated step heights is the step specimen's surface finish.

---

*See page 32 for the definition of s.

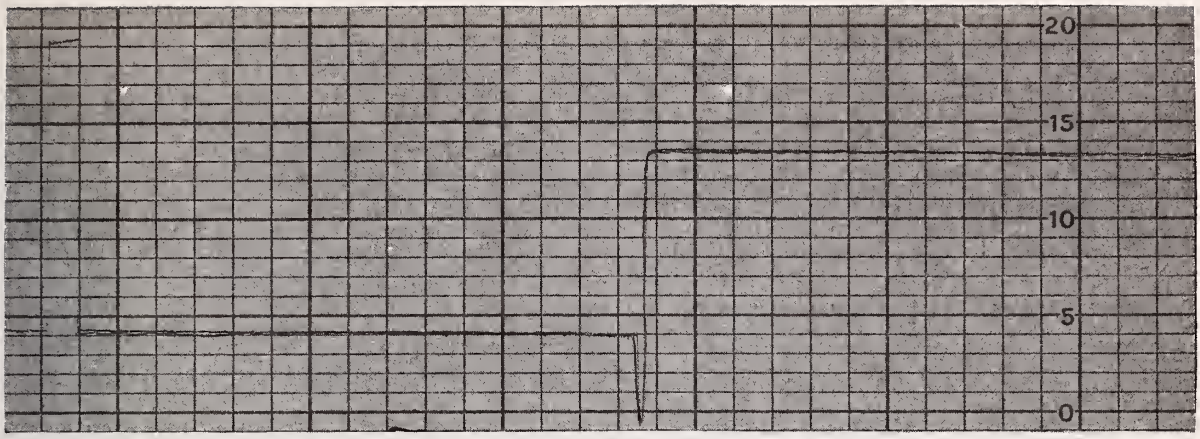

Figure 33a: Profile of 12.8 μm Step with Surface Finish of 13 nm AA. Vertical Magnification ≃ 2000; Horizontal Magnification ≃ 20.

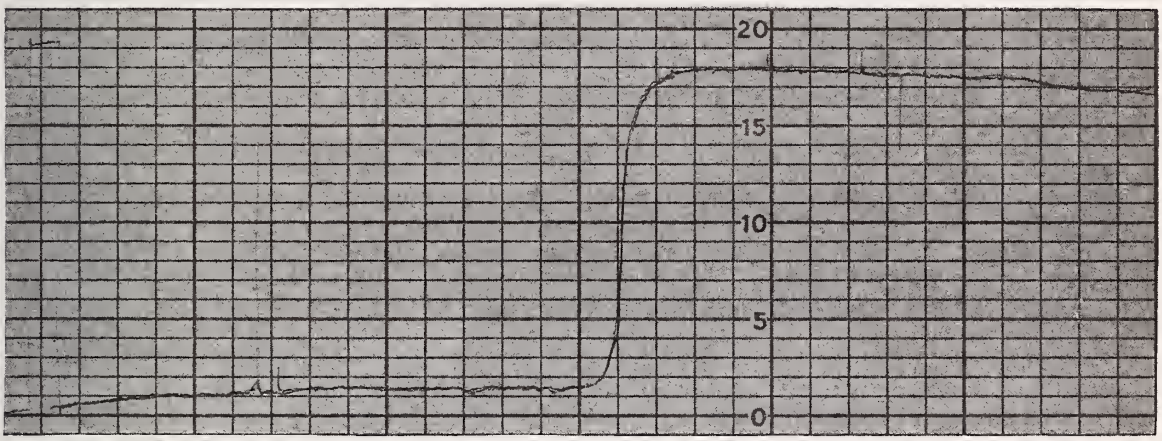

Figure 33b: Profile of 503 nm Step with Surface Finish of 8 nm AA. Vertical Magnification ≃ 100,000; Horizontal Magnification ≃ 20.

Figure 33: Profiles of Steps Used for Taking Statistics on Step Height Measurements.

```
IN
FFFFE480 FD22A000 FFFFD2C0 04AD5000 0000A488 079E78A0
H1       H3       H5       H7       HM
00010035 00010031 00010028 00010024 00010029
IN
FFFFE540 FD227000 FFFFD520 04AC9800 0000A488 079D4BB0
H1       H3       H5       H7       HM
00010028 00010025 00010022 00010018 00010023
IN
FFFFE600 FD214000 FFFFD520 04AC1800 0000A488 079D8E90
H1       H3       H5       H7       HM
00010030 00010026 00010023 00010020 00010024
IN
FFFFE700 FD206000 FFFFD580 04AB6000 0000A488 079D1C40
H1       H3       H5       H7       HM
00010028 00010024 00010021 00010017 00010022
IN
FFFFE620 FD205800 FFFFD2A0 04ABD800 0000A488 079E5F20
H1       H3       H5       H7       HM
00010035 00010031 00010027 00010023 00010028
IN
FFFFE680 FD204000 FFFFD360 04AB8800 0000A488 079DDEF0
H1       H3       H5       H7       HM
00010032 00010028 00010024 00010021 00010025
IN
FFFFE400 FD1AE000 FFFFD160 04A5C800 0000A488 079F19B0
H1       H3       H5       H7       HM
00010038 00010035 00010031 00010027 00010032
IN
FFFFE540 FD17F000 FFFFD220 04A3F800 0000A488 079F7230
H1       H3       H5       H7       HM
00010040 00010036 00010033 00010029 00010034
IN
FFFFE3E0 FD17E800 FFFFD3A0 04A2D800 0000A488 079EFF00
H1       H3       H5       H7       HM
00010037 00010034 00010030 00010027 00010031
IN
FFFFE480 FD166000 FFFFD260 04A28800 0000A488 079FF970
H1       H3       H5       H7       HM
00010043 00010039 00010035 00010032 00010036
IN
FFFFE360 FD16E800 FFFFD1C0 04A29000 0000A488 07A02BD0
H1       H3       H5       H7       HM
00010043 00010040 00010036 00010033 00010037
IN
FFFFE3C0 FD169000 FFFFD340 04A13000 0000A488 079ECA00
H1       H3       H5       H7       HM
00010036 00010033 00010029 00010026 00010030
IN
FFFFE4A0 FD159800 FFFFD260 04A10800 0000A488 079F2F40
H1       H3       H5       H7       HM
00010039 00010035 00010031 00010028 00010032
IN
FFFFE760 FD148800 FFFFD320 04A0B800 0000A488 079E4D80
H1       H3       H5       H7       HM
00010035 00010031 00010027 00010023 00010028
```

Table 7a: Measurements on Height of 12.8 μm Step with Surface Finish of 13 nm AA.

Mean of all 28 = 10032 ± (3σ = 16 or 0.16%)

```
IN
FFFFE320 FD14B800 FFFFD200 04A04000 0000A488 07A02A50
H1       H3       H5       H7       HM
00010043 00010040 00010036 00010033 00010037
IN
FFFFE680 FD13A000 FFFFD400 049F2000 0000A488 079E0840
H1       H3       H5       H7       HM
00010033 00010029 00010025 00010022 00010026
IN
FFFFE620 FD125800 FFFFD2E0 049D6800 0000A488 079DE940
H1       H3       H5       H7       HM
00010032 00010029 00010025 00010021 00010026
IN
FFFFE300 FD11A000 FFFFD180 049CC000 0000A488 079FE040
H1       H3       H5       H7       HM
00010042 00010038 00010035 00010031 00010036
IN
FFFFE180 FD112000 FFFFD160 049B4800 0000A488 079FC570
H1       H3       H5       H7       HM
00010041 00010038 00010034 00010031 00010035
IN
FFFFE3A0 FD0FF800 FFFFD060 049BA800 0000A488 07A02FC0
H1       H3       H5       H7       HM
00010044 00010040 00010036 00010033 00010037
IN
FFFFE2C0 FD10B000 FFFFD480 049B8000 0000A488 079F6E20
H1       H3       H5       H7       HM
00010038 00010036 00010033 00010030 00010033
IN
FFFFE320 FD125800 FFFFD560 049E6800 0000A488 07A06300
H1       H3       H5       H7       HM
00010043 00010040 00010038 00010035 00010038
IN
FFFFE540 FD117000 FFFFD3E0 049E8800 0000A488 07A05910
H1       H3       H5       H7       HM
00010044 00010041 00010037 00010034 00010038
IN
FFFFE400 FD11C000 FFFFD420 049DF800 0000A488 07A02910
H1       H3       H5       H7       HM
00010043 00010040 00010036 00010033 00010037
IN
FFFFE2E0 FD128800 FFFFD180 049E8000 0000A488 07A0CA70
H1       H3       H5       H7       HM
00010047 00010043 00010040 00010036 00010040
IN
FFFFE480 FD116000 FFFFD3C0 049D9000 0000A488 079FE120
H1       H3       H5       H7       HM
00010042 00010038 00010035 00010032 00010036
IN
FFFFE4E0 FD104800 FFFFD440 049CF000 0000A488 07A016D0
H1       H3       H5       H7       HM
00010043 00010039 00010036 00010033 00010037
IN
FFFFE3E0 FD10A800 FFFFD360 049CC800 0000A488 07A034E0
H1       H3       H5       H7       HM
00010043 00010040 00010037 00010033 00010037
```

Table 7b: Measurements on Height of 12.8 μm Step with Surface Finish of 13 nm AA.

```
2534G
IN
FFFF5C40 F8E7F000 FFFEC3A0 057F7800 00005FB4 0D0B1400
H1       H3       H5       H7       HM
00010011 00009997 00009983 00009968 00009986
IN
FFFFB060 F92E4800 FFFFABC0 06577000 00005FB4 0D5BE7C0
H1       H3       H5       H7       HM
00010229 00010228 00010228 00010227 00010228
IN
00003920 F9361800 FFFF67C0 06741000 00005FB4 0D2A2D40
H1       H3       H5       H7       HM
00010114 00010094 00010074 00010055 00010079
IN
FFFFF120 F94C9800 FFFF8640 0685F000 00005FB4 0D4B1B40
H1       H3       H5       H7       HM
00010195 00010185 00010175 00010165 00010178
IN
FFFFF260 F96E4800 00000700 067B8000 00005FB4 0D143AC0
H1       H3       H5       H7       HM
00010010 00010012 00010014 00010016 00010014
IN
000047C0 F9431000 FFFF6080 068C4000 00005FB4 0D2DD980
H1       H3       H5       H7       HM
00010128 00010106 00010085 00010063 00010090
IN
00000220 F9515800 FFFF8880 066D4000 00005FB4 0D241040
H1       H3       H5       H7       HM
00010081 00010070 00010058 00010047 00010061
IN
FFFFFA00 F945E000 FFFFACE0 0663C800 00005FB4 0D27BA80
H1       H3       H5       H7       HM
00010085 00010077 00010070 00010063 00010072
IN
FFFFB980 F9440000 FFFF82E0 065CC800 00005FB4 0D49A980
H1       H3       H5       H7       HM
00010182 00010177 00010172 00010167 00010173
IN
00004000 F8FB8000 FFFF60E0 0659C800 00005FB4 0D473680
H1       H3       H5       H7       HM
00010203 00010182 00010161 00010140 00010166
IN
FFFFFF20 F9091800 FFFF6A60 0636E800 00005FB4 0D39FCC0
H1       H3       H5       H7       HM
00010151 00010137 00010123 00010109 00010127
IN
FFFFD680 F9378000 FFFF6C20 066FD800 00005FB4 0D5AEA80
H1       H3       H5       H7       HM
00010242 00010232 00010223 00010213 00010225
IN
000006C0 F9053000 FFFF6FE0 063AE800 00005FB4 0D3D3C00
H1       H3       H5       H7       HM
00010161 00010147 00010133 00010119 00010136
IN
00000880 F8F4E000 FFFF3760 0637A800 00005FB4 0D4DBD80
H1       H3       H5       H7       HM
00010220 00010200 00010181 00010161 00010186
```

Table 8a. Measurement on Height of 503nm Step with Surface Finish of 8nm AA.

M = 10143 $\pm$ (3σ = 207 or 2.0%)

```
IN
00002460 F8E86800 FFFF5AA0 06397800 00005FB4 0D49CE40
H1       H3       H5       H7       HM
00010207 00010188 00010169 00010150 00010174
IN
FFFFEF20 F8EFD800 FFFF4D40 06417000 00005FB4 0D68EB40
H1       H3       H5       H7       HM
00010293 00010278 00010263 00010248 00010267
IN
FFFFB480 F8FD4000 FFFF96E0 061BC800 00005FB4 0D509F80
H1       H3       H5       H7       HM
00010199 00010196 00010194 00010191 00010194
IN
00000500 F91CA000 FFFFAFE0 0647C800 00005FB4 0D2EA480
H1       H3       H5       H7       HM
00010107 00010099 00010091 00010083 00010093
IN
00001340 F8FEF000 FFFF4680 063BA000 00005FB4 0D408080
H1       H3       H5       H7       HM
00010180 00010160 00010141 00010122 00010146
IN
FFFFCD00 F90C0000 FFFF4E40 063AB000 00005FB4 0D58DD00
H1       H3       H5       H7       HM
00010240 00010228 00010216 00010204 00010219
IN
00001CC0 F8FED000 FFFFBEC0 062C1000 00005FB4 0D226680
H1       H3       H5       H7       HM
00010071 00010063 00010054 00010045 00010056
IN
FFFFD3C0 F903D000 FFFF9220 06381800 00005FB4 0D556900
H1       H3       H5       H7       HM
00010219 00010213 00010207 00010201 00010209
IN
FFFFF420 F8FAD800 FFFF7600 062A8000 00005FB4 0D410640
H1       H3       H5       H7       HM
00010168 00010156 00010145 00010133 00010148
IN
FFFFECC0 F8D97000 FFFF87C0 06039000 00005FB4 0D3E3280
H1       H3       H5       H7       HM
00010156 00010146 00010137 00010127 00010139
IN
FFFFB620 F8E1B800 FFFF7FA0 0604B800 00005FB4 0D5601C0
H1       H3       H5       H7       HM
00010219 00010214 00010209 00010204 00010210
IN
FFFFEC80 F8E02000 FFFF5740 061F5000 00005FB4 0D573000
H1       H3       H5       H7       HM
00010238 00010224 00010210 00010196 00010214
IN
00001680 F8F02000 FFFF9520 061BB800 00005FB4 0D277680
H1       H3       H5       H7       HM
00010092 00010080 00010068 00010056 00010071
IN
000039C0 F91F5000 FFFF3D60 0672A800 00005FB4 0D428400
H1       H3       H5       H7       HM
00010193 00010170 00010146 00010123 00010152
```

Table 8b. Measurements on 503nm Step with Surface Finish of 8 nm AA.

APPENDIX L

MEASUREMENTS OF THE STYLUS-TRANSDUCER AND INTERFACE HARDWARE NON-LINEARITIES

Stylus-transducer non-linearity was measured by recording the transducer's voltage output as a function of an interferometrically measured displacement input. Displacement inputs were generated either by driving a linear-translation-stage with a differential screw or directly from the differential screw. The differential screw was constructed so that a 360° rotation of the instrument's barrel produced a 6.4 μm displacement of the output screw. The linear-translation-stage [13] employed parallel-arm flexure pivots to obtain a reduction-ratio between input and output displacements of 69. Displacements input to the linear-translation-stage or directly to the stylus were measured with a Hewlett-Packard 5526 laser measurement system including its associated remote interferometer and retroflector. Direct displacements were therefore measured with a resolution of 25 nm; displacements from the linear-translation-stage were measured with a resolution of 0.4 nm.

All components used in generating and measuring the displacements were clamped together and to the Talysurf's base to form a stiff structure. With the stylus tip resting on the displacement-stage mechanical vibrations had approximately twice the arithmetic average value as found with the tip resting on a solid specimen i.e., 12 nm.

Output voltages were measured with a digital voltmeter having a non-linearity of ± one digit on the readout over the range from ± 0.100 to ± 1.000 volts. Thus, this roundoff non-linearity ranged in the measurements from ± 0.1% to ± 1% of the readout values, typically 0.2% or less. Analytic non-linearities of this magnitude and less may however be extracted from the measurements by statistical analysis since the data subjected to roundoff were random i.e., the next digit was representative of the system noise level.

Non-linearity for purposes of these measurements is defined as the maximum deviation of a quadratic least-squares fit from a linear least-squares fit to the experimental data. (This definition was adopted after an unsuccessful search for a commonly accepted definition of non-linearity.) Computer printouts of the data on stylus displacement versus transducer output voltage and the results of analyses are given in tables 9 and 10. Table 9, gives the results obtained while using the Talysurf's sensitivity of "1000"; table 10 gives the results obtained while using the Talysurf's sensitivity of "50,000". In both tables: column 4 is the output voltage in millivolts; column 42 is the deviation of the data from a linear-least squares fit; column 52 is the deviation of the data from a quadratic-least-squares fit; column 53 is the difference between a linear and a quadratic least squares fit; and column 54 is this difference expressed as a percentage of its respective datum value. In table 10 column 2 is interferometrically measured displacements in microinches input to the linear-translation-stage; stylus displacements are therefore, the numbers given in column 2 divided by 69. In table column 2 gives the direct stylus displacements in microinches.

The measurements given in table 9 cover the entire range of the Talysurf on the "1000" sensitivity so that the maximum deviation between the linear and quadratic least-squares fit is the non-linearity of the instrument's transducer. The "500" sensitivity is rarely employed for measurements at NBS and thus was not used for the non-linearity tests. Measurements of non-linearity, on the "50,000 magnification" were performed to verify that the non-linearity of the transducer would be less over the limited range and that smaller scale variations not resolved at the "1000 magnification" were not present.

On the "1000 magnification" with the stylus tip being displaced $\pm$ 25.4 μm from an arbitrary zero the measured non-linearity, as defined earlier, was 0.4%; on the "50,000 magnification" the non-linearity was 0.2%. Expressed in an analytical form the results were:

$$\left(\frac{dV\ out}{dy\ in}\right)_{linear} = (37.25 \pm .06)\ \ mV/\mu m,$$

$$\left(\frac{dV\ out}{dy\ in}\right)_{quadratic} = [(37.15 \pm .10) + (3.4 \pm 9.3) \times 10^{-3}y]\ mV/\mu m,$$

for "1000 magnification" and:

$$\left(\frac{dV\ out}{dy\ in}\right)_{linear} = (1.445 \pm .007)\ volts/\mu m,$$

$$\left(\frac{dV\ out}{dy\ in}\right)_{quadratic} = [(1.443 \pm .035) + (0.004 \pm .056)y]\ volts/\mu m,$$

for the "50,000 magnification." The $\pm$ values after each coefficient are the 3 standard deviations of the coefficients estimated from the data analysis. For both the "1000 and 50,000 magnifications" the quadratic coefficient is less than its 3 standard deviation value. Thus, the non-linearities quoted are values based on the small probability that a quadratic component is present in the transducer's output voltage versus stylus displacement.

The signal path from the transducer's output to data storage in the minicomputer was tested and analyzed in a similar manner. For these measurements a voltage source with an accuracy of 100 μV was used as the input to the filter-amplifier (appendix A) whose output was in turn used as the input to the analog-to-digital converter, ADC. The output of the ADC was then stored in the minicomputer memory and printed at the teletype as a function of the voltage input. Input voltages were stepped over the range from -1.000 to + 1.000 volts producing outputs from the filter-amplifier of - 10.0 to + 10.0 volts. At the input to the ADC, noise was approximately 1 mv RMS, or 0.2 of the ADC's resolution. Effects from the noise were further minimized by sampling the analog signal 16 times at 30 ms intervals to obtain the average value printed at the teletype. An analysis of the data for memory stored values versus filter-amplifier input voltage performed according to the same procedure described for the transducer gave a non-linearity of 0.06%.

OMNITAB

COLUMN 2	COLUMN 4	COLUMN 42	COLUMN 52	COLUMN 53	COLUMN 54
313.00000	-926.00000	-1.0760728	-1.5696273	.49355453	-.053361635
350.00000	-890.00000	-.083549568	-.50492772	.42137816	-.047350305
385.00000	-856.00000	.80126949	.44549554	.35577395	-.041523509
488.00000	-757.00000	2.3480298	2.1702554	.17777443	-.023411456
599.00000	-655.00000	-.67440051	-.68552518	.011124671	-.0017001735
673.00000	-585.00000	-.68935408	-.60388783	-.085466251	.014626851
728.00000	-532.00000	.27250653	.42224390	-.14973737	.028131713
962.00000	-312.00000	-1.1261183	-.77460785	-.35151041	.11307171
1057.0000	-223.00000	-2.0101782	-1.6098760	-.40030214	.18114053
1172.0000	-112.00000	.18280159	.61657279	-.43377120	.38666461
1457.0000	158.00000	.53062727	.92652404	-.39589677	-.25141191
1554.0000	250.00000	.75427149	1.0980071	-.34373562	-.13791033
1666.0000	353.00000	-2.2142994	-1.9555994	-.25870004	-.072829287
1739.0000	422.00000	-2.2831051	-2.0941429	-.18896222	-.044536824
1795.0000	474.00000	-3.2673924	-3.1395838	-.12780857	-.026779238
1876.0000	553.00000	-.90537412	-.87778077	-.027593344	-.0049815989
1938.0000	613.00000	.43344738	.37493643	.058510948	.0095517698
2011.0000	681.00000	-.63535460	-.80569094	.17033634	.024989364
2074.0000	739.00000	-2.2426774	-2.5186011	.27592373	.037224479
2141.0000	802.00000	-2.6345918	-3.0320379	.39744610	.049394607
2222.0000	883.00000	1.7274155	1.1703492	.55706629	.063211575
2250.0000	914.00000	6.2352737	5.6197954	.61547828	.067801518
2168.0000	830.00000	-.18058938	-.62969700	.44910762	.054097581
2074.0000	740.00000	-1.2426774	-1.5186011	.27592373	.037224479
2018.0000	687.00000	-1.2583937	-1.4400465	.18165281	.026393113
1947.0000	624.00000	2.9181197	2.8464325	.071687192	.011542309
1860.0000	540.00000	1.2329726	1.2814838	-.048491150	-.0090003932
1791.0000	473.00000	-.48280072	-.35040360	-.13239713	-.027962394
1765.0000	448.00000	-.88295108	-.72155498	-.16139610	-.035955052
1722.0000	409.00000	.80141323	1.0076247	-.20621148	-.050517439
1613.0000	307.00000	1.9315441	2.2337982	-.30225414	-.099077478
1535.0000	233.00000	1.7310838	2.0866072	-.35552341	-.15372727
1512.0000	211.00000	1.4924879	1.8612569	-.36876905	-.17601710
1141.0000	-140.00000	1.5133908	1.9408997	-.42750888	.30209782
1010.0000	-269.00000	-3.5412222	-3.1626681	-.37855405	.14260370
983.00000	-292.00000	-.99522828	-.63128537	-.36394291	.12506424
728.00000	-532.00000	.27250653	.42224390	-.14973737	.028131713
668.00000	-588.00000	1.0413892	1.1206947	-.079305470	.013463480
520.00000	-728.00000	1.0712890	.94423697	.12705204	-.017426559
480.00000	-767.00000	-.082786785	-.27358097	.19079418	-.024878068
390.00000	-849.00000	3.0705335	2.7239196	.34661388	-.040679013
280.00000	-958.00000	-1.8532023	-2.4135785	.56037620	-.058607757

Table 9: Voltage Output Versus Displacement for Stylus Instrument Using the X1000 Magnification

OMNITAB

COLUMN 2	COLUMN 4	COLUMN 42	COLUMN 52	COLUMN 53	COLUMN 54
353.00000	-456.00000	-1.0311200	-1.3671559	.33603592	-.073859098
514.00000	-372.00000	-2.6956620	-2.9145902	.21892822	-.059281246
689.00000	-280.00000	-3.8093028	-3.9176023	.10829955	-.039211875
825.00000	-208.00000	-4.1718930	-4.2062038	.034310818	-.016833212
1389.0000	92.0000000	-4.2638317	-4.1031826	-.16064906	-.16688413
1592.0000	199.00000	-5.2756507	-5.0889515	-.18669927	-.091395753
1682.0000	248.00000	-4.1626614	-3.9718853	-.19077617	-.075655994
1789.0000	302.00000	-7.0949991	-6.9053493	-.18964982	-.061356483
1952.0000	394.00000	-1.8236995	-1.6482368	-.17546275	-.044328511
2067.0000	460.00000	2.9873410	3.1437351	-.15639403	-.034220941
2239.0000	550.00000	1.4699375	1.5838230	-.11388545	-.020761933
2414.0000	645.00000	3.3563010	3.4097286	-.053427607	-.0083266782
2575.0000	731.00000	3.6917548	3.6742318	.017522991	.0024092935
2705.0000	798.00000	1.5216262	1.4360940	.085532278	.010738807
2839.0000	867.00000	-.77681436	-.94247313	.16565877	.019090021
2908.0000	908.00000	3.5093093	3.2989221	.21088713	.023315580
3061.0000	983.00000	-2.8981128	-3.2189139	.32080117	.032538977
2962.0000	927.00000	-6.2224020	-6.4705674	.24816543	.026592314
2787.0000	837.00000	-3.1087612	-3.2421178	.13335660	.015873730
2614.0000	750.00000	1.9407171	1.9037970	.036920086	.0049354490
2472.0000	675.00000	2.4957819	2.5253425	-.029560655	-.0043956088
2295.0000	581.00000	2.6735744	2.7700018	-.096427321	-.016673511
2120.0000	489.00000	3.7872109	3.9322937	-.14508271	-.029900842
1938.0000	390.00000	1.6253912	1.8026636	-.17727239	-.045644691
1767.0000	300.00000	2.6107154	2.8011267	-.19041130	-.064027625
1589.0000	202.00000	-.67941778	-.49293342	-.18648437	-.092009523
1437.0000	122.00000	.19642731	.36534433	-.16891703	-.13867986
742.00000	-241.00000	6.9905692	6.9123501	.078219116	-.031541165
593.00000	-346.00000	9.1571952	8.9307333	.22646189	-.060364532

Table 10: Voltage Output Versus Displacement for Stylus Instrument Using the X50,000 Magnification

APPENDIX M

THE EFFECT OF FINITE RECORD LENGTH ON MEASURED ROOT-MEAN-SQUARE AND ARITHMETIC AVERAGE VALUES

Consider first the case of estimating the uncertainty in the mean square value, q^2, calculated from a finite length L of the profile y(x). By definition:

$$q^2 = \frac{1}{L} \int_o^L y^2(x)\, dx.$$

For convenience and brevity in the following discussion, the definitions listed below will be used [14].

Sample space = the set of points representing the possible outcomes of a measurement.

$\phi(k)$ ≡ a real number, called the random variable, which represents the outcome of a measurement indexed by k.

$$p(\phi) \equiv \lim_{\Delta\phi \to o} \frac{\text{Probability } [\phi < \phi(k) \leq \phi + \Delta\phi]}{\Delta\phi}$$

$E[g(\phi(k))]$ ≡ the expected value of any real single-valued continuous function $g(\phi)$ of the random variable $\phi(k)$. It is given by:

$$E[g(\phi(k))] = \int_{-\infty}^{+\infty} g(\phi)p(\phi)\, d\phi.$$

As an example the mean square value of y(x) is given by:

$$E[y^2(x)] = \int_{-\infty}^{+\infty} y^2(x)p(x)\, dx.$$

$E[y^2(x)]$ will be defined as $\overline{q}^2$. $\overline{q}^2$ is that value approached by q^2 as the record length L approaches infinity or that value obtained for the mean q^2 of a large number of finite samplings. The variance of y(x) is defined by:

$$\text{var}\ \{y\} = E[(y-\overline{y})^2] = \int_{-\infty}^{+\infty} (y-\overline{y})^2 p(x)\, dx.$$

Similarly the variance in q^2 is defined by:

$$\text{var}\left\{q^2\right\} = E[(q^2-\overline{q}^2)^2].$$

For the special case when y(x) is a bandwidth limited Gaussian waveform with zero mean, Bendat and Piersol [14] show that;

$$\frac{\text{var}\left\{q^2\right\}}{\overline{q}^4} = \frac{2L^*}{L}\left[1-e^{-2L/L^*}\right] + \frac{L^*}{L}\left[\left(2\frac{L}{L^*}+1\right)e^{-2L/L^*}-1\right],$$

where L* is shift distance required for the ACF to drop by 63% of its zero shift value. If L>>L* the relation reduces to:

$$\frac{\text{var}\left\{q^2\right\}}{\overline{q}^4} = 2\,\frac{L^*}{L}$$

The propogration of error formulae discussed by Ku [17] may be used to relate the variance of the root-mean-square value = RMS = $\sqrt{q^2}$ to this variance of q^2. Results given in table 1 of this reference show that if:

$$\frac{\text{var } q^2}{\overline{q}^4} = \varepsilon, \text{ then } \frac{\text{var RMS}}{\overline{q}^2} = \frac{\varepsilon}{4}$$

Thus, the normalized 3 standard deviations limit, 3SD in the root-mean-square values calculated from randomly sampled length, L, of a Gaussian profile with a correlation length L* is given by:

$$\text{3SD limit of RMS} = \frac{3}{2}\sqrt{\frac{2L^*}{L}} = 2.1\sqrt{\frac{L^*}{L}} \equiv \text{3SDR}$$

Whitehouse and Archard [3] report reasonable confirmation of this result for their test specimens which had approximately Gaussian profiles. The importance of this result is stated very clearly by Whitehouse and Archard [3]. "The variance of measured RMS or AA values for the roughness of a surface may be found easily if one knows the standard deviation of a large number of such measurements made upon the same surface. Alternatively one may predict the variance from a knowledge of the correlation length of a typical profile of the test surface." The argument just given for the 3SD limit partially fulfills the "it can be shown" statement by Whitehouse and Archard.

Unfortunately these results do not apply for periodic waveforms such as that of the precision roughness specimens. However, the principles of calculation are still applicable. Consider the example of a sinusoidal waveform:

$$y(x) = A \sin(\omega\chi+\theta).$$

The waveform is sampled for a length L with the phase angle θ considered as the random variable of the sample space. θ will be considered as having a uniform distribution over values from 0 to 2π i.e.

$p(\theta) = \frac{1}{2\pi}$, $0<\theta<2$ and $p(\theta) = 0$, for all other values of θ.

According to the definitions given earlier:

$$q^2 = \frac{1}{L} \int_0^L [A \sin(\omega\chi+\theta) - \frac{A}{\omega L} \left\{ \cos\theta - \cos(\omega L+\theta) \right\}]^2 \, dx.$$

The last term under the integral is the mean value of y as a function of θ. Evaluation of the integral yields;

$$q^2 = \frac{A}{2} \left[1 - \frac{\sin 2(\delta+\theta)}{2\omega L} + \frac{\sin 2\theta}{2\omega L} \right]$$

where $\delta = \omega L - 2n\pi$ and terms of order n^{-2} have been dropped. The mean square uncertainty in q^2 is given by:

$$E[(q^2-\bar{q}^2)^2] = \frac{1}{2\pi} \int_0^{2\pi} [\frac{A^2}{2} (1 - \frac{\sin 2(\delta+\theta)}{2\omega L} + \frac{\sin 2\theta}{2\omega L}) - \frac{A^2}{2}]^2 \, d\theta$$

Evaluation of the integral yields:

$$\text{var } q^2 = \frac{A^4 \ (1-\cos 2\delta)}{16 \ \omega^2 L^2}$$

Thus, if the record length includes an integral number of periods the var $q^2 = 0$. But, if we take the more likely case when the range of experimentally measured wavelengths is such that δ has a distribution like that of θ, the result averaged with respect to δ is

$$(\text{var } q^2)_\delta = \frac{A^4}{16 \ \omega^2 L^2} \quad \text{or} \quad \frac{(\text{var } q^2)_\delta}{\bar{q}^4} = \frac{1}{4 \ \omega^2 L} .$$

Use of the same relationships between var q^2 and var RMS given earlier yields:

$$\frac{\text{var RMS}}{\overline{q^2}} = \frac{1}{16\ \omega^2 L^2} ,$$

or normalized 3SD limit of RMS $= \dfrac{0.75}{\omega L} \equiv$ 3SDP.

For the 3.17 μm (125 μin) patch of a precision roughness specimen, $\omega L = 80\pi$ with the standard 3.81 μm record length; for the 0.5 μm (20 μin) patch, $\omega L = 500\pi$. Thus,

$$3SDP_{125} = 0.3\%,$$

$$3SDP_{20} = 0.05\%.$$

These estimates neglect small effect expected from the waveform differences between the analyzed sine wave and the triangular waveform of a precision roughness specimen. One would also expect that the normalized 3SD of the AA value would be approximately equal to that just found for the RMS value since both quantities are similar measures of the sampled profile's density function.

The major source of additional uncertainty not accounted for is that produced by the imperfect waveforms of the precision roughness specimens. These imperfections are illustrated in section 3.4. The illustrations show that the distortions may be produced by either an additive random function together with phase modulation or by the combination of random amplitude and phase modulation. The additive random function is the only error which can be readily analyzed. For this case the RMS value of the sum of two uncorrelated waveforms adds in an RMS manner. The use of the propagation of error formulae derived by Ku [17] then yields:

$$3SD = 1.5 \left(2a\ L^*/L + \frac{b}{4\ \omega^2 L^2} \right)^{\frac{1}{2}}$$

where $a = \left(1 + \dfrac{q_R^2}{q_P^2}\right)^{-2}$, $b = \left(1 + \dfrac{q_P^2}{q_R^2}\right)^{-2}$ and

$q^2_{P,R}$ = mean square values of periodic and random components, respectively. Both q_P^2/q_R^2 and L^*/L are difficult to estimate from the investigatory experiments performed so far on the precision roughness specimens. However, for the 0.5 µm (20 µin) roughness waveform preliminary estimates are $L = 20L^*$ and $q_R^2 = 0.01\ q_P^2$. With these estimates the 3SD limit, for the waveform sampled for 250 periods would be dominated by the uncertainty from the random component; this would increase the limit to a 3SD of 0.3%. These same values of L^* and q_R^2 are insignificant for the 3.17 µm precision roughness specimen since now $q_R^2 = 2.8 \times 10^{-4}\ q_P^2$.

APPENDIX N

SOME CONSIDERATIONS OF THE SYSTEM'S TRANSIENT RESPONSE CHARACTERISTICS

Ideally the system response, the storage of a datum point V(t) in memory at time t, would be directly proportional to the stylus tip displacement input y(t) at time t. The stored signal would be unchanged from that of y(t) except for a possible delay t_o; i.e.,

$$V(t) = Ay(t-t_o),$$

where A is a proportionality constant equal to the inverse of KCAL. In any real system the relationship between V(t) and y(t) is typically a complex function of the system's properties such as its mechanical and electrical resonance frequencies, passband or cutoff frequencies and response times. One way of characterizing systems is to determine the step response function S(t), which is the response of an initially relaxed system to a unit step input U(t) defined by the relations:

$$U(t) = 1 \quad t \geq 0,$$

$$= 0 \quad t < 0.$$

In terms of S(t) the response to an arbitrary excitation y(t) is given by [15]:

$$V(t) = y(o)\ s(t) + \int_o^t y'(\Gamma)\ s(t-\Gamma)\ d\Gamma.$$

Thus, the step response of an ideal system would be S(t) = A U(t-t_o), with A and t_o as defined earlier. Employing this approach to analytically characterize the stylus instrument/minicomputer system response is very difficult. The difficulty is in producing a realistic and known input for V(t) that has none of the undesirable properties for which the system is being tested. However, the concept of this technique was used to assess the magnitude of the system transient errors and the range of response because of its simplicity relative to other techniques such as the vibrating platform approach discussed by Spragg [16].

The measurement procedure was as follows: the stylus was traversed across a step formed by two closely spaced gage blocks wrung to a platen; the generated profile was stored in the minicomputer memory. The step input was measured and recorded by traversing the stylus across the step at the Talysurf's slowest speed, 12 µm/sec. The transient response was then measured by traversing the stylus across the same position on the step at the speed used for

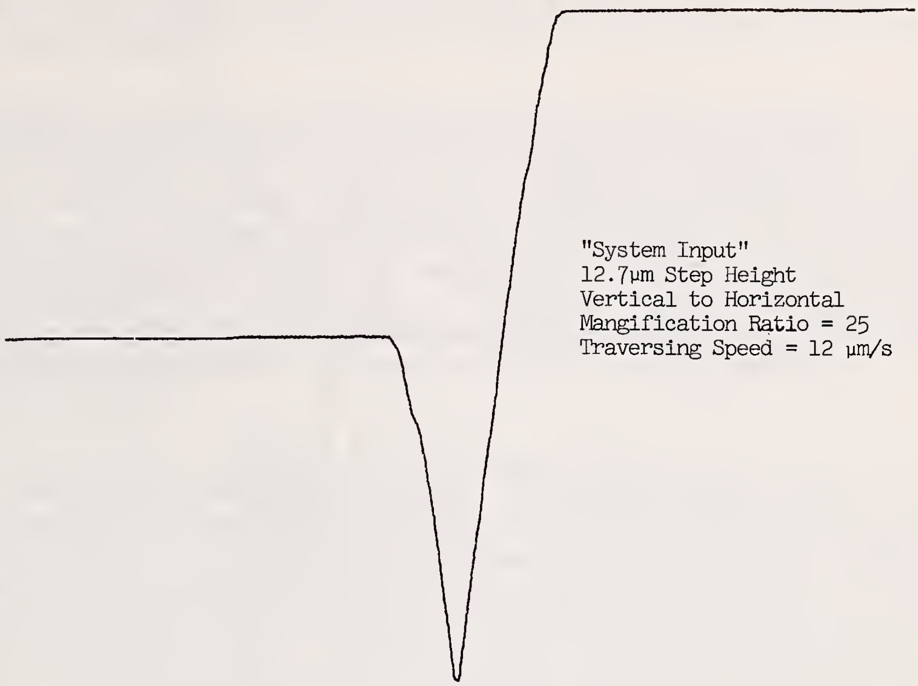

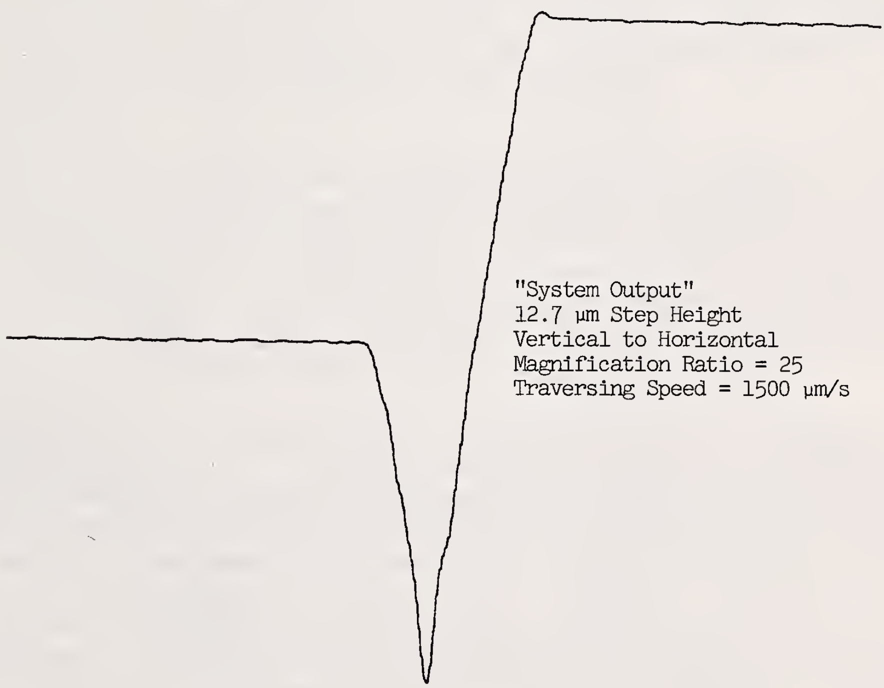

Figure 34a: Step Response of System

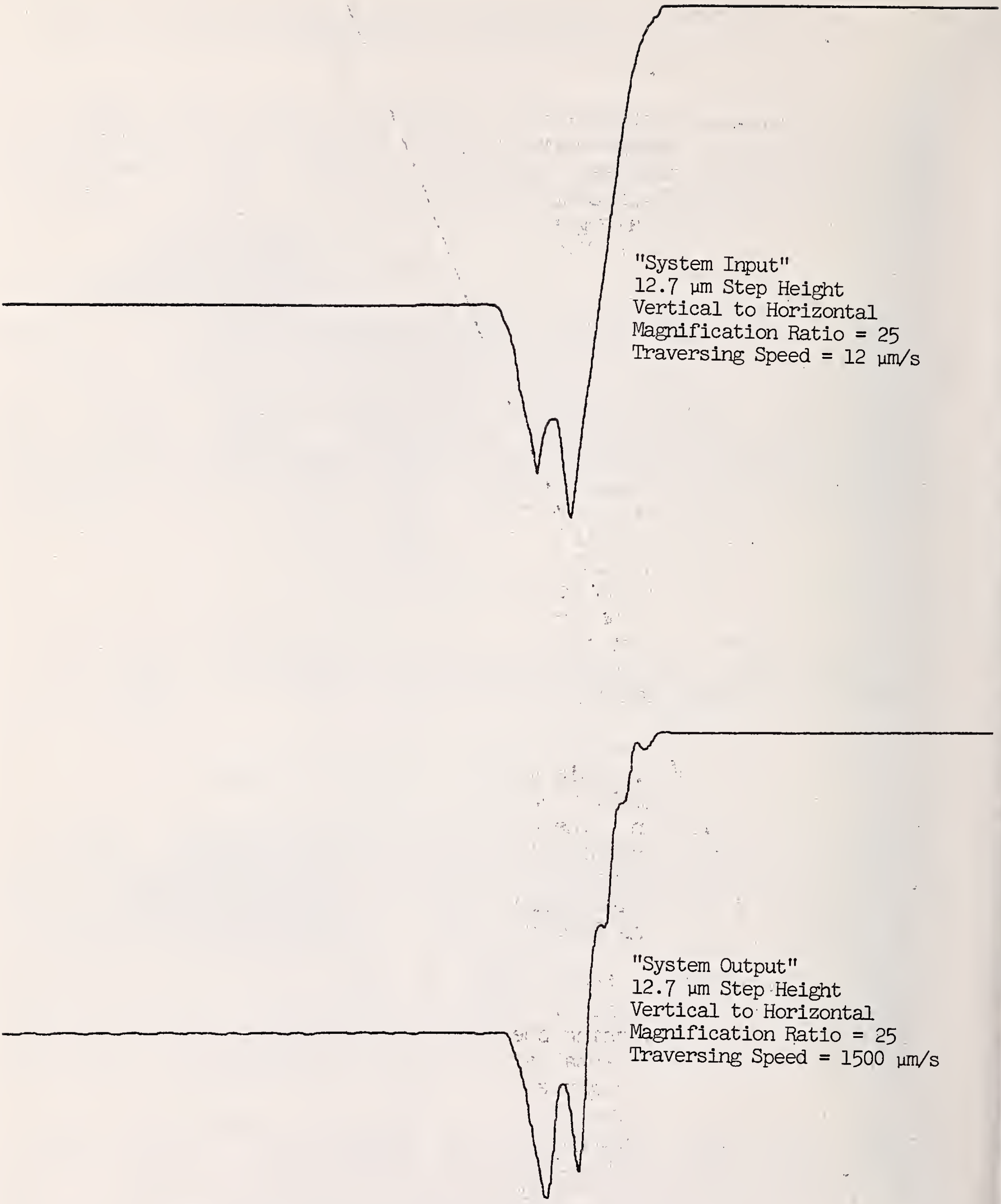

Figure 34b: Step Response of System

roughness measurements, 1500 μm/sec. Figures 34a and 34b demonstrate the results for steps near the borderline before "ringing" or "bouncing" began to occur. Steps with a crevice between the gage blocks were intentionally used to obtain profiles with both directions of acceleration present.

The ringing present in the "double-crevice" profile of figure 34b was also found in the system response to a larger step height. No ringing or overshoot was found in the transient response to steps smaller that the 12.7 μm step used for the measurements illustrated. At several positions along the step edge the gradient in the step was not as great as shown in figure 34a. Profiles at these positions also showed no evidence of overshoot or ringing. Thus, the transients produced by these steps are an approximate upper limit for which the system's characteristics may be represented by the step response $S(t) = A\ U(t-t_o)$.

The most suspect component of the system which would cause the ringing is the stylus instrument pickup. In use the stylus tip is held in contact with the specimen surface by the force of a flexure-pivot spring. This force, the internal damping of the spring, and the moving mass of the pick-up determine the maximum acceleration to which the pick-up may be subjected before the stylus tip will no longer follow the surface profile. A quantitative estimate of the value of acceleration at which the bouncing is initiated may be obtained from figure 34a. Using conservative estimates for the transition time between the two sides of the crevice and the transition time between the drop and rise to the high side of the step, the accelerations necessary to cause bouncing are greater than 0.25 m/s^2.

For comparison, a value for this acceleration obtained from Spragg [16] is 5 m/s^2. This value is estimated from his curve of the peak to peak amplitudes necessary to cause bouncing versus frequency of vibration. The acceleration needed to cause bouncing was found to be independent of frequency, to first order. Differences between the two values may be attributed to the different pick-up properties; NBS stylus force was 500 μN vs 1000 μN used by Spragg; the NBS moving mass was larger than that of the Spragg system.

For perspective, the acceleration generated by the fundamental sinewave component of the 0.5 μm (20 μin) AA precision roughness specimen at a traversing speed of 1500 μm/s is only 0.01 m/s^2; that generated by the fundamental sinewave component of the 3.17 μm (125 μin) AA precision roughness specimen is 2.4×10^{-3} m/s^2. Using the acceleration limit estimated from the step response study, the maximum sharpness triangular waveform which the NBS system could reliably reproduce at the 1500 μm/s traversing speed would be one with an included angle at the peak or valley of 140° or greater. (This does not include errors resulting from the finite tip radius.) The included angle on a precision roughness specimen is 150°; for typical machined surfaces it is about 160°.

APPENDIX O

MEASUREMENTS OF THE RECORD LENGTH AND TRAVERSING SPEED

Record Length

For meaningful average slope and wavelength measurements from the stored digital profiles the horizontal motion of the stylus must be calibrated to the accuracies desired for slope and wavelength. With the computerized system the calibration may be performed easily by adjusting the data acquisition rate so that a known length between two or more index points on a specimen occupies the correct proportion of the record length in memory. The data acquisition rate is adjusted by entering at the teletype the necessary count rate (appendix B).

The rulings of a 3.17 μm (125 μin) precision roughness specimen proved to be very convenient for calibrating the traversing length since they produce a clean profile in memory and their spacings may be measured with a length measuring microscope. The particular length measuring microscope employed was one designed so that the calibrated scale and the cross-hair used for measuring stage, and specimen, displacement were observed with separate microscopes. Mean spacing of the rulings was (95 ± 8) μm. The uncertainty stated is the sum of the 3 standard deviation limit estimated from values obtained in 20 measurements and the systematic error of the microscope estimated as 2 μm.

The traversing length required for five 762 μm (0.030 in) cutoff lengths is therefore equivalent to 40.2 periods of the 3.17 μm roughness waveform. Using a plot of the contents of memory the count number was adjusted to give 40 periods in the stored profile. This accuracy is considered sufficient for the present applications of average wavelength and slope. With this adjustment the sampling interval is (0.93 ± 0.07) μm.

Traversing Speed

To measure accuracy and uniformity of traversing speed a retroflector was attached to the motor drive of the Talysurf by means of modeling clay. The motion of the retroflector was then measured with a Hewlett-Packard 5526 laser measurement system. Speed values were recorded at rates up to 10 per sec. with a digital recorder. Analysis of the data showed:

at nominal speed = 1.52 mm/s (0.060 in/s)
measured speed = (1.52 ± 0.04) mm/s,
at nominal speed = 0.305 mm/s (0.012 in/s)
measured speed = (0.305 ± 0.013) mm/s.

A plot of the speed versus time from start of traverse exhibited some periodic behavior. The data was therefore Fourier analyzed to determine the magnitude of any dominant components. The maximum magnitude was only 0.7% of the mean speed; this occurred for a component with period approximately equal to 1/3 of the traverse length.

The primary concern in measuring the traversing speed was to ascertain the uniformity of the samplings of the roughness profile for use in the AA, average slope, average wavelength and the step height LSQ fit calculations.

APPENDIX P

SAMPLE TEST REPORT CONTAINING CALCULATIONS OF STATISTICAL PARAMETERS AND FUNCTIONS

U.S. DEPARTMENT OF COMMERCE
NATIONAL BUREAU OF STANDARDS
WASHINGTON, D.C. 20234

November 6, 1974

REPORT OF CALIBRATION 232.08/211071

For: Two Copper Gravure Printing Plates - Segments of Cylindrical Printing Surfaces

Submitted by:

On each of the two plates roughness measurements have been made to obtain profiles at appropriate magnifications, arithmetic average (AA) values, amplitude density functions, average profile slopes and profile wavelengths.

Table I gives the average AA value obtained from 3 traverses in each of 10 positions on both sample A and sample D. The positions are indicated schematically in figure 1. Average wavelength and average slope calculations for the profiles of positions 4, 8, 10 were made. The resulting values are also shown in table I. For positions 4 and 8 profile graphs at a horizontal magnification of 100, with vertical magnifications as indicated, and amplitude density functions were obtained. The graphs are displayed in figures 2 to 4.

The property of surface roughness in the 5 μm (200 microinch) AA range and below is measured at NBS by means of a minicomputer/stylus instrument system. Using an interferometrically measured step the system is calibrated on each value of magnification employed during a measurement. Surface profiles are taken according to the American National Standard B-46.1-1962 using a 0.76 mm (0.030 inch) cutoff length and a 3.80 μm (150 μin) stylus tip radius. Data is stored in the minicomputer memory employing 12 bit analog to digital conversion and a sampling rate of 1 point/μm (1 point/40 μin) over the traversing length. AA values are then calculated as described in Appendix A of the same American National Standard. The other parameters or functions may also be calculated from the stored profile data.

A conservative estimate* of the systematic error (3σ = 3 standard deviations) resulting from stylus pickup nonlinearity, interface hardware, software computations and analog to digital conversion is 1% for any type of uniform roughness specimen. Other errors are due to stylus tip radius uncertainty [3σ = 5 nm (0.2 μin)], to the surface finish of the step specimen [3σ of step transfer = 25 nm (1 μin)] and to the interferometric

*At the time this report was written the classifications of uncertainty components was slightly different from that in section 2.6. All subsequent reports conform to the classifications in section 2.6.

measurements of step heights [3σ = 25 nm (1 μin)]. The use of a step height approximately equal to the surface profile peak to valley height then gives a net systematic error for the calibration procedure of 2.8% (3σ) for AA values in the 0.25 μm (10 μin) range and 12% (3σ) for AA values in the 0.05 μm (2 μin) range.

From the data in table I and the measured system noise level the computed value for the average surface roughness of the specimen marked A is 0.226 μm (8.9 μin) AA with an uncertainty of 0.055 μm (2.2 μin).

Similarly, the computed value for the average surface roughness of the specimen marked D is 0.43 μm (1.71 μin) AA with an uncertainty of 0.13 μm (0.52 μin).

The uncertainties quoted are the sum of the systematic errors just described and the 3σ limit estimated from an analysis of the values from the 10 positions on each of the specimens. Values given as the average value have been corrected from the small effect of noise by assuming that the noise and signal from the specimen were not correlated. With this assumption the true value was calculated from the equation:

$$\text{true value} = [(\text{measured value})^2 - (\text{noise value})^2]^{\frac{1}{2}}.$$

The measured AA value of the noise during the time of roughness measurements was 0.0035 μm.

The amplitude density function of a surface profile or waveform describes the probability that the profile line will assume a value within some defined range at any point along the sampling length. The probability that the profile f(x) assumes a value between the range f and (f + Δf) is obtained by taking the ratio of L_X/L, where L_X is the total length that f(x) falls inside the range (f, f + Δf) over the sampling length L.

In equation form, for small Δf, one has:

$$\lim_{\Delta f \to 0} \text{Prob} \quad f < f(x) \leq f + \Delta f \quad = \lim_{\Delta f \to 0} \frac{L_X}{L} \quad = \text{ADF}(f)\ df$$

Calculation of the amplitude density function proceeds according to the definition given above by dividing the minicomputer data storage (12 bits) into 512 increments of 8 units width. The attached plots of the estimated amplitude density function (ADF) obtained with these finite increments are therefore the percentage of the profile data within the respective intervals as a function of the average ordinate value of the interval. Further interpretation of the ADF graphs may be obtained by comparing the experimental forms with the "ideal" Gaussian ADF for a theoretically random waveform which has a symmetrical bell shape. In addition to the information obtainable from the form of the ADF, one may measure the maximum peak to valley height of the profile from the extension of the graph and the scales indicated in figures 2 to 4. The scales shown in the figures are based on measurements of the ADF of a step of known height.

I In figures 3 and 4 the graphs of the ADF contain a flat portion for ordinate values near the mean ordinate. These regions are due to saturating the graphing system at the magnifications chosen for the ADF graphs. The large magnification was chosen to reveal more structure of the ADF's trailing edge, which would have been lost at magnifications not causing saturation.

The average profile slope is computed as the ratio of Arithmetic Average of the ordinate difference between successively sampled points to the mean sample spacing. Angles given in table I are the arc tangent of the computed value. The average wavelength is calculated with the equation:

$$\text{Average Wavelength} = 2\pi \, \frac{\text{profile AA}}{\text{AA of profile slope}} \, .$$

Measurements made by E. Clayton Teague
Fredric E. Scire

For the Director,

Russell D. Young
Russell D. Young
Chief, Optics and Micrometrology Section
Optical Physics Division, IBS.

TABLE 1

Summary of Parameter Measurements

Sample A

Position	AA(μm)	Average Slope Degrees	Average Wavelength (μm)
1	.1927		
2	.2323		
3	.2334		
4	.2236	5.8	11.8
5	.2504		
6	.2203		
7	.2087		
8	.2351	5.9	15.2
9	.2261		
10	.2406	6.3	12.9

Sample D

Position	AA(μm)	Average Slope Degrees	Average Wavelength (μm)
1	.0411		
2	.0475		
3	.0431		
4	.0398	1.2	12.5
5	.0430		
6	.0443		
7	.0475		
8	.0459	1.3	13.0
9	.0413		
10	.0412	1.1	12.9

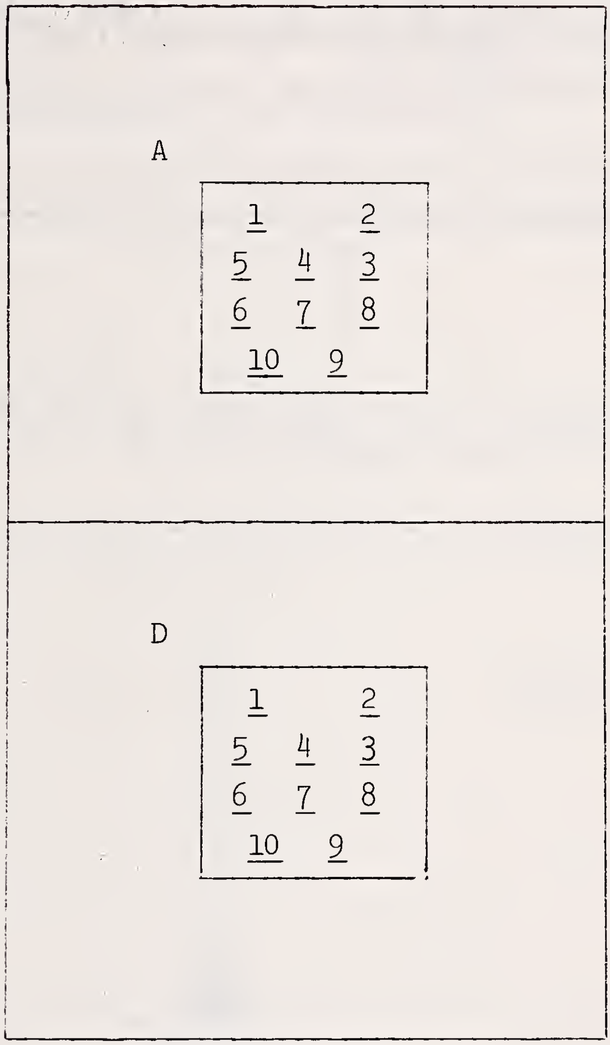

The points indicated on the sketch above are not to scale but are used to represent the approximate areas at which measurements were taken on each specimen.

Figure 1: Schematic of Measurement Positions

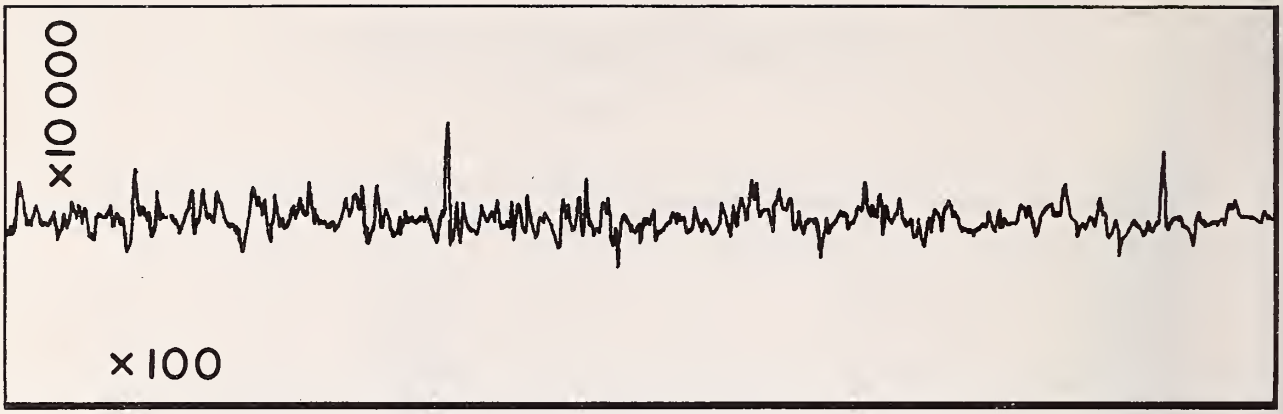

Surface Profile

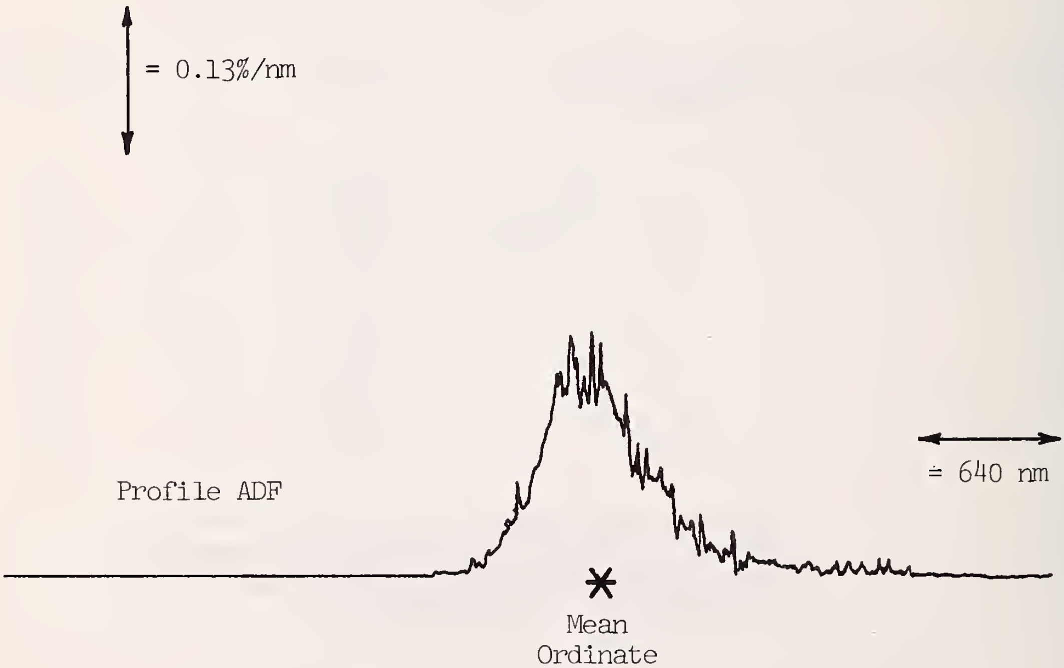

Figure 2: Profile and ADF of Area 4 on Sample A.

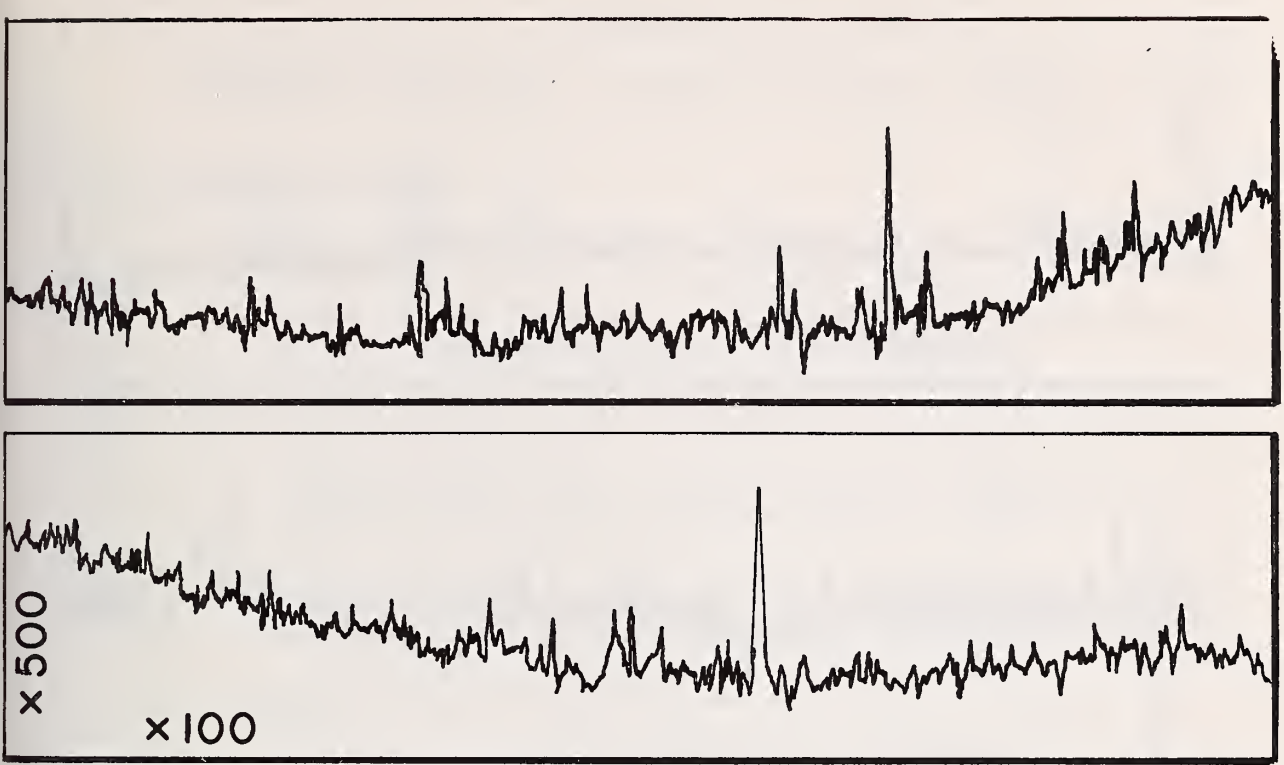

Surface Profile

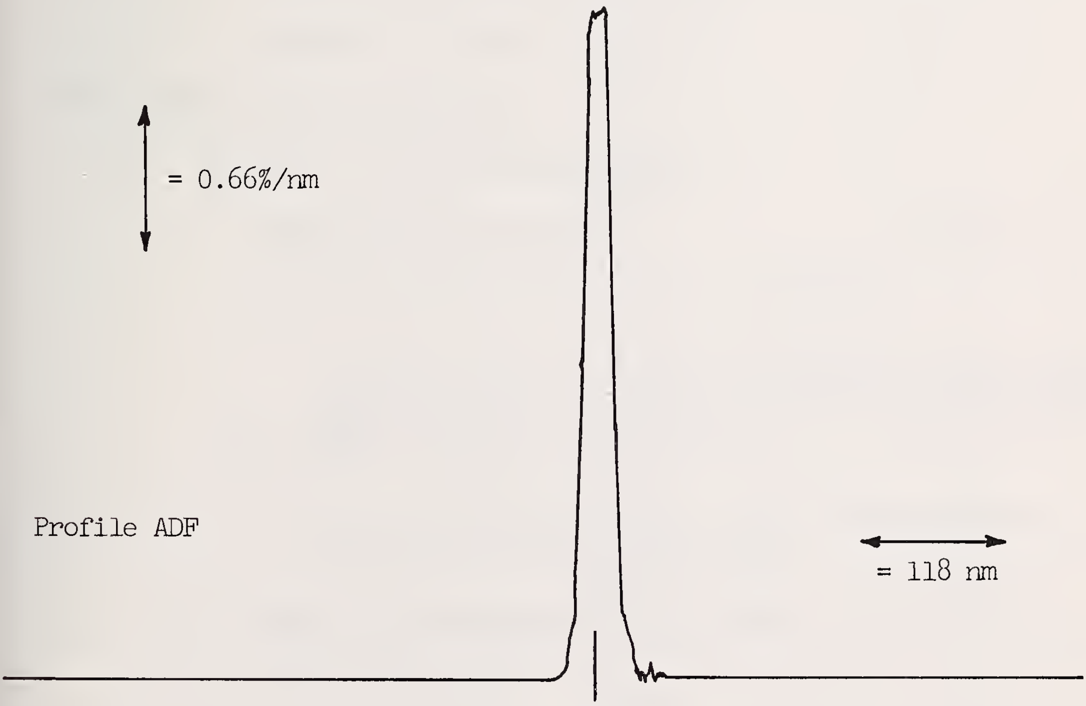

Figure 3: Profiles and ADF of Area 4 on Sample D.

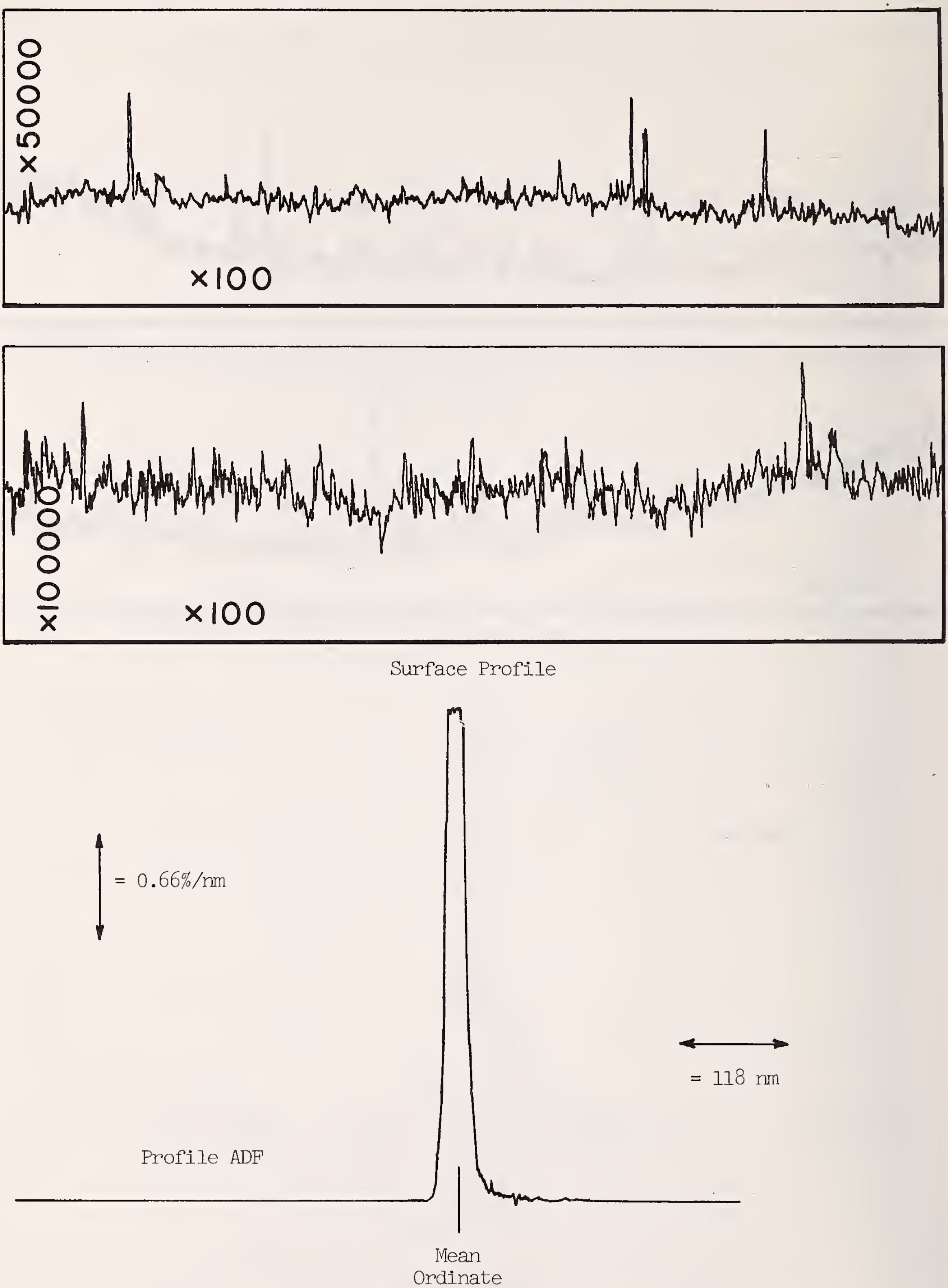

Figure 4: Profile and ADF Graphs of Area 8 on Sample D.

APPENDIX Q*

OPERATOR'S INSTRUCTIONS: INTERDATA 3/TALYSURF 4 SYSTEM

I. Preliminary Set-up

A. Instrumentation: the following connections are necessary:

1. those on the Talysurf for normal operation as indicated by the Talysurf Operating Instrumentions manual;

2. those internal to the A/D converter as shown in figure 35a;

3. the power cord of the interface electronics as in figure 35b (N. B. Disconnect main power line to computer when connecting this line).

4. The external leads between the Talysurf, interface electronics and A/D converter as in figure 35c.

B. Software: the following programs must reside in memory;

1. the hexadecimal monitor (3A80-3FFF);

2. the arithmetic subroutines (3010-3A00);

3. the master program (0080-1000).

II. General System Operation

A. Calibration of Stylus Instrument

1. Magnification Selection

(a) Align unknown specimen on Talysurf;

(b) traverse stylus with chart recorder on and select magnification on Talysurf electronic unit to obtain approximately three-quarters of maximum on-scale deflection of recorder pen;

(c) turn off recorder and select calibration step artifact of appropriate size.

2. Input of Calibration Step: Step-up

(a) Set switches

*Revised from DASR

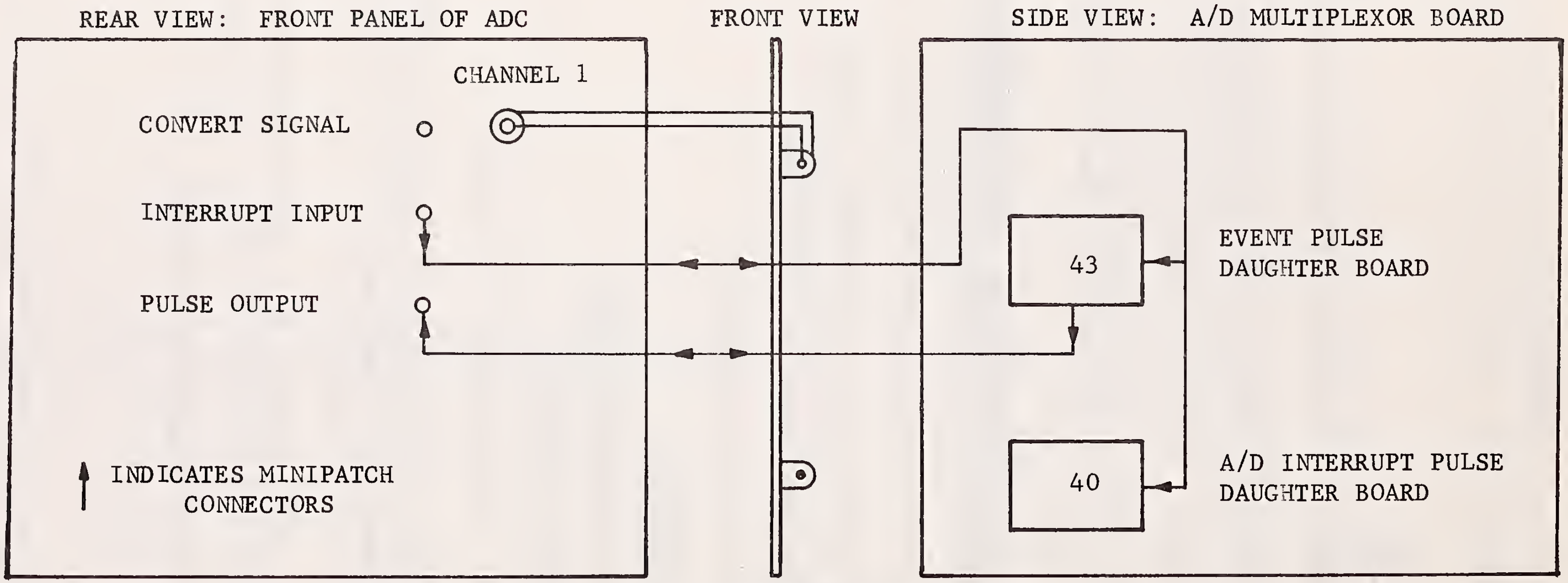

A/D CONVERTER BOARD

INTERNAL LEAD CONNECTIONS

FIGURE 35a

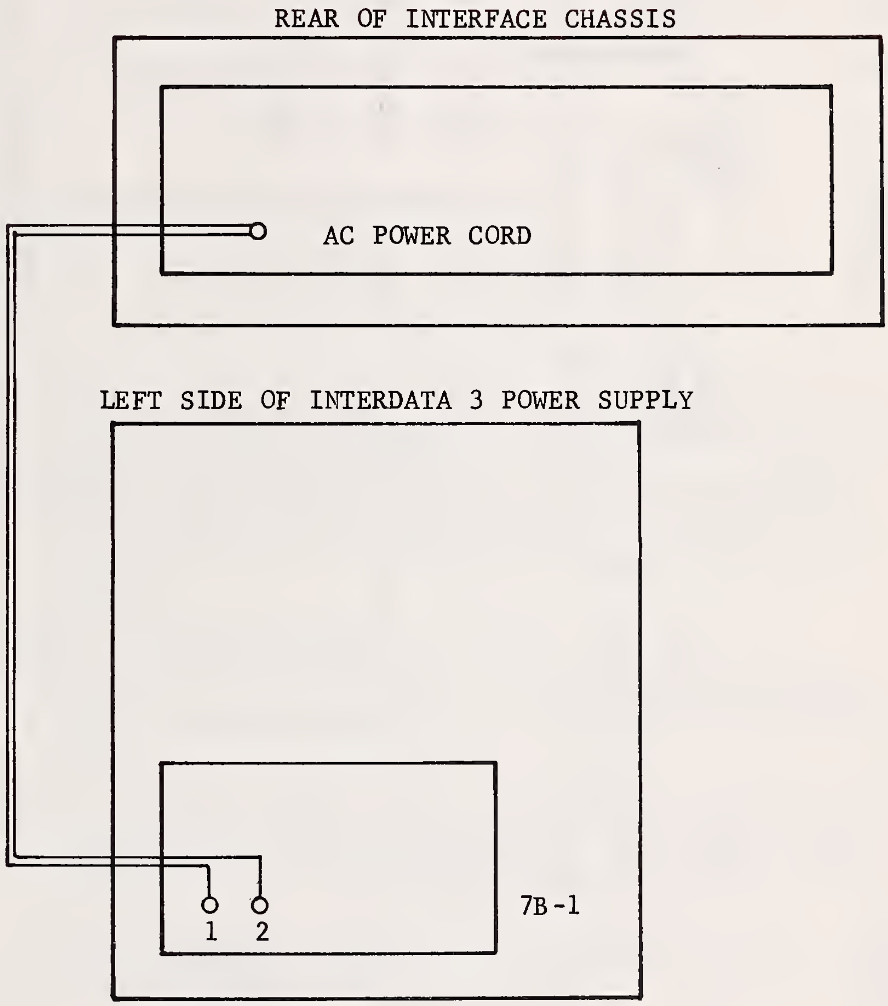

INTERFACE ELECTRONICS: AC POWER CONNECTION

FIGURE 35b

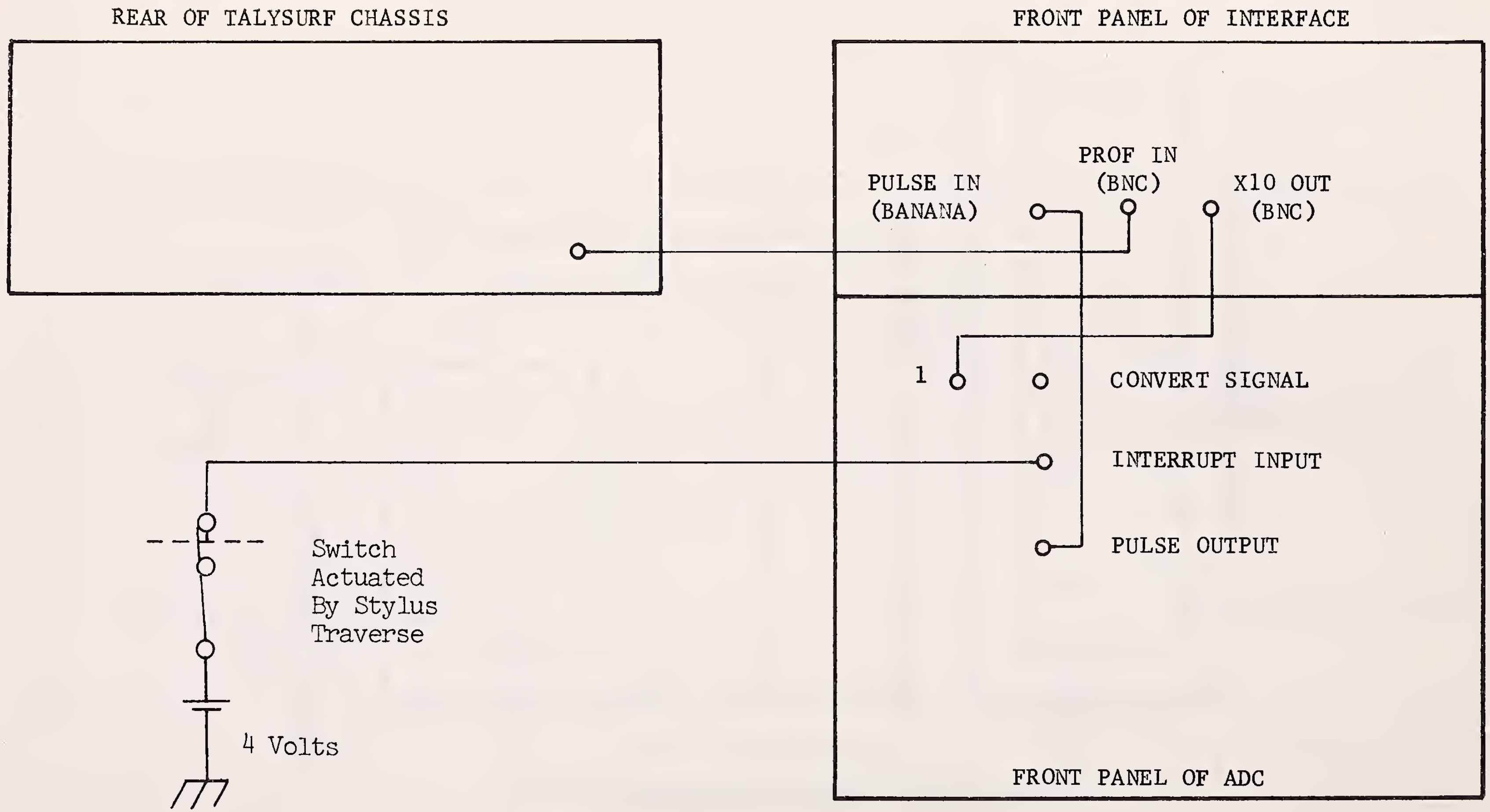
REAR OF TALYSURF CHASSIS
FRONT PANEL OF INTERFACE
PULSE IN
(BANANA)
PROF IN
(BNC)
X10 OUT
(BNC)
1
CONVERT SIGNAL
INTERRUPT INPUT
PULSE OUTPUT
Switch
Actuated
By Stylus
Traverse
4 Volts
FRONT PANEL OF ADC

FIGURE 35c

(1) Talysurf Electronic Control Unit

(1) Magnification: as determined in II.A.1

(2) Cut-off: K

(3) Operation: N

(2) Talysurf Gear Box

(1) Stroke knob: L

(2) Speed knob: X20

(3) Interface Electronics

(1) Mode Select: 10X

(2) Cut-off: Step

(b) Align artifact and traverse stylus to obtain trace with step edge in proper position relative to the event mark (See appendix E).

(c) Rotate the Talysurf Setting Lever to the left (CCW) position (see p. 4 of Talysurf Manual and Note 1 below).

3. <u>Input of Calibration Step</u>: Program Execution

(a) Begin program executive from TTY Control (Enter an "S")

(b) At "Enter Data": turn on the chart recorder and gently move and Setting Lever to the right (CW); data will be read for twenty-five seconds.

(c) At In: shut off the chart recorder and tear off the recorded trace;

(d) A1 and A2 selection:

(1) with the "Step Locator Scale," determine the position in mm of the step edge relative to the trailing edge of the event mark (see appendix E);

(2) select A1 and A2 symmetrically about the step edge.

(3) Record on the strip chart the mm and address locations of A1 and A2;

(e) At "Enter HO": type in the step height value as four digits and depress the space bar on the TTY;

(f) At "Enter Units": type in a two character unit symbol (do not press the space bar);

(g) At "Enter A1"; type in the four-digit address A1 and depress the space bar;

(h) At "Enter A2"; either A2 as above; the computer will now print out the computed step heights H1, H2 and HM with units.

(i) At "More?":

(1) If the computed step heights are unsatisfactory, type N and repeat the procedure for step 3a:

(2) If the heights are satisfactory, type Y.

B. Calibration of Unknown Specimen

1. Align the specimen on the Talysurf and traverse the stylus to obtain a properly centered trace.

2. Calibration of a Step

(a) Repeat procedure in IIA2, b and c;

(b) At "H or R?": type in H;

(c) At "Enter Data", follow procedure from IIA3, b thru h;

3. Calibration of a Roughness

(a) Select filter cut-off on interface; select X4 stroke speed on Talysurf; type R.

(b) At "Enter Data," rotate the Setting Lever to right position (CW); data will be read for 3.5 seconds.

(c) The computed AA and units will now be printed.

4. At "More?":

(a) If a step is to be calibrated, type Y; then at "H or R?", type H.

(b) If a roughness is calibrated, type Y, then at "H or R?", type R.

(c) If no more measurements are to be made, exit from program by typing N.

Note 1. The Event Marker appears on the chart recorder at the "Start of cut-off average" position in the stroke. With the stroke knob on the gear box at position L, the event mark appears when the marks on the gear box window are aligned as indicated below. Therefore, in returning the Setting Lever to the left (CCW) position, it is necessary only for L mark to be to the left of the rightmost mark on the upper scale.

APPENDIX R

CHECKLIST FOR PROPER ELECTRICAL OPERATION

Talysurf Outputs

(1) The profile Output should produce a voltage of nominally +1 volt when the pen is at the 2 inch mark on the strip chart and -1 volt at the zero inch mark.

(2) The interrupt signal should be a positive - going step of four volts near the "Start of cut-off average" position of the stylus stroke (see Talysurf Manual).

A/D Outputs

(1) With the Talysurf's interrupt signal lead connected to the Interrupt Input terminal on the A/D converter front panel. the A/D output at the Pulse Output terminal should be a zero to four volts pulse of about one second duration; (simultaneously the computer interrupt should trigger internally).

Interface Electronics Outputs

(1) With the system fully wired (figure 35), the output at the X10 OUT should be the amplified, filtered Profile Signal;

(2) A one-second pulse of nominally one volt should be present at the "PROFILE IN" terminal (and a similar one recorded on the chart recorder) at the "Start of cut-off average" stroke position.

Internal A/D Signals (A/D Multiplex or Board).

With the Talysurf's interrupt signal present at the Interrupt Input:

The output of the A/D Interrupt pulse (daughter board 40) should be a 50 microsecond positive-going pulse of about four volts.

NBS-114A (REV. 7-73)

U.S. DEPT. OF COMM. BIBLIOGRAPHIC DATA SHEET	1. PUBLICATION OR REPORT NO. NBS TN-902	2. Gov't Accession No.	3. Recipient's Accession No.

4. TITLE AND SUBTITLE Evaluation, Revision and Application of the NBS Stylus/Computer System for the Measurement of Surface Roughness	5. Publication Date April 1976
	6. Performing Organization Code
7. AUTHOR(S) E. Clayton Teague	8. Performing Organ. Report No.
9. PERFORMING ORGANIZATION NAME AND ADDRESS NATIONAL BUREAU OF STANDARDS DEPARTMENT OF COMMERCE WASHINGTON, D.C. 20234	10. Project/Task/Work Unit No. 2320184
	11. Contract/Grant No.
12. Sponsoring Organization Name and Complete Address (Street, City, State, ZIP) Same as No. 9	13. Type of Report & Period Covered Final
	14. Sponsoring Agency Code

15. SUPPLEMENTARY NOTES

16. ABSTRACT *(A 200-word or less factual summary of most significant information. If document includes a significant bibliography or literature survey, mention it here.)*

This report describes in detail the hardware and software used at NBS to implement on a stylus instrument/minicomputer system the process of calibrating the system with an interferometrically measured step and the calculation of important characterizations of surface profiles. The characterizations of a profile which may be calculated include the arithmetic average value, the mean square value, the amplitude density function, the autocorrelative function and the average wavelength. The report also includes a statistical evaluation, using empirical and analytical techniques, of the calibration procedures's long term stability.

17. KEY WORDS *(six to twelve entries; alphabetical order; capitalize only the first letter of the first key word unless a proper name; separated by semicolons)*

Amplitude density function; arithmetic average; autocorrelation function; average wavelength; kurtosis; minicomputer software; random error; skewness; surface micro-topography; surface roughness; surface texture; systematic error.

18. AVAILABILITY	19. SECURITY CLASS (THIS REPORT)	21. NO. OF PAGES
[X] Unlimited [ ] For Official Distribution. Do Not Release to NTIS	UNCLASSIFIED	151
[X] Order From Sup. of Doc., U.S. Government Printing Office Washington, D.C. 20402, SD Cat. No. C13. 46:902 [ ] Order From National Technical Information Service (NTIS) Springfield, Virginia 22151	20. SECURITY CLASS (THIS PAGE) UNCLASSIFIED	22. Price **$2.70**

USCOMM-DC 29042-P74

U.S. GOVERNMENT PRINTING OFFICE: 1976-210-801/210

NBS TECHNICAL PUBLICATIONS

PERIODICALS

JOURNAL OF RESEARCH reports National Bureau of Standards research and development in physics, mathematics, and chemistry. It is published in two sections, available separately:

- **Physics and Chemistry (Section A)**

Papers of interest primarily to scientists working in these fields. This section covers a broad range of physical and chemical research, with major emphasis on standards of physical measurement, fundamental constants, and properties of matter. Issued six times a year. Annual subscription: Domestic, $17.00; Foreign, $21.25.

- **Mathematical Sciences (Section B)**

Studies and compilations designed mainly for the mathematician and theoretical physicist. Topics in mathematical statistics, theory of experiment design, numerical analysis, theoretical physics and chemistry, logical design and programming of computers and computer systems. Short numerical tables. Issued quarterly. Annual subscription: Domestic, $9.00; Foreign, $11.25.

DIMENSIONS/NBS (formerly Technical News Bulletin)—This monthly magazine is published to inform scientists, engineers, businessmen, industry, teachers, students, and consumers of the latest advances in science and technology, with primary emphasis on the work at NBS. The magazine highlights and reviews such issues as energy research, fire protection, building technology, metric conversion, pollution abatement, health and safety, and consumer product performance. In addition, it reports the results of Bureau programs in measurement standards and techniques, properties of matter and materials, engineering standards and services, instrumentation, and automatic data processing.

Annual subscription: Domestic, $9.45; Foreign, $11.85.

NONPERIODICALS

Monographs—Major contributions to the technical literature on various subjects related to the Bureau's scientific and technical activities.

Handbooks—Recommended codes of engineering and industrial practice (including safety codes) developed in cooperation with interested industries, professional organizations, and regulatory bodies.

Special Publications—Include proceedings of conferences sponsored by NBS, NBS annual reports, and other special publications appropriate to this grouping such as wall charts, pocket cards, and bibliographies.

Applied Mathematics Series—Mathematical tables, manuals, and studies of special interest to physicists, engineers, chemists, biologists, mathematicians, computer programmers, and others engaged in scientific and technical work.

National Standard Reference Data Series—Provides quantitative data on the physical and chemical properties of materials, compiled from the world's literature and critically evaluated. Developed under a world-wide program coordinated by NBS. Program under authority of National Standard Data Act (Public Law 90-396).

NOTE: At present the principal publication outlet for these data is the Journal of Physical and Chemical Reference Data (JPCRD) published quarterly for NBS by the American Chemical Society (ACS) and the American Institute of Physics (AIP). Subscriptions, reprints, and supplements available from ACS, 1155 Sixteenth St. N. W., Wash. D. C. 20056.

Building Science Series—Disseminates technical information developed at the Bureau on building materials, components, systems, and whole structures. The series presents research results, test methods, and performance criteria related to the structural and environmental functions and the durability and safety characteristics of building elements and systems.

Technical Notes—Studies or reports which are complete in themselves but restrictive in their treatment of a subject. Analogous to monographs but not so comprehensive in scope or definitive in treatment of the subject area. Often serve as a vehicle for final reports of work performed at NBS under the sponsorship of other government agencies.

Voluntary Product Standards—Developed under procedures published by the Department of Commerce in Part 10, Title 15, of the Code of Federal Regulations. The purpose of the standards is to establish nationally recognized requirements for products, and to provide all concerned interests with a basis for common understanding of the characteristics of the products. NBS administers this program as a supplement to the activities of the private sector standardizing organizations.

Federal Information Processing Standards Publications (FIPS PUBS)—Publications in this series collectively constitute the Federal Information Processing Standards Register. Register serves as the official source of information in the Federal Government regarding standards issued by NBS pursuant to the Federal Property and Administrative Services Act of 1949 as amended, Public Law 89-306 (79 Stat. 1127), and as implemented by Executive Order 11717 (38 FR 12315, dated May 11, 1973) and Part 6 of Title 15 CFR (Code of Federal Regulations).

Consumer Information Series—Practical information, based on NBS research and experience, covering areas of interest to the consumer. Easily understandable language and illustrations provide useful background knowledge for shopping in today's technological marketplace.

NBS Interagency Reports (NBSIR)—A special series of interim or final reports on work performed by NBS for outside sponsors (both government and non-government). In general, initial distribution is handled by the sponsor; public distribution is by the National Technical Information Service (Springfield, Va. 22161) in paper copy or microfiche form.

Order NBS publications (except NBSIR's and Bibliographic Subscription Services) from: Superintendent of Documents, Government Printing Office, Washington, D.C. 20402.

BIBLIOGRAPHIC SUBSCRIPTION SERVICES

The following current-awareness and literature-survey bibliographies are issued periodically by the Bureau:

Cryogenic Data Center Current Awareness Service

A literature survey issued biweekly. Annual subscription: Domestic, $20.00; foreign, $25.00.

Liquefied Natural Gas. A literature survey issued quarterly. Annual subscription: $20.00.

Superconducting Devices and Materials. A literature survey issued quarterly. Annual subscription: $20.00. Send subscription orders and remittances for the preceding bibliographic services to National Bureau of Standards, Cryogenic Data Center (275.02) Boulder, Colorado 80302.

Electromagnetic Metrology Current Awareness Service

Issued monthly. Annual subscription: $24.00. Send subscription order and remittance to Electromagnetics Division, National Bureau of Standards, Boulder, Colo. 80302.